Identification, Control and Optimization Strategies for Thermo-Mechanical Pulping (TMP) Processes

by

Eranda Harinath Puwakkatiya-Kankanamge

B.Sc., University of Moratuwa, 2003
M. Eng., Memorial University of Newfoundland, 2007

A THESIS SUBMITTED IN PARTIAL FULFILLMENT OF
THE REQUIREMENTS FOR THE DEGREE OF

DOCTOR OF PHILOSOPHY

in

The Faculty of Graduate Studies

(Electrical and Computer Engineering)

THE UNIVERSITY OF BRITISH COLUMBIA

(Vancouver)

June 2012

Abstract

The focus of this thesis is to develop an advanced control system for existing and to-be developed Thermo-Mechanical Pulping (TMP) refining processes. Therefore, the thesis has two parts. The first part developed two different but yet complementary closed-loop identification methods to update the models used in the low-level control layer of the current advanced control systems for TMP refiners. These newly developed identification methods are specific to closed-loop systems controlled by Model Predictive Control (MPC) techniques, and successfully tailored to the presence of the MPC.

By updating the existing process models, the current advanced control systems can be operated to give better performance. However, these control systems may not be able to provide optimal performance due to process disturbances. Hence, a novel economically oriented advanced control system is developed for the existing two-stage TMP refiner processes for their optimal operation when disturbances are present. This novel technique dynamically optimizes the TMP processes as opposed to conventional two-layer methods which perform process optimization at steady-state, and has shown a potential economical benefit through reduction of total specific energy of a two-stage TMP process in a simulation study.

In the second part, a novel TMP process with multi-stages of Low Consistency (LC) refining is studied for its optimal operation. The proposed Nonlinear Model Predictive Control (NMPC) technique dynamically optimizes the process and provides better performance when disturbances are present. This economically oriented NMPC (econNMPC) minimizes the total specific energy consumption of the process while respecting all the process constraints and achieving final desired pulp quality. In simulation studies, a TMP process with multiple stages of LC refining was able to save significant specific energy consumption with set-point tracking control when disturbances are present. Moreover, further reduction of specific energy has been achieved with the developed econNMPC technique.

Preface

Chapter 3 is based on two published papers:

1. Rui Huang, Eranda Harinath, and Lorenz T. Biegler. Lyapunov stability of economically oriented NMPC for cyclic processes. *Journal of Process Control*, 21(4):501-509, 2011, and

2. Rui Huang, Lorenz T. Biegler, and Eranda Harinath. Robust stability of economically oriented infinite horizon NMPC that include cyclic processes. *Journal of Process Control*, 22(1):51-59, 2012.

This research was initiated by Dr. Huang and Dr. Biegler, Department of Chemical Engineering, Carnegie Mellon University (CMU). Dr. Huang was a former Ph. D. student at CMU and worked with Dr. Biegler. Dr. Huang is currently working in the United Technologies Research Center, USA. I contributed to the analysis of infinite horizon NMPC and wrote sections of the manuscripts. The rest of the analysis and paper writing were done by Dr. Huang and Dr. Biegler.

A part of Chapter 4 is based on a published paper,

1. Jun Yan, Eranda Harinath, Guy A. Dumont. Closed-loop identification for model predictive control: Direct method. *Proceeding of the* 48^{th} *IEEE Conference on Decision and Control*, 2592-2597, Shanghai, China, Dec 16-18, 2009.

The idea of use of explicit solutions of MPC stemmed from a discussion between myself and Dr. Yan, who was a post doctoral fellow at the Department of Electrical and Computer Engineering, University of British Columbia (UBC), and worked with Dr. Dumont. Dr. Yan is currently working in Hirain Technologies, China. I contributed to the analysis, section writing, and simulation studies. Dr. Dumont kindly reviewed the theoretical proofs.

Versions of Chapter 5 are published in two papers:

1. Eranda Harinath, Lorenz T. Biegler, and Guy A. Dumont. Control and optimization strategies for thermo-mechanical pulping processes: Nonlinear model predictive control. *Journal of Process Control*. 21(4):519-528, 2011, and

2. Eranda Harinath, Lorenz T. Biegler, and Guy A. Dumont. Advanced Step Nonlinear Model Predictive Control for Two-stage Thermo Mechanical Pulping Process. *the* 18^{th} *IFAC world congress*, Milan, Italy, Aug. 28 - Sept. 02, 2011.

I performed the complete analysis, simulation study, and paper writing for these research works. Dr. Biegler assisted to formulate the optimization problems and provided necessary softwares to solve the problems. Dr. Dumont and Dr. Biegler gave useful feedback during the research study and kindly reviewed the papers.

A version of Chapter 6 is submitted for publication.

1. Eranda Harinath, Guy A. Dumont, and Lorenz T. Biegler. Predictive optimal control for thermo-mechanical pulping processes with multi-stage low consistency refining, 2012.

I performed the complete analysis, simulation study, and paper writing for this research work. Dr. Biegler provided necessary softwares to solve the problems. Dr. Dumont and Dr. Biegler gave useful feedback during the research study and kindly reviewed the paper.

The other papers which are published or submitted for publication during my Ph. D. study but not included in this thesis are:

1. Eranda Harinath, Jun Yan, and Guy A. Dumont. Advanced control of a TMP refiner line: A simulation study. *the* 95^{th} *Annual Meeting of PAPTAC*, Montreal, Quebec, Canada, Feb 2-3, 2010.

In this research work, I performed the complete analysis, simulation study, and paper writing. Dr. Dumont and Dr. Yan gave useful feedback during the research study and kindly reviewed the paper.

2. Jun Yan, Eranda Harinath, and Guy A. Dumont. Tuning and Identification for Model Predictive Control: An Iterative Approach. *In Proceedings of IFAC Symposium on System Identification*, St. Malo, France, July 6-8, 2009. This research was initiated by Dr. Yan. I contributed to the analysis and simulation studies. Dr. Dumont kindly reviewed theoretical proofs and gave useful feedback during the research study.

3. X. Shi, Eranda Harinath, D. M. Maijer and Guy A. Dumont, Nonlinear Model Predictive Control in a Low Pressure Die Casting Process, submitted for publication, 2012.
   This research was initiated by X. Shi, Dr. Maijer and Dr. Dumont. Dr. Maijer is with the Department of Materials Engineering at the University of British Columbia, and X. Shi is a Ph. D. student of Dr. Dumont and Dr. Maijer. In this research, I contributed to the analysis of system identification and designing of nonlinear controller.

Table of Contents

List of Tables

List of Figures

Symbols

$\in$	belongs to
$\subseteq$	subset of
$\sum$	summation
$\|x\|$	norm of a vector x
$Q^T\,(x^T)$	transpose of a matrix Q (a vector x)
$\|x\|_Q^2$	weighted norm $x^T Qx$
$R > 0$	a positive definite matrix R
min	minimum
$\forall$	for all
$\neq$	not equal
$\mathbb{R}$	set of real numbers
$\mathbb{R}_{\geq 0}$	non-negative real numbers
$\mathbb{R}^n$	n-dimensional Euclidean space
$f : \mathbb{R}^n \times \mathbb{R}^m \to \mathbb{R}^n$	a function f mapping a space $\mathbb{R}^n \times \mathbb{R}^m$ into a space $\mathbb{R}^n$
$\emptyset$	empty set
ln	natural logarithm
∇f	gradient of a function f
$\nabla^2 L$	Hessian of a function L
$diag(w)$	a diagonal matrix with w vector in the diagonal
lim	limit
∞	infinity
$\to$	tends to
deg	degree

Abbreviations

TMP	Thermo Mechanical Pulping
HC	High Consistency
RTO	Real-Time Optimization
LC	Low Consistency
NMPC	Nonlinear Model Predictive Control
econNMPC	economically oriented NMPC
LTI	Linear Time Invariant
NLP	Nonlinear Programming
IPOPT	Interior Point OPTimizer
asNMPC	advanced step NMPC
MPC	Model Predictive Control
MPHC	Model Predictive Heuristic Control
DMC	Dynamic Matrix Control
GPC	Generalized Predictive Control
CARIMA	Control Auto-Regressive Integrated Moving-Average
ISS	Input to State Stability
RPI	Robustly Positively Invariant
KKT	Karush Kuhn Tucker
LICQ	Linear Independent Constraint Qualification
SSOC	Sufficient Second Order Condition
SC	Strict Complementary
PEM	Prediction Error Method
LRPI	Long Range Predictive Identification
QP	Quadratic Programming
FIR	Finite Impulse Response
ARX	Auto-Regressive Exogenous

RLS	Recursive Least Square
MIMO	Multi-Input Multi-Output
SISO	Single-Input Single-Output
CSF	Canadian Standard Freeness
LFC	Long Fiber Content
SC	Shive Content
sptNMPC	setpoint tracking NMPC
AMPL	A Modeling Language for Mathematical Programming
MATLAB	MATrix Laboratory
MHE	Moving Horizon Estimation
EKF	Extended Kalman Filter
BJ	Box-Jenkins

Acknowledgements

First, I would like to offer my sincere gratitude to my advisor, Prof. Guy A. Dumont at the Department of Electrical Engineering, the Faculty of Applied Science, for giving me an opportunity to pursue my Ph.D. studies. I express my sincere gratitude to him for providing an excellent research environment, guidance, valuable discussions, encouragement, and friendly attitude during the course of study. I also like to thank Prof. James A. Olson, the Director of Pulp and Paper centre (PPC), UBC, for providing me the financial support, guidance, and valuable discussions throughout the course.

It was an honor to work with many research collaborators who have contributed significantly to this research work, and their help and guidance are greatly acknowledged. Many thanks to Prof. Lorenz T. (Larry) Biegler in the Department of Chemical Engineering at Carnegie Mellon University (CMU), and Dr. Rui Huang. I also like to thank Dr. Rodrigo López-Negrete and all the other members in the Centre for Advanced Process Decision-making (CAPD) at CMU, who helped me during my research visit. I also want to thank Prof. Frank Allgöwer in the Institute for Systems Theory and Automatic Control (IST) at University of Stuttgart, and Prof. Christian Ebenbauer, Dr. Shuyou Yu, Christoph Maier, and all other members in IST, who helped me during my research visit. Many thanks to Dr. Jun Yan who is now with Hirain Technologies, China, and XinMei Shi for having fruitful discussions. I gratefully acknowledge the supports given by all other members in the PPC.

I gratefully acknowledge the financial contributions and supports from the Michael Smith Foreign Study Supplements Scholarship, NSERC, British Columbia Innovation Council, Advanced Fiber Technologies, Andritz, Arkema, BC Hydro, Canfor, Catalyst Papers, CEATI/ Ontario Power Authority, Honeywell, Howe Sound Pulp and Paper, Paprican, Westcan, and West Fraser Quesnel River Pulp.

Dedication

To My Parents, Lisie and Peter
To My Sisters
To My Loving Wife Ruvini

Chapter 1

Introduction

Thermo-Mechanical Pulping (TMP) is a dominant process in the pulping industry. In the TMP process, wood chip refiners, which are required to run uniformly, are used to convert wood chips to pulp. The TMP refiners consume large amounts of electric energy - in British Columbia, Canada, around 10% of the total electrical energy production is consumed by seven mechanical pulping plants [1]. Conventional TMP processes have two stages of High Consistency (HC) refining. The consistency can simply be defined as *mass ratio of dry-fiber to the mixture of dry-fiber and water*. The HC refiners play the main role in achieving the paper-making properties of pulp, yet are high energy consuming; nearly 80% of the total energy consumption in a TMP process is due to the HC refiners [1].

Although the TMP process is a mainstay of the pulping industry [2], TMP mills face a number of challenges due to the increase in electricity costs, and initiatives to reduce green house gas emissions. TMP mills need to reduce electrical energy consumption, thereby reducing production cost and environmental impact [3] [4]. In addition, pulp mills have to produce improved pulp with less variability in pulp quality in order to maintain competitiveness and retain customers [5]. At present, TMP mills are seeking advanced process control techniques to minimize energy consumption and improve pulp quality in order to address the above challenges.

1.1 Two-stage TMP Process

Fig. 1.1 shows the basic operational units of a typical TMP process. There are mainly three operational areas in the TMP process [6]. In the wood chips pre-treatment, wood chips are first screened to remove under and over sized particles, and are then steamed at atmospheric pressure around 100^{o}C for preheating. Following this, the wood chips are fed to the washing system, which operates around

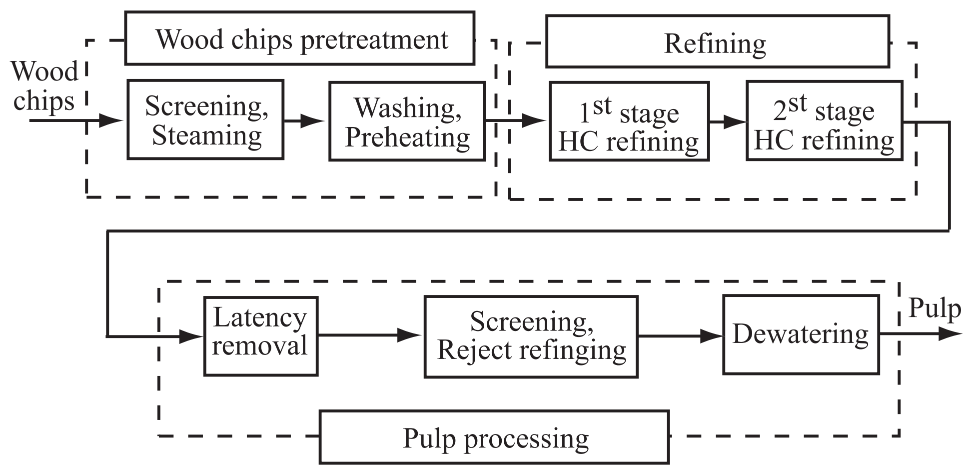

Figure 1.1: Basic schematic of a two-stage TMP process

70 – 85^{o}C to maintain chip moisture, to remove contaminants like sand, saw-dust and stones from the wood chips [2]. Before feeding to the primary refining stage, the wood chips are preheated to soften lignin binding wood fibers in order to facilitate their further separation, maximizing long fiber content and minimizing shive content [6].

The smooth operation of wood chip refiners is critical, as they play a major role in achieving paper-making properties of the pulp. There are two stages of HC refining: primary and secondary. The wood chips are fed to the primary refiner using a screw feeder which is manipulated to control the production rate. The primary refiner is used to convert wood chips to individual wood fibers; the refining plates of the refiners are made such that wood chips are gradually broken into fibers in the refining zone. The second stage of refining is used to develop the pulp qualities. The primary and secondary refiners are operated at HC, and dilution water is fed to the refiners to control the consistencies.

The pulp processing, done at Low Consistency (LC), is performed to achieve the required properties of the pulp. After the secondary stage of HC refining, the pulp is fed to the latency chest for latency removal, i.e. relieving of internal stresses and removal of curl, resulting in improved pulp properties such as strength. The screening and reject refining are then performed to remove contaminants and decrease shive content of the pulp. In the dewatering process, optical properties of the pulp are improved.

The refining process is, inherently, a Multi-Input Multi-Output (MIMO) process with complex dynamics and severe interactions among process variables. To understand the refining process with a view to controlling it, the process variables are divided into four categories: manipulated variables, operating variables, pulp-quality variables, and disturbance variables [6, 7].

Manipulated Variables (MVs)

The Manipulated Variables (MVs) are the main input variables for any refiner, and must be controlled in order to achieve the desired operational conditions. In the case of primary and secondary refining, the MVs include chip transfer screw speed (considered at the primary refiner only), plate gap, and dilution water flow [8, 9]. The temperature of the wood chips entering the primary refiner can also be considered as an input variable and assumed to be the same as the pre-heater temperature which softens the wood chips. However, the temperature of the wood chips entering the primary refiner is not considered as a MV [2, 7].

Operating Variables (OVs)

The Operating Variables (OVs) are the key variables, and are highly correlated with pulp quality. By controlling the MVs, the OVs are kept at *optimum setpoints* (OSPs); the OSPs are determined by economical operation of the refining process. The main OVs in all stages of refining are: motor load, consistency, and production rate. Among them, the motor load is believed to be an important OV [7, 10, 11]. In the literature, specific energy and refining intensity are also considered as OVs; however, they are correlated with the above OVs for a given refiner. Therefore, the effect of specific energy and refining intensity on pulp quality can be controlled through motor load, consistency and production rate [12, 13].

Pulp Quality Variables (PQVs)

The Pulp Quality Variables (PQVs) define the paper-making properties of the pulp, and the choice of different properties depends on the end users. The main PQVs that characterize the refining process are: freeness, fiber size distribution, and shive content [11, 12]. Online measurement of PQVs is possible with a *Pulp-Quality Monitor* (PQM), and is important to determine the optimum economical operation of the refiner units.

Disturbance Variables (DVs)

The variables that cannot generally be manipulated with and are independent of the input variables are called Disturbance Variables (DVs). These variables appear in the refining process mainly through wood chips and the refiner unit itself. The DVs influence the operating conditions of the refiner process, thereby changing the pulp quality. The important DVs in wood chips are wood-chip species, chip size distribution, moisture content, and chip-bulk density. The back-flow of steam from the refiner and refiner plate wear are the main disturbances in the refiner unit [6, 7].

A comprehensive understanding of these process variables is necessary to develop refiner process control strategies.

1.2 Research Motivation

Chips refiners are the most energy intensive units in the TMP process; approximately 80% of the total energy is consumed by HC refiners [1]. Therefore, there is considerable literature on implementation of advanced control systems for them [5], [14], [8]. However, it has been reported that advanced control systems have failed to perform well over for a long period: over 90% of all advanced control applications have been turned off within a year [5]. Major reasons for poor performance of advanced control systems are 1) less attention being paid to low-level regulatory control and 2) the linearity assumption of the TMP process. In addition, operator training and servicing after installation need to be improved for reliable and continuing operation of advanced control systems.

Multi-layer architecture is commonly used in the decision making hierarchy of industrial processes, and economical operation of a process is usually performed using an advanced process control system with a two-layer structure. Fig. 1.2 shows the two-layer control strategy for a TMP process. The two-layer structure consists of a higher layer, implementing Real-Time Optimization (RTO), followed

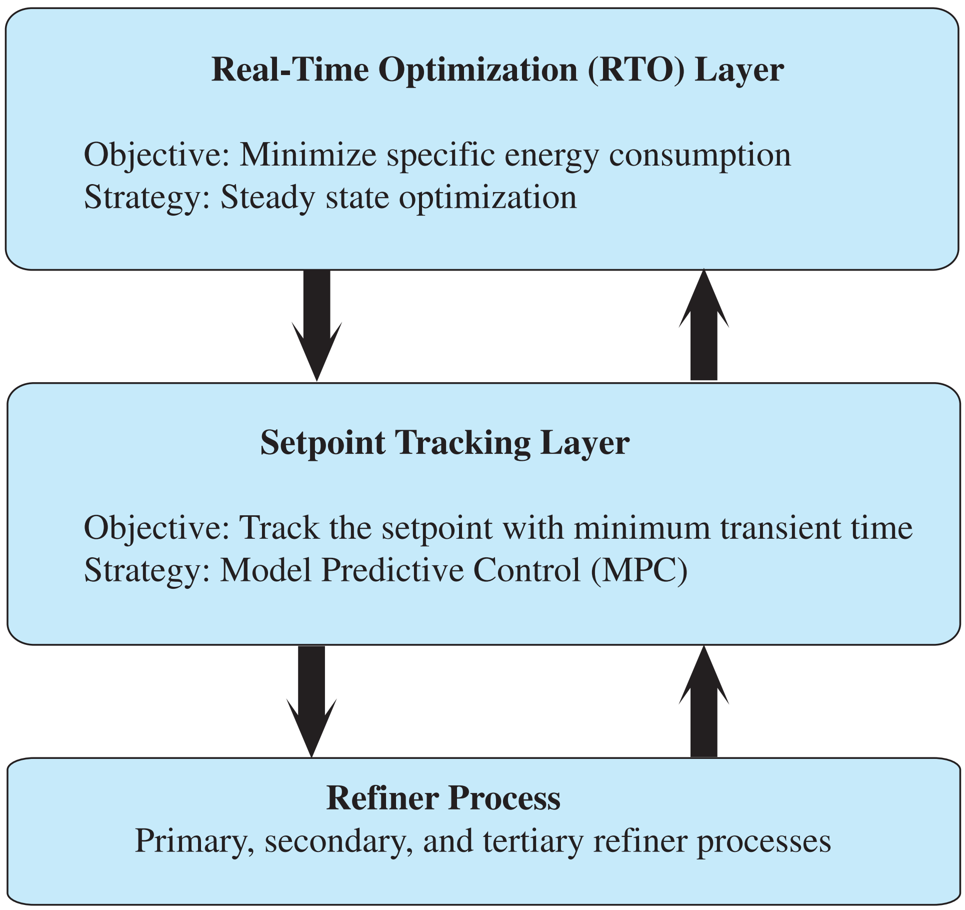

Figure 1.2: Current control strategy of TMP refiner processes: the conventional two-layer architecture

by a lower layer for setpoint tracking or regularization control. The RTO layer computes optimal steady-state setpoints using a steady-state process model, and provides these setpoints to the setpoint tracking layer, in order to maximize an economical objective while keeping product quality constraints within safe values.

The performance of the advanced control systems installed in TMP mills directly rely on the basic low-level regulatory control system; only the basic low-level control system has direct access to the TMP refiner process and can change the control input variables [5, 15], such as the refiner plate gap. Therefore, the proper monitoring of the regulatory layer is essential for economical operation of the TMP process. Most existing advanced control systems installed in TMP processes are based on a linear model of the process. Periodic update of this linear process model would be required for satisfactory performance of the controller, as the performance of the closed-loop system may deteriorate due to model/process mismatch caused by physical changes of the process over time, such as wear and tear of the refiner plates. However, setpoint tracking control would be difficult with a controller based on a linear model since TMP refiner processes are inherently complex processes, consisting of nonlinear dynamics. Moreover, the inconsistency of the two models used in the RTO and setpoint layers could result inconsistent and unreachable setpoint [16, 17]. Furthermore, optimum setpoints are not always at steady-state due to dynamically changing disturbances, like chip bulk density, chip moisture content, and model-plant mismatch. Therefore, it is sub-optimal to minimize transition time between setpoints. These problems have been noticed in one of our industrial partner's TMP control system. On the other hand, LC refining technology is emerging. More attention has been paid towards research and development of LC refiners, mainly because the LC refiners are more energy efficient than HC refiners [1, 18]. The inclusion of the third stage LC refiner in the mainline has led to the reconsideration of advanced control system to optimally coordinate the HC and LC refiners. Therefore, time is ripe to develop an advanced control technique for the existing TMP processes with two-stage HC refiners, and new TMP processes which are to be developed with HC and LC refiners.

1.3 Research Objective

The main objective of this thesis is to propose strategies to improve the performance of the existing TMP processes and the new TMP processes. For that purpose, closed-loop identification techniques, and nonlinear model based control and optimization strategies are presented for TMP processes.

1.4 Summary of Contributions

The following are the summary of contributions in this research.

1. Development of two closed-loop identification schemes. The first scheme is a novel attempt while the second scheme is an extension of an existing method with a meaningful identification criteria. Both the schemes can be applied for Linear Time-Invariant (LTI) systems controlled by constrained MPC laws.

2. Design of a novel control and optimization strategy based on Nonlinear Model Predictive Control (NMPC) technique for a two-stage TMP process.

3. Design of economically oriented control strategy for a novel TMP process which consists of HC and LC refiners using NMPC framework. This research work is one of the first contributions that investigates dynamic optimization of TMP processes with multi-stages of LC refiners.

4. Analysis of nominal and robust stabilities of an infinite horizon NMPC with a general economic objective function. Since the stability analysis of this class of problem is still in early stage of its development, this research work will be a significant contribution to the field.

1.5 Organization of the Thesis

The rest of the thesis is organized as follows. Chapter 2 presents the basic principle of NMPC techniques and introduces some definitions and assumptions which are used throughout the thesis. The material presented in the Chapter 2 serves as the basis for the subsequent chapters. Chapter 3 discusses economically oriented NMPC (econNMC) framework for the optimal operation of a process. In particular, infinite horizon econNMPC with a general economic objective function is discussed. The nominal and inherent robustness properties are discussed for econNMPC in Chapter 3. Chapter 4 presents closed-loop identification methods which can be applied to an LTI system controlled by a constrained MPC law. In Chapter 5, economical operation of two-stage TMP process is studied. The setpoint tracking and econNMPC techniques are discussed, and closed-loop simulation studies also presented for two-stage TMP processes. Chapter 6 studies two types of TMP processes for optimal operation: a conventional two-stage TMP process with a LC refiner, an improved TMP process with two-stages of LC refining. Both processes are dynamically optimized with econNMPC techniques. Simulation studies are presented for both processes to realize potential economical benefits through reduction in total specific energies.

Chapter 2

Model Predictive Control (MPC)

2.1 Summary

In this chapter, the basic principles of Nonlinear Model Predictive Control (NMPC) are presented for discrete time nonlinear systems. The nominal and robust stability of setpoint tracking NMPC problems are reviewed. Solution strategies for the resulting Nonlinear Programing (NLP) problem of NMPC framework are discussed; specifically, the basic formulation of the Interior Point OPTimizer (IPOPT) solver is presented. Furthermore, the advanced step NMPC (asNMPC) concept, which is a fast approximate solution technique of the resulting NLP to reduce on-line computational time, is discussed. The review of NMPC presented in this chapter is not exhaustive, but rather provides the basis for the following chapters.

2.2 Receding Horizon Control

In MPC, at each sample time k, first the future dynamic behavior of the process is predicted using a model of the process over a *prediction horizon* N. Next the optimal control moves over a *control horizon* M are determined by minimizing an objective functional subject to the process dynamics, and input and state constraints. Although M control moves are calculated, only the first control move is applied to the process until the next sample time $k+1$. At sample time $k+1$, the process evolves to new states which, in practice, will not be equal to the model predicted states at sample time $k+1$, due to model-process mismatch and disturbances. Hence, a new constrained optimization problem is formulated over the prediction horizon N with the state information at sample time $k+1$ and is solved for M optimal control moves. This strategy is also known as *receding horizon* or *moving horizon* control, and the MPC law is implemented in this receding horizon

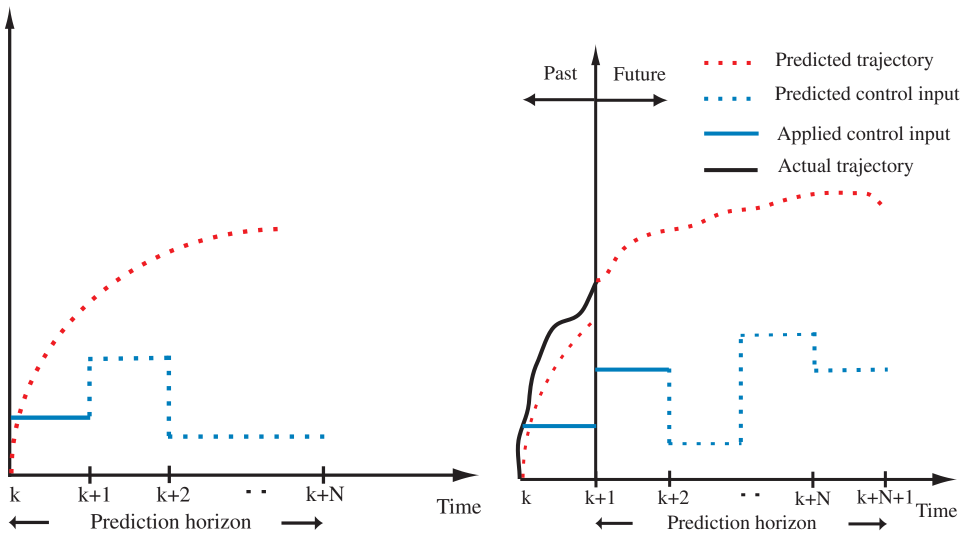

(a) At sample time k (b) At sample time $k+1$

Figure 2.1: The basic of MPC

framework. The basic concept of MPC is illustrated in Fig. 2.1 and summarized in the following algorithm.

Algorithm 1 The basic steps of MPC framework at sample time k

1: Predict the future dynamic behavior of the process over the prediction horizon using the state information at sample time k.
2: Determine the optimal control inputs over the control horizon by solving the constrained optimization problem.
3: Apply only the first control move to the process until next sample time $k+1$.
4: $k \rightarrow k+1$, go the step 1

2.3 Basic NMPC Problem Set-up

Consider a discrete time nonlinear system described by

$$x_{k+1} = f(x_k, u_k), \quad k \geq 0, \tag{2.1a}$$

subject to the control and state constraints,

$$u_k \in \mathbb{U} \quad \text{and} \quad x_k \in \mathbb{X}, \tag{2.1b}$$

where $x_k \in \mathbb{R}^n$ and $u_k \in \mathbb{R}^m$ are the state and control input variable vectors of the system, respectively. $\mathbb{U} \subseteq \mathbb{R}^m$ is the control constraint set, and $\mathbb{X} \subseteq \mathbb{R}^n$ is the state constraint set. $f : \mathbb{R}^n \times \mathbb{R}^m \to \mathbb{R}^n$ is the nominal nonlinear system function. In the sequel, $z \in \mathbb{R}^n$ and $v \in \mathbb{R}^m$ are used to denote the model predicted state and computed control input vectors in the controller, respectively.

Using the current process state x_k as initial conditions, the dynamic optimization problem for NMPC is formulated at sample time k as follows.

$$\min_{\mathbf{v}} \quad J(z(\cdot), v(\cdot)) \tag{2.2a}$$

$$\text{s. t. :} \quad z_{i+1} = f(z_i, v_i), \quad z_0 = x_k \quad i = 0, \ldots, N-1, \tag{2.2b}$$

$$z_i \in \mathbb{X} \quad i = 0, \ldots, N, \quad \text{and} \tag{2.2c}$$

$$v_i \in \mathbb{U} \quad i = 0, \ldots, N-1 \tag{2.2d}$$

where N is, for simplicity, the length of the horizons in sample times, without differentiating the control and the prediction horizons. x_k is the current, measured or estimated, state vector of the process. $\mathbf{v} = \{v_0, v_1, \ldots, v_{N-1}\} \in \mathbb{U}_N(x_k)$ where $\mathbb{U}_N(x_k)$ is the set of *feasible* control moves which satisfy the constraints (2.2b)-(2.2d). $J : \mathbb{R}^n \times \mathbb{R}^m \to \mathbb{R}$ is a cost functional, sometimes called *performance index* or *objective functional*, is defined over the horizon N,

$$J(z(\cdot), v(\cdot)) = \sum_{i=0}^{N-1} l(z_i, v_i) \tag{2.3}$$

where $l : \mathbb{R}^n \times \mathbb{R}^m \to \mathbb{R}$ is the stage cost.

There are mainly three ingredients in MPC: 1) the internal model, 2) the objective functional, and 3) the constraints. A basic categorization of different MPC strategies can be obtained via the selection of the internal model and objective function in their formulations. An MPC formulation is, in general, referred to as *linear* or *nonlinear* if the model used is linear or nonlinear. With the type of stage cost, for example *setpoint tracking* or *economic*, MPC techniques used in the linear and nonlinear MPC frameworks are different. Linear MPC techniques are widely popular and have been successfully applied in industrial processes [19].

The receding horizon concept, one of the key ideas of MPC, was first conceptualized in [20] to apply linear programming techniques in optimization-based control problems. The description of perhaps the earliest application of MPC, Model Predictive Heuristic Control (MPHC), was presented in [21]. In the MPHC formulation, an impulse response model was used with a quadratic stage cost, and input and output constraints. Within the family of linear MPC strategies, the Dynamic Matrix Control (DMC) [22] and the Generalized Predictive Control (GPC) [23, 24] were key formulations in the early stage of MPC development in both academia and industry, and have been successfully implemented in many industrial processes. The DMC formulation uses a linear step-response model while the GPC formulation uses a Controlled Auto-Regressive Integrated Moving-Average (CARIMA) model for setpoint tracking. Thorough reviews of MPC techniques are provided in [19, 25]. The theory of linear MPC is quite mature at present [26]. In this chapter, the setpoint tracking NMPC formulation is reviewed for its nominal and robust stability.

2.4 Nominal Stability of NMPC

For the setpoint tracking NMPC, a quadratic stage cost is generally used in the cost functional, i.e.

$$l(z,v) = \|z - x_s\|_Q^2 + \|v - u_s\|_R^2 \tag{2.4}$$

where $x_s \in \mathbb{R}^n$ and $u_s \in \mathbb{R}^m$ are state and control setpoint vectors, respectively. Although the use of the reference control input vector u_s is not necessary if there is no degree of freedom in the controller i.e. $n = m$, this formulation might be useful when changing the operating conditions especially for nonlinear processes [27]. $Q \in \mathbb{R}^{n\times n} > 0$ and $R \in \mathbb{R}^{m\times m} > 0$ are *positive definite* weighting matrices for state and control vectors, respectively. To simplify the formulation of expressions in this chapter, the setpoint vectors are considered, without loss of generality, as $x_s = 0$

and $u_s = 0$. The following definitions and lemmas have been used throughout the chapter.

Definition 2.4.1 *[28, 29] Let $\mathbb{U}_N(x)$ be the set of feasible control moves which satisfy the constraints* (2.2b)-(2.2d) *with the initial state x. Then the admissible set $\mathbb{Z}_N$ can be defined as,*

$$\mathbb{Z}_N = \{(x, \mathbf{v}) | x \in \mathbb{X} \textit{ and } \mathbf{v} \in \mathbb{U}_N(x)\},$$

and the set of admissible states $\mathbb{X}_N \subseteq \mathbb{X}$ can be defined as,

$$\mathbb{X}_N = \{x | \mathbb{U}_N(x) \neq \emptyset\}. \tag{2.5}$$

Definition 2.4.2 *[30] Consider the system $x_{k+1} = f(x_k, u_k)$ with the control law $\kappa : \mathbb{R}^n \to \mathbb{R}^m$ defined by $u = \kappa(x)$, and $f(0,0) = 0$. Then for the closed-loop system,*

$$x_{k+1} = f(x_k, \kappa(x_k)) = h(x_k) \tag{2.6}$$

the set $\mathbb{X}_{pi}$ is said to be a positively invariant set if

$$h(x_k) \in \mathbb{X}_{pi}, \quad \forall\, x_k \in \mathbb{X}_{pi}, \quad \forall\, k \geq 0.$$

Further, if $\mathbb{X}_{pi} \subseteq \mathbb{X}_N$, then $\mathbb{X}_{pi}$ is called output admissible set which is a domain of attraction of the origin [31, 32].

Definition 2.4.3 *[30] A continuous function $\alpha : [0, a) \to [0, \infty)$, where $a \in \mathbb{R}_{\geq 0}$, is a class $\mathcal{K}$ function if it is strictly increasing and $\alpha(0) = 0$. It is a class $\mathcal{K}_\infty$ function if $\alpha(a) \to \infty$ as $a \to \infty$.*

Definition 2.4.4 *[30] A continuous function $\beta : [0, a) \times [0, \infty) \to [0, \infty)$ is a class $\mathcal{K}\mathcal{L}$ function if, for each fixed $s \in \mathbb{R}_{\geq 0}$, $\beta(\cdot, s)$ is a class $\mathcal{K}$ function, and for each $r \in \mathbb{R}_{\geq 0}$, $\beta(r, s) \to 0$ as $s \to \infty$.*

Definition 2.4.5 *[30] A function $V(\cdot)$ is called a Lyapunov function for the system* (2.6) *if there exists a set $\mathbb{M}$ and $\mathcal{K}_\infty$ functions α_{v1}, α_{v2}, and α_{v3} such that*

$$\begin{aligned} \alpha_{v1}(x) \le V(x) \le \alpha_{v2}(x), \\ V(h(x)) - V(x) \le -\alpha_{v3}(x) \quad \text{for all } x \in \mathbb{M}. \end{aligned} \tag{2.7}$$

Lemma 2.4.1 *[32, 33] Let $V(\cdot)$ be a Lyapunov function for the system* (2.6)*, and $V(\cdot)$ is defined in an admissible positive invariant set $\mathbb{X}_{pi}$ containing the origin in its interior. Then the origin is asymptotically stable. Further, if $\alpha_{v1} = a_{v1}\|x\|^{b_v}$, $\alpha_{v2} = a_{v2}\|x\|^{b_v}$, $\alpha_{v3} = a_{v3}\|x\|^{b_v}$, for real positive a_{v1}, a_{v2}, a_{v3}, and b_v then the origin is an exponentially stable equilibrium point.*

The constrained optimization problem is formulated for the setpoint tracking NMPC problem at sample time k to achieve the nominal stability of the closed-loop system as,

$$V_N(x) = \min_{\mathbf{v}} \quad \sum_{i=0}^{N-1} l(z_i, v_i) + F(z_N) \tag{2.8a}$$

$$\text{s. t. :} \quad z_{i+1} = f(z_i, v_i), \quad z_0 = x_k, \tag{2.8b}$$

$$z_i \in \mathbb{X}, \quad v_i \in \mathbb{U}, \tag{2.8c}$$

$$z_N \in \mathbb{X}_F, \quad i = 0, \dots, N-1, \tag{2.8d}$$

where $F(\cdot)$ is a *terminal cost* (or called *terminal penalty term*). $\mathbb{X}_F \subseteq \mathbb{X}$ is a *terminal set* (an output admissible set). The above constrained optimization problem is denoted as $P_N(k)$, and the solution of $P_N(k)$ is denoted by $\mathbf{v}^* = \{v_0^*, v_1^*, \dots, v_{N-1}^*\}$. Since the controller is implemented according to the receding horizon fashion, the MPC control law $h_{mpc} : \mathbb{R}^n \to \mathbb{R}^m$ can be defined by

$$h_{mpc}(x_k) = v_0^*. \tag{2.9}$$

Then the closed-loop system can be described as

$$x_{k+1} = f(x_k, h_{mpc}(x_k)). \tag{2.10}$$

In the following, some fundamental properties of the nonlinear system function f, stage cost l, terminal cost F, constraint sets $\mathbb{U}$ and $\mathbb{X}$, and terminal set $\mathbb{X}_F$ are assumed to show the nominal stability of the closed-loop system (2.10).

Assumption 2.4.1 *f is continuous, and $f(0,0)=0$. Thus the origin is an equilibrium point of the system* (2.1a).

Assumption 2.4.2 *l is Lipschitz continuous with Lipschitz constant L_l. $l(0,0)=0$, and $\alpha_l(\|x\|) \le l(x,u) \le \beta_l(\|x\|)$ where α_l and β_l are $\mathscr{K}$ functions.*

Assumption 2.4.3 *$\mathbb{U}$ is compact, and $\mathbb{X}$ is closed. The origin $(0,0)$ is an interior point of $\mathbb{X} \times \mathbb{U}$.*

Assumption 2.4.4 *$\mathbb{X}_F \subseteq \mathbb{X}_N$ is compact and contains the origin in its interior, i.e. $0 \in \mathbb{X}_F$.*

Assumption 2.4.5 *F is Lipschitz in $\mathbb{X}_F$ with Lipschitz constant L_F. $F(0)=0$, and $\alpha_F(\|x\|) \le F(x) \le \beta_F(\|x\|)$ where α_F and β_F are $\mathscr{K}$ functions.*

Assumption 2.4.6 *For a given auxiliary (or called local) continuous control law $h_F : \mathbb{R}^n \to \mathbb{R}^m$, the following expressions hold:*

1. *h_F is Lipschitz continuous in X_F with Lipschitz constant L_{hf},*
2. *$h_F(\mathbb{X}_F) \in \mathbb{U}$,*
3. *$f(x,h_F(x)) \in \mathbb{X}_F$, and*
4. *$F(f(x,h_F(x))) - F(x) \le -l(x,h_F(x))$ for all $x \in \mathbb{X}_F$.*

The Assumption 2.4.4, and the conditions 2 and 3 in Assumption 2.4.6 imply $\mathbb{X}_F$ is an output admissible set for the closed-loop $f(x,h_F(x))$ system under the local control law h_F. The condition 4 in Assumption 2.4.6 implies that F is decreasing along the trajectory of closed-loop $f(x,h_F(x))$, which is required to prove the closed-loop stability.

The following theorem expresses the nominal stability of the closed-loop system (2.10).

Theorem 2.4.1 *[28, 32] Let Assumptions 2.4.1-2.4.6 hold. Then the origin is an asymptotically stable equilibrium point for the closed-loop system,*

$$x_{k+1} = f(x_k, h_{mpc}(x_k)),$$

with a region of attraction $\mathbb{X}_N$*. Further, if* $\alpha_l = a_l\|x\|^{b_l}$, $\beta_F = a_F\|x\|^{b_l}$*, for real positive* a_l, a_F*, and* b_l*, then the origin is an exponentially stable equilibrium point in* $\mathbb{X}_N$*.*

The proof of the theorem can be found in [28, 32] where $V_N(x)$, the value function, is shown as an Lyapunov function for the closed-loop (2.10) by showing that

$$\alpha_l(\|x\|) \leq V_N(x) \leq \beta_F(\|x\|) \tag{2.11a}$$

$$V_N(f(x, h_{mpc}(x))) - V_N(x) \leq -\alpha_l(\|x\|) \quad \forall\, x \in \mathbb{X}_N. \tag{2.11b}$$

In the view of Lemma (2.4.1), asymptotic and exponential stability can be proven.

For guaranteeing closed-loop stability, there are three main ingredients in the NMPC formulation (2.8) : 1) the terminal cost F, 2) the terminal set $\mathbb{X}_F$, and 3) the local control law h_F. Depending on the different selection of these three F, $\mathbb{X}_F$, and h_F, many techniques have been proposed to ensure the stability [34–40]. The formulation in [34] was first to propose the use of an equality constraint on the terminal state ($z_N = 0,\ i.e.\ \mathbb{X}_F = \{0\}$ in (2.8d)) to guarantee the stability of the closed-loop system, yet it faces some difficulties on implementation due to the requirement of exact satisfaction of nonlinear constraint, which is difficult and computationally expensive. The exact equality terminal constraint was therefore relaxed in a later development called the *dual-mode* MPC in [36]. In [36], the terminal state z_N is forced to stay inside some neighborhood of the origin $\mathbb{X}_{\mathbb{F}}$, i.e. $z_N \in \mathbb{X}_{\mathbb{F}}$. The basic idea of the dual-mode MPC is to apply the local stabilizing linear controller h_F inside the terminal set $\mathbb{X}_{\mathbb{F}}$ and the MPC law h_{mpc} outside the terminal set $\mathbb{X}_{\mathbb{F}}$, to guarantee the stability of the closed-loop system. In another development [37], the terminal cost F was proposed to add to the objective functional (2.8a) to ensure the closed-loop stability without the need of terminal constraint (2.8d). In this formulation, the finite horizon objective functional with the terminal cost F approximates the infinite horizon objective functional. Later, different ideas were proposed in the literature with the combination of all three components: the terminal cost F, the terminal set $\mathbb{X}_F$, and the local control law h_F. A key development called *quasi-infinite* horizon MPC was proposed in [39]. In the quasi-infinite horizon MPC technique, both the terminal constraint (2.8d) and the terminal cost F were employed to approximate the infinite horizon cost and to ensure the stability, respectively, yet the local controller h_F was not applied inside the terminal set $\mathbb{X}_F$.

Over the years, the classical Lyapunov stability theory has been applied to prove the stability of the closed-loop system with the MPC control law. The standard approach is to consider the value function as a candidate Lyapunov function for the closed-loop system [34], and to prove the stability, assuming that both the nonlinear system and value functions are continuous (see Assumptions 2.4.1 and 2.4.2). The requirements of the nonlinear system and value function for being continuous were questioned in [41]. In [41], stability was proven without requiring that the MPC control law for being continuous, but by assuming the continuity of the nonlinear system function on a neighborhood of the origin. It was shown [42] that the MPC technique sometimes need to produce a discontinuous control law in order to ensure the closed-loop stability.

2.5 Robust Stability of NMPC

In this section, the inherent robustness of the NMPC controller presented in section 2.4 is analyzed using the Input-to-State Stability (ISS) framework. The ISS definition [32, 43, 44] can be extended to analyze the stability of the system.

2.5.1 Inherent Robustness of NMPC

Consider the nominal system f (2.1a) with uncertainty as

$$\begin{aligned} x_{k+1} &= f(x_k,u_k) + g(x_k,u_k,w_k), \\ &:= f_{cl}(x_k,u_k,w_k), \qquad (2.12a) \\ & x_k \in \mathbb{X}, \quad u_k \in \mathbb{U}, \quad w_k \in \mathbb{W}, \quad k \geq 0, \qquad (2.12b) \end{aligned}$$

where $w_k \in \mathbb{R}^d$ is the disturbance vector, and $\mathbb{W} \subseteq \mathbb{R}^d$ is the compact uncertain region. $g : \mathbb{R}^n \times \mathbb{R}^m \times \mathbb{R}^d \to \mathbb{R}^n$ is the uncertain part of the system f and assumed to be Lipschitz continuous as follows.

Assumption 2.5.1 *The uncertain term $g(\cdot,\cdot,\cdot)$ is Lipschitz continuous with respect to all its arguments with Lipschitz constant $L_g \geq 0$ such that for all $(z_1, v_1), (z_2, v_2) \in \mathbb{Z}$, and $w_1, w_2 \in \mathbb{W}$, i.e.*

$$\|g(z_1, v_1, w_1) - g(z_2, v_2, w_2)\| \leq L_g \|(z_1, v_1, w_1) - (z_2, v_2, w_2)\|. \tag{2.13}$$

This system (2.12) is considered to be controlled by the NMPC control law (2.9). Then the closed loop can be written as

$$x_{k+1} = f_{cl}(x_k, h_{mpc}(x_k), w_k). \tag{2.14}$$

For robust stability analysis, the following definitions, assumptions, and lemmas, which are common in the NMPC stability analysis, have been used in this section.

Definition 2.5.1 *[43, 44] A set $\mathbb{X}_{rpi} \in \mathbb{X}_N$ is an admissible robust positive invariant (RPI) set for the system* (2.12) *if*

$$f_{cl}(x_k, \kappa(x), w_k) \in \mathbb{X}_{rpi}, \quad \forall\, x_k \in \mathbb{X}_{rpi}, \quad \forall\, w_k \in \mathbb{W}, \quad \text{and } k \geq 0. \tag{2.15}$$

with the control law $\kappa : \mathbb{R}^n \to \mathbb{R}^m$ defined by $u = \kappa(x)$. Correspondingly, $\mathbb{Z}_{RP} = \{(x, \mathbf{v}) | x \in \mathbb{X}_{rpi},$ and $w \in \mathbb{W}.\}$

Definition 2.5.2 *[43, 44] The closed-loop system f_{cl} is said to be ISS if there exists a $\mathscr{K}\mathscr{L}$ function $\gamma(\cdot,\cdot)$, and a $\mathscr{K}$ function $\delta(\cdot)$ such that,*

$$\|x_k\| \leq \gamma(x_0, k) + \delta(\|w\|), \quad \forall k \geq 0, \quad \forall w \in \mathbb{W}, \quad \forall x_0 \in \mathbb{X}_{rpi} \tag{2.16}$$

Furthermore, an ISS-Lyapunov function is defined for the closed-loop system as follows.

Definition 2.5.3 *[44] A function $V(\cdot)$ is called an ISS-Lyapunov for the system* (2.12a) *if there exists a set $\mathbb{N}$ containing the origin in its interior, $\mathscr{K}_\infty$ functions*

$\alpha_{v1}(\cdot), \alpha_{v2}(\cdot), \alpha_{v3}(\cdot)$, *and a* $\mathscr{K}$ *function* $\delta_{v1}(\cdot)$ *such that for all* $x \in \mathbb{N}$ *and all* $w \in \mathbb{W}$,

$$\begin{aligned} V(x) &\geq \alpha_{v1}(\|x\|) \\ V(x) &\leq \alpha_{v2}(\|x\|) \\ V(f_{cl}(x_k, \kappa(x_k), w_k)) - V(x, w) &\leq -\alpha_{v3}(\|x\|) + \delta_{v1}(\|w\|). \end{aligned} \tag{2.17}$$

Lemma 2.5.1 *(see [32, 43]) Let* $\mathbb{X}_{rpi}$ *be an admissible RPI set for the system* (2.12), *containing the origin, and* $V(\cdot)$ *be an ISS-Lyapunov function defined in* $\mathbb{X}_{rpi}$ *for the system* (2.12), *then the resulting closed-loop system is ISS in* $\mathbb{X}_{rpi}$.

The following theorem expresses the ISS property of the closed-loop system (2.14).

Theorem 2.5.1 *Let Assumptions 2.4.1 - 2.5.1 hold, then the closed-loop system* (2.14) *is ISS in an admissible RPI set* $\mathbb{X}_{rpi}$ *for any perturbation* $g(\cdot,\cdot,\cdot)$ *such that*

$$\|g(x, u_k, 0)\| \leq \frac{r}{L_v}\alpha_l(\|x\|) \tag{2.18}$$

where $r \in \mathbb{R}$ *and* $0 < r < 1$ *is an arbitrary real number.* L_v *is Lipschitz constant of* $V(\cdot)_N$ *in* (2.11).

The proof of the theorem can be found in [32] where it is shown that

$$V_N(f_{cl}(x_k, h_{mpc}(x_k), w_k)) - V_N(x, w) \leq -(1-r)\alpha_l(\|x_k\|) + L_v L_g \|w_k\| \tag{2.19}$$

Since the closed-loop system has nominal stability, the condition (2.11b) still holds. Therefore, according to Definition 2.5.3, $V_N(\cdot)$ is an ISS Lyapunov function for the closed-loop system. Then it can be concluded from Lemma 2.5.1 that the closed-loop system (2.14) is ISS at the origin.

2.5.2 Robust Design of NMPC

In addition to the inherent robustness of the closed-loop system, provided by the nominal NMPC framework, the designing of the NMPC techniques to ensure robust closed-loop stability of uncertain systems has gained much attention among researchers. These robust NMPC controller designing techniques should ensure 1) recursive feasibility, 2) robust constraint satisfaction, and 3) some closed-loop performance [44, 45]. In *min-max* approach, a H_∞ objective function is first maximized with respect to disturbances, and then minimized with respect to control moves over the horizon [46, 47]. Although it seems that the min-max approach is the general way to handle uncertain systems, they are computationally demanding. To overcome the computational complexity of min-max approaches, tightening constraints approaches are alternative methods where the robust stability is guaranteed by tightening the constraint of the nominal optimization problem for any admissible disturbances [48]. However, this approach can create to small constraint sets or even lead to infeasible problems [32] due to the exponential increase of the uncertainty margin with the increase of the prediction horizon. The tube based NMPC approach, *tube-NMPC*, is also a constraint tightening method. Compared to the min-max approaches, this method provides stronger robust stability and is computationally attractive [49, 50]. In tube-NMPC, a feedback auxiliary controller is utilized with the nominal controller in order to force the trajectory of the closed-loop uncertain system to be inside a tube centered with nominal trajectory. The discussion of robust NMPC designing techniques can be found in [51, 52].

2.6 Solution of NMPC Optimization Problem

One drawback of the NMPC technique is that it needs to repeatedly solve a nonlinear optimization problem at each sample time. Depending on the size of the problem, this could take a considerable amount of time without guarantee of a solution within a specified sample time. Therefore, the application of NMPC was restricted to slow processes at early stages of its development. NLP solvers can exploit a special structure of the NMPC problem to improve the computational performance. The NMPC problem has a special structure due to two main features: the sparsity of the problem and the availability of good initial solutions [53], [54]. One way of exploiting the block structure is to consider the system equations (output or/and state) as equality constraints in the NLP. Then the Hessian of the objective function and the Jacobian of constraints can be made sparse. In the absence of disturbance and setpoint changes, a feasible solution can be found using the solution of the problem at previous time samples, and this feasible solution can be considered as an initial solution to the current problem [54], [55]. In recent years, researchers have developed fast MPC algorithms such as explicit NMPC [56] and Newton-type controllers [57]. While the explicit NMPC algorithms are suitable for systems with few states, the on-line NMPC algorithms such as Newton-type controllers are more efficient alternatives for large systems [58]. In this work, The IPOPT solver presented in [59] is used to solve the resulting NLP problem of the NMPC formulation (2.8), and the computational burden is further improved with the asNMPC concept presented in [58].

2.6.1 IPOPT

IPOPT uses a primal-dual interior-point algorithm, with a filter line-search strategy, to solve the general form of NLP problem as

$$\min_{w} \quad f(w) \tag{2.20a}$$

$$\text{s. t. :} \quad c(w) = 0, \tag{2.20b}$$

$$w \geq 0, \tag{2.20c}$$

where $w \in \mathbb{R}^n$ is variable vector. $f : \mathbb{R}^n \to \mathbb{R}$ and $c : \mathbb{R}^{n_c} \to \mathbb{R}^{m_c}$, with $m_c \leq n_c$, are the objective function and the equality constraints, which are assumed to be twice continuously differentiable. In the context of NMPC formulation, the resulting NLP problem $P_N(k)$ (2.8) can be recast in the form of

$$\min_{w} \quad f(w, \theta) \tag{2.21a}$$

$$\text{s. t. :} \quad c(w, \theta) = 0, \tag{2.21b}$$

$$w \geq 0, \tag{2.21c}$$

where θ is a parameter vector, and $\theta \equiv x_k$ where x_k is the initial state variable vector at k^{th} sample time. Note that the sample time dependence is omitted in the equations. IPOPT computes a series of approximate solutions to a sequence of barrier problems

$$\min_{w} \quad f(w,\theta) - \delta \sum_{j=1}^{n_c} \ln(w^j)) \tag{2.22a}$$

$$\text{s. t. :} \quad c(w,\theta) = 0, \tag{2.22b}$$

with a decreasing sequence of barrier parameters, $\delta \to 0$. The barrier terms, $\ln(w^j)$ where w^j denotes the j^{th} component of the vector w, are added to the objective function in order to handle the inequality constraints (2.21c). With a fixed value of δ, the IPOPT first computes an approximate solution to the barrier problem (2.22) by solving the Karush-Kuhn-Tucker (KKT) conditions:

$$\nabla_w f(w,\theta) + \nabla_w c(w,\theta)\lambda - \eta = 0 \tag{2.23a}$$

$$c(w,\theta) = 0 \tag{2.23b}$$

$$ENe - \delta e = 0 \tag{2.23c}$$

where $\lambda \in \mathbb{R}^{m_n}$ and $\eta \in \mathbb{R}^{n_c}$ are Lagrange multipliers for the equality constraints and the bound constraints, respectively. Here $E = diag(w)$ and $N = diag(\eta)$ are diagonal matrices, and $e = [1,1,\cdots,1]^T$ is vector of ones. Then by decreasing the barrier parameter, a new barrier problem is solved with the approximate solution of the previous problem. IPOPT solves each barrier problem using Newton's method for nonlinear equations applied to the KKT conditions (2.23). Let us consider a fixed value of δ_k, and an iteration i, $(w_i(\theta), \lambda_i(\theta), \eta_i(\theta))$, of the Newton step. Then the search directions $(\Delta w_i, \Delta\lambda_i, \Delta\eta_i)$ are obtained by solving following system of linear equations.

$$\begin{bmatrix} H_i & A_i & -I \\ A_i^t & 0 & 0 \\ N_i & 0 & E_i \end{bmatrix} \begin{bmatrix} \Delta w_i \\ \Delta\lambda_i \\ \Delta\eta_i \end{bmatrix} - \begin{bmatrix} \nabla_w f(w_i,\theta) + A_i\lambda_i \\ c(w_i,\theta) \\ E_i N_i e - \delta_k e \end{bmatrix} = 0, \tag{2.24}$$

where the matrix $H_i = \nabla^2_{ww} L(w_i, \lambda_i, \eta_i)$ is the Hessian of the Lagrange function $L = f(w,\theta) + c(w,\theta)^T\lambda - \eta^T w$, and the matrix $A_i = \nabla c(w_i,\theta)$ is the Jacobian of the constraint (2.21c). I and 0 denote identity and zero matrices with appropriate dimensions. Let us denote

$$s_k^* = [w^*(\theta)^T, \lambda^*(\theta)^T \eta^*(\theta)^T], \tag{2.25}$$

the solution for the linear system when $\delta = 0$ at a fixed parameter value θ. The above description is a basic formulation of the IPOPT solver, and more details can be found in [59].

2.6.2 asNMPC

The asNMPC algorithm consists of two main steps: 1) solving a nominal NLP problem in advance, and 2) updating the nominal solution with new information. Suppose at sample time k the control action u_k is known. Then the next state z_{k+1} of the process can be predicted through a forward simulation of the process model (2.8b), and solve the predicted nominal problem $P_N(k+1|k)$ with $\theta = \theta_0 = z_{k+1}$. With this strategy, the control policy for $k+1$ sample time, $\mathbf{v}^*(k+1|k)$, is readily available when time reaches $k+1$, provided that the predicted nominal problem $P(k+1|k)$ can be solved within a sample time. In the presence of disturbances there is a mismatch between the predicted state z_{k+1} and actual state x_{k+1}. The asNMPC algorithm then updates the nominal solution

$$s_{k+1|k}^* = [w^*(\theta_0)^T, \lambda^*(\theta_0)^T \eta^*(\theta_0)^T], \tag{2.26}$$

by solving the perturbed KKT system with $\theta = x_{k+1}$

$$K^*(\theta_0)\Delta s(\theta) = -\varphi(s_{k+1|k}^*, \theta). \tag{2.27}$$

The above equation is closely related to (2.24) where $K^*(\theta_0)$ is the KKT matrix evaluated at θ_0 and $s_{k+1|k}^*$. The vector $\varphi(s_{k+1|k}^*, \theta)$ has the same form as in (2.24) but is evaluated at $s_{k+1|k}^*$ and $\theta = x_{k+1}$. With the assumption that the active-set at the nominal solution is as for the perturbed system, the factorization of the KKT matrix is readily available for the above system from (2.24). As a result, a fast approximate solution can be computed to the problem with a single back-solve. This section presents only a basic description of the method. Detailed discussion about optimality, stability and robustness of asNMPC formulation can be found in [58, 60].

2.7 Conclusion

This chapter provides the basics of NMPC formulation, establishing a foundation for processes that will be discussed in the following chapters. First, the basic idea of receding horizon control is depicted. Next, a mathematical representation of NMPC formulation is presented, along with their basic assumptions. Finally, nominal and robust stability of NMPC concepts are introduced. In particular, inherent robustness of the nominal NMPC technique and designing robust NMPC methods are discussed for uncertain nonlinear systems. The basic formulation of the IPOPT solver is presented to solve the resulting NLP problem of NMPC. Using the as-NMPC concept, a fast approximation of the NLP problem is sought with aims to reduce the on-line computational time.

Chapter 3

Economically Oriented NMPC

3.1 Summary

In this chapter, an economically oriented process control technique is presented. The NMPC framework discussed in Chapter 2 is utilized to explicitly consider an economical objective function in the formulation. The nominal and robust stability properties are discussed for a nonlinear system with the infinite horizon econNMPC technique.

3.2 Introduction

The economical operation of a process is usually conducted using an advanced control system with a two-layer structure. The conventional two-layer structure consists of a higher layer to implement RTO, followed by a lower layer to track the setpoint. The RTO layer computes optimal steady-state setpoints using a steady-state process model, and provides them to the setpoint tracking layer in order to maximize an economical objective while keeping product quality constraints within safe values. The setpoint tracking layer uses advanced control strategies, most commonly NMPC techniques. The conventional two layer structure has some drawbacks mainly due to 1) low frequency of operation of the RTO layer, and 2) assumption of slow variation of the disturbances on the process [15]. Due to the use of nonlinear steady-state modeling of the process in the RTO layer, the resulting constrained optimization problem can take considerable amount of time. Therefore, it might not be able to operate simultaneously with the NMPC dynamic optimization layer. The slow variation of disturbances during setpoint update is also not a valid assumption in many industrial processes.

Literature on this topic generally discusses few alternatives to this two layers approach. The basic idea is to recalculate or modify the setpoints using less-detailed steady-state process models, most commonly linear models within the lower-level [61]. This modification can be performed with a separate optimization within the setpoint tracking layer or can be integrated with the dynamic optimization problem in NMPC formulation [62]. The main issues with the application of NMPC with detailed nonlinear models are due to computational burden and lack of theoretical support for stability [63, 64]. However, with the increase of computational power and development of efficient Nonlinear Programing (NLP) solvers, the economical objective and setpoint tracking objective tasks could be simultaneously implemented with a single layer, with detailed nonlinear models in the advanced control system [65–68]. With an application of economical objective function of specific energy, we have recently demonstrated a potential reduction of about 13% in total specific energy for a two-stage TMP process in a simulation study [67]. In another simulation study [69], a cost reduction of about 30% has been realized for an air separation unit by taking into account the periodically changing electricity price. Practical economical benefits are discussed in [70–72] for optimal operation of processes. Although the stability theories of these economically oriented NMPC techniques are still in early stages, there are interesting developments in the literature [29, 69, 73–76]. Nominal stability properties of two economically oriented NMPC schemes for cyclic processes are presented in [69], and robust stability of economically oriented infinite horizon NMPC is presented in [74]. A discount factor, which projects future profit to the present value, is introduced in [77] for NMPC formulation to maximize the net present value of the economical objective function. In our recent paper [69], nominal stability of infinite horizon NMPC with a discount factor for cyclic processes was proved by introducing a transformed system. In this chapter, a general infinite horizon NMPC technique is discussed with an economic objective, and more work on this topic can be found in [69, 74].

3.3 Infinite Horizon economically oriented NMPC (econNMPC)

Consider a discrete time nonlinear system described by

$$x_{k+1} = f(x_k, u_k), \quad k \geq 0, \tag{3.1a}$$

subject to the control and state constraints,

$$u_k \in \mathbb{U} \quad \text{and} \quad x_k \in \mathbb{X}, \tag{3.1b}$$

where $x \in \mathbb{R}^n$ and $u \in \mathbb{R}^m$ are the state and control variable vectors of the system, respectively. $\mathbb{U} \subseteq \mathbb{R}^m$ is the control constraint set, and $\mathbb{X} \subseteq \mathbb{R}^n$ is the state constraint set. $f : \mathbb{R}^n \times \mathbb{R}^m \to \mathbb{R}^n$ is the nominal nonlinear system function, and k is the sample time. In a sequel, z and v are denoted as the predicted state and control vectors, respectively, by the model f.

In the econNMPC framework, the following performance index $J : \mathbb{R}^n \times \mathbb{R}^m \to \mathbb{R}^1$ is considered with a general economic stage cost functional $l : \mathbb{R}^n \times \mathbb{R}^m \to \mathbb{R}^1$, for the system (3.1a) - (3.1b).

$$J(x_{(\cdot)}, u_{(\cdot)}) = \lim_{N \to \infty} \frac{1}{N} \sum_{k=0}^{N} l(x_k, u_k). \tag{3.2}$$

The objective of the infinite horizon optimal control problem at the k^{th} sample time is to find a control law $u_k = h(x_k)$ where $h : \mathbb{R}^n \to \mathbb{R}^m$, by minimizing the performance index J subject to the nonlinear dynamic system (3.1a), and the state and control constraints (3.1b), such that the closed-loop system (3.3) is feasible.

$$x_{k+1} = f(x_k, h(x_k)). \tag{3.3}$$

This infinite horizon optimal control problem is referred as P_∞, assuming that there exists a unique optimum steady-state (x^*, u^*) such that $l(x^*, u^*) < l(x_k, u_k)$, $(x_k, u_k) \neq (x^*, u^*)$, for all $u_k \in \mathbb{U}$, $x_k \in \mathbb{X}$. Further, the following assumptions are made in this chapter, as discussed in [29, 69].

Assumption 3.3.1 *$f(\cdot,\cdot)$ and $l(\cdot,\cdot)$ are Lipschitz continuous on the admissible set $\mathbb{Z}_N$ (see Definition 2.4.1. Here, $\mathbb{Z}_N$ is defined accordingly for the problem P_∞), with Lipschitz constants L_f and $L_l \geq 0$ such that for all (z_1, v_1), $(z_2, v_2) \in \mathbb{Z}_N$, i.e.*

$$\begin{aligned} \|f(z_1,v_1) - f(z_2,v_2)\| &\leq L_f\|(z_1,v_1) - (z_2,v_2)\| \\ \|l(z_1,v_1) - l(z_2,v_2)\| &\leq L_l\|(z_1,v_1) - (z_2,v_2)\| \end{aligned} \tag{3.4}$$

Assumption 3.3.2 *There exists a $\mathscr{K}_\infty$ function $\gamma(\cdot)$ such that for every state $x \in \mathbb{X}_N$, where $\mathbb{X}_N$ is the admissible state set (see Definition 2.4.1. Here, $\mathbb{X}_N$ is defined accordingly for the problem P_∞), there exists $\mathbf{u}$ such that $(x, \mathbf{u}) \in \mathbb{Z}_N$ and*

$$\sum_{k=0}^{N-1} \|u_k - u^*\| \leq \gamma(\|x - x^*\|), \tag{3.5}$$

and $(x_k, u_k) = (x^*, u^*)$ for all $k \geq N$. The Assumption 3.3.2 means that some degree of system controllability is needed [29, 34]; starting from an initial state x, the system can be steered to the steady-state in N steps with a bounded input sequence, while satisfying the input and state constraints.

In the following section, an econNMPC is presented with a modified stage cost.

The econNMPC with a Regularization Term

In this section, an econNMPC problem is formulated with a regularization term in the economic stage as

$$\min_{(z_i,v_i)} \sum_{i=0}^{\infty} l(z_i,v_i) + \|z_i - z_{i+1}\|_Q^2 + \|v_i - v_{i+1}\|_R^2 \tag{3.6a}$$

$$\text{s.t.}: \quad z_{i+1} = f(z_i, v_i) \tag{3.6b}$$

$$z_0 = x_k \tag{3.6c}$$

$$z_i \in \mathbb{X}, \quad \text{and} \quad v_i \in \mathbb{U},\ i = 1, \ldots, \infty. \tag{3.6d}$$

The regularization terms $\|z_i - z_{i+1}\|_Q^2 + \|v_i - v_{i+1}\|_R^2$, where Q and R are positive definite weighting matrices, force the system to converge to a steady-state. And also, it ensures the optimization problem (3.6) is well-posed and the solution is locally unique. The discussion on strong convexity requirement for the stage cost can be found in our recent paper [74]. The following assumption states the well-posedness of the problem (3.6) [78].

Assumption 3.3.3 *The constrained optimization problem* (3.6) *satisfies the Linear Independent Constraint Qualification (LICQ), Sufficient Second order Condition (SSOC), and Strict Complementarity (SC) at the solution.*

3.4 Nominal Stability of the econNMPC

The nominal stability of the econNMPC is analyzed in this section. The notion of transformed system [69] is considered and nominal stability is proved using Lyapunov stability theory. The transformed system is defined by subtracting the optimal steady-state from the original system (3.1a)-(3.1b) as

$$\bar{z}_{i+1} = f(\bar{z}_i + x^*, \bar{v}_i + u^*) - x^* := \bar{f}(\bar{z}_i, \bar{v}_i), \tag{3.7}$$

$$\bar{v}_i \in \bar{\mathbb{U}} \quad \text{and} \quad \bar{z}_i \in \bar{\mathbb{X}}, \tag{3.8}$$

where $\bar{v}_i = v_i - u^*$ and $\bar{z}_i = z_i - x^*$. $\bar{f} : \mathbb{R}^n \times \mathbb{R}^m \to \mathbb{R}^n$ is the nominal transformed nonlinear system function. $\bar{\mathbb{U}} \subseteq \mathbb{R}^m$ and $\bar{\mathbb{X}} \subseteq \mathbb{R}^n$ are corresponding constrained sets for the transformed variables $\bar{z}$ and $\bar{v}$, respectively. Here it can be seen that when $(\bar{z}_i, \bar{v}_i) \to (0,0)$, then $(z_i, v_i) \to (x^*, u^*)$, i.e. the original system will converge to the optimal steady-state (x^*, u^*) if the transformed system is steered from an initial state to 0. The nominal stability of the original system is proved using Lemma (3.4.1).

Lemma 3.4.1 *(see [69]) The stability of the transformed system* (3.7) *at* $(0,0)$ *is equivalent to the stability of the original closed-loop system* (3.1a) *at the steady-state* (x^*, u^*).

Further, the original objective function (3.6a) is modified to have the transformed objective as

$$
\begin{aligned}
V_\infty(\bar{x}_k) &= \sum_{i=0}^{\infty} L_i(\bar{z}_i, \bar{v}_i) \\
&:= \sum_{i=0}^{\infty} l(\bar{z}_i + x^*, \bar{v}_i + u^*) - l(x^*, u^*) + \\
&\qquad \|(z_i - x^*) - (z_{i+1} - x^*)\|_Q^2 + \|(v_i - u^*) - (v_{i+1} - u^*)\|_R^2 \\
&= \sum_{i=0}^{\infty} \bar{l}(\bar{z}_i, \bar{v}_i) + \|(z_i - x^*) - (z_{i+1} - x^*)\|_Q^2 + \|(v_i - u^*) - (v_{i+1} - u^*)\|_R^2,
\end{aligned}
\tag{3.9}
$$

where $\bar{x}_k = x_k - x^*$ at sample time k, and $\bar{l} = l(\bar{z}_i + x^*, \bar{v}_i + u^*) - l(x^*, u^*)$. Similar to the original system, the following assumptions are made on Lipschitz continuity and weak controllability for the transformed system.

Assumption 3.4.1 *$\bar{f}(\cdot,\cdot)$ and $L_i(\cdot,\cdot)$ are Lipschitz continuous on the admissible set of the transformed system, $\bar{\mathbb{Z}}_N$, with Lipschitz constants $L_{\bar{f}}$ and $L_L \geq 0$ such that for all (z_1, v_1), $(z_2, v_2) \in \bar{\mathbb{Z}}_N$, i.e.*

$$
\begin{aligned}
\|\bar{f}(z_1, v_1) - \bar{f}(z_2, v_2)\| &\leq L_{\bar{f}} \|(z_1, v_1) - (z_2, v_2)\| \\
\|L_i(z_1, v_1) - L_i(z_2, v_2)\| &\leq L_L \|(z_1, v_1) - (z_2, v_2)\|.
\end{aligned}
\tag{3.10}
$$

Assumption 3.4.2 *There exists a $\mathcal{K}_\infty$ function $\gamma_\infty(\cdot)$ such that for every state $\bar{x} \in \bar{\mathbb{X}}_N$, there exists $\bar{\mathbf{u}}$ such that $(\bar{x}, \bar{\mathbf{u}}) \in \bar{\mathbb{Z}}_N$ and*

$$
\sum_{k=0}^{N-1} \|\bar{u}_k\| \leq \gamma_\infty(\|\bar{x}\|),
\tag{3.11}
$$

where $\bar{\mathbf{u}}$ is a feasible input sequence, and $\bar{\mathbb{X}}_N$ is the admissible state set for the transformed system, respectively.

The validity of Assumptions 3.4.1 and 3.4.2 can be easily seen in the view of Assumptions 3.3.1 and 3.3.2, respectively. The Assumption 3.4.2 means that starting from an initial state $\bar{x}$, the transformed system can be steered to $(0,0)$

in N steps with a bounded input sequence, while satisfying the input and state constraints of the transformed system. For this particular feasible solution $(\hat{z}_i, \hat{v}_i)$, the expression (3.12) holds.

$$L_i(\hat{z}_i, \hat{v}_i) = 0 \quad i \geq N \tag{3.12}$$

Furthermore, Assumption 3.4.3 is made on the transformed stage cost $L_i(\cdot,\cdot)$.

Assumption 3.4.3 *There exits a $\mathscr{K}_\infty$ function $\beta_\infty(\cdot)$ such that the stage cost $L_i(\cdot,\cdot)$ defined in* (3.9)*, satisfies*

$$L_i(\bar{z}, \bar{v}) \geq \beta_\infty(\|\bar{z} - 0\|). \tag{3.13}$$

Note that Assumption 3.4.3 may not hold for general economic objective functions. An alternative approach, a modification of $L_i(\bar{z}, \bar{v})$, is proposed using rotated stage cost in [29] while a generalization of that is developed in our recent paper [74].

The constrained optimization problem in the transformed econNMPC formulation is expressed as

$$\min_{(\bar{z}_i, \bar{v}_i)} \sum_{i=0}^{\infty} L_i(\bar{z}, \bar{v}) \tag{3.14a}$$

$$\text{s.t}: \quad \bar{z}_{i+1} = \bar{f}(z_i, v_i) \tag{3.14b}$$

$$\bar{z}_0 = x_k - x^* \tag{3.14c}$$

$$\bar{z}_i \in \bar{\mathbb{X}}, \quad \text{and} \quad \bar{v}_i \in \bar{\mathbb{U}},\ i = 1, \ldots, \infty. \tag{3.14d}$$

The following theorem expresses asymptotic stability of the nominal system at the optimal steady-state (x^*, u^*) in the view of asymptotic stability of the transformed system at origin $(0,0)$.

Theorem 3.4.1 *Let Assumptions 3.3.1 - 3.4.3 hold, then at time step k, the value function $V_\infty(\bar{x}_k)$ defined by* (3.9) *is a Lyapunov function, and the transformed system* (3.7) *is asymptotically stable at $(0,0)$ with the controller based on* (3.14)*. Consequently, the original closed-loop system controlled by the econNMPC* (3.6) *is asymptotically stable at the optimal steady-state (x^*, u^*).*

The proof of the Theorem 3.4.1 is given in [69]. That $V_\infty(\bar{x}_k)$ is a Lyapunov function for the transformed system is proven in [69], by showing

$$\beta_\infty(\|\bar{x}_k\|) \leq V_\infty(\bar{x}_k) \leq \alpha_\infty(\|\bar{x}_k\|), \tag{3.15}$$

$$V_\infty(\bar{f}(\bar{x}_k, \bar{u}_k)) - V_\infty(\bar{x}_k) \leq -\beta_\infty(\|\bar{x}_k\|), \tag{3.16}$$

where $\alpha_\infty(\cdot)$ is a $\mathscr{K}_\infty$ function. In the view of Lemma (3.4.1), the proof is completed for the original system. Further, $V_\infty(\cdot)$ is Lipschitz continuous with Lipschitz constant $L_v \geq 0$.

3.5 Robust Stability of the econNMPC

In this section, the inherent robustness of the econNMPC controller presented in the previous section is analyzed using the ISS framework. Consider the nominal system f with uncertainty as

$$\begin{aligned} x_{k+1} &= f(x_k, u_k) + g(x_k, u_k, w_k) \\ &:= h(x_k, u_k, w_k), \\ & x_k \in \mathbb{X}, \quad u_k \in \mathbb{U}, \quad w_k \in \mathbb{W}, \end{aligned} \tag{3.17}$$

where $w_k \in \mathbb{R}^d$ is the disturbance vector, and $\mathbb{W} \subseteq \mathbb{R}^d$ is the compact uncertain region. $g : \mathbb{R}^n \times \mathbb{R}^m \times \mathbb{R}^d \to \mathbb{R}^n$ is the uncertain part of the system f, and the Lipschitz continuity of g is assumed with respect to all its arguments, as follows.

Assumption 3.5.1 *The uncertain term $g(\cdot,\cdot,\cdot)$ is Lipschitz continuous with respect to all its arguments with Lipschitz constant $L_g \geq 0$ such that $\forall\ (z_1, v_1), (z_2, v_2) \in \mathbb{Z}$, and $w_1, w_2 \in \mathbb{W}$, i.e.*

$$\|g(z_1, v_1, w_1) - g(z_2, v_2, w_2)\| \leq L_g \|(z_1, v_1, w_1) - (z_2, v_2, w_2)\|. \tag{3.18}$$

The transformed system can be defined for the system (3.17), similar to the nominal system in (3.7),

$$\begin{aligned}\bar{x}_{k+1} &= f(\bar{x}_k + x^*, \bar{u}_k + u^*) + g(\bar{x}_k + x^*, \bar{u}_k + u^*, w_k) \\ &= \bar{f}(\bar{x}_k, \bar{u}_k) + \bar{g}(\bar{x}_k, \bar{u}_k, w_k) \\ &:= \bar{h}(\bar{x}_k, \bar{u}_k, w_k),\end{aligned} \tag{3.19}$$

where $\bar{g} : \mathbb{R}^n \times \mathbb{R}^m \times \mathbb{R}^d \to \mathbb{R}^n$ is the uncertainty part of the transformed system $\bar{f}$, and $\bar{g}(\bar{x}_k, \bar{u}_k, w_k) = g(\bar{x}_k + x^*, \bar{u}_k + u^*, w_k)$. The transformed nominal system $\bar{f}(\cdot,\cdot)$ is Lipschitz continuous with the Lipschitz constant $L_{\bar{f}} \geq 0$ (3.4.1). In the view of Assumptions (3.3.1) and (3.5.1), it can be seen that $\bar{g}(\cdot,\cdot)$ is also Lipschitz continuous with the Lipschitz constant $L_{\bar{g}}$ for all (z_1, v_1), $(z_2, v_2) \in \mathbb{Z}_N$, and $w_1, w_2 \in \mathbb{W}$, such that

$$\|\bar{g}(\bar{z}_1, \bar{v}_1, w_1) - \bar{g}(\bar{z}_2, \bar{v}_2, w_2)\| \leq L_{\bar{g}} \|(\bar{z}_1, \bar{v}_1, w_1) - (\bar{z}_2, \bar{v}_2, w_2)\|. \tag{3.20}$$

For the robust stability analysis of the transformed system (3.19), the following definitions and lemmas which are adopted for the transformed system are used.

Definition 3.5.1 *(Robust positively invariant set: Transformed system) [32, 43, 44] A set* $\bar{\mathbb{X}}_N$ *is a RPI set for the transformed system* (3.19) *if* $\bar{h}(\bar{x}_k, \bar{u}_k, w_k) \in \hat{\mathbb{X}}_N$, *for all* $\bar{x}_k \in \hat{\mathbb{X}}_N$, $w_k \in W$.

The ISS definition [32, 43, 44] can be extended to analyze the stability of the transformed system.

Definition 3.5.2 *(Input-to-state stability: Transformed system) [74] The transformed closed-loop system, the system* (3.19) *controlled by the controller* (3.14), *is said to be ISS if there exits a* $\mathscr{K}\mathscr{L}$ *function* $\gamma_s(\cdot,\cdot)$*, and a* $\mathscr{K}$ *function* $\delta(\cdot)$ *such that,*

$$\|\bar{x}_k\| \leq \gamma_s(\bar{x}_0, k) + \delta(\|w\|), \forall k \geq 0,\ \forall \bar{x}_0 \in \hat{\mathbb{X}}_N. \tag{3.21}$$

Further, ISS-Lyapunov function is defined for the transformed system as follows.

Definition 3.5.3 *(ISS-Lyapunov function: Transformed system) [74] A function* $V_\infty(\cdot)$ *is called an ISS-Lyapunov for the transformed system* (3.19) *if there exists a RPI set* $\hat{\mathbb{X}}_N$ *containing the origin in its interior,* $\mathscr{K}_\infty$ *functions* $\alpha_1(\cdot), \alpha_2(\cdot), \alpha_3(\cdot)$ *and* $\delta_1(\cdot)$ *such that* $\forall \bar{x} \in \hat{\mathbb{X}}_N$ *and* $\forall w \in W$*,*

$$\begin{aligned} V_\infty(\bar{x}) &\geq \alpha_1(\|\bar{x}\|) \\ V_\infty(\bar{x}) &\leq \alpha_2(\|\bar{x}\|) \\ \Delta V_\infty(\bar{x}, w) = V_\infty(\bar{h}(\bar{x}, \bar{u}, w)) - V_\infty(\bar{x}) &\leq -\alpha_3(\|\bar{x}\|) + \delta_1(\|w\|). \end{aligned} \tag{3.22}$$

Lemma 3.5.1 *(see [32, 43]) Let* $\hat{\mathbb{X}}_N$ *be a RPI set for the transformed system* (3.19)*, containing the origin, and let* $V_\infty(\cdot)$ *be an ISS-Lyapunov function for the transformed system* (3.19)*, then the resulting closed-loop system is ISS in* $\hat{\mathbb{X}}_N$*.*

Similar to Lemma (3.4.1), the ISS of the original closed-loop system, the system (3.1a) controlled by the controller (3.6), can be investigated using Lemma (3.5.2).

Lemma 3.5.2 *(see [74]) The ISS stability of the transformed closed-loop system, the system* (3.19) *controlled by the controller* (3.14)*, at* 0 *is equivalent to the ISS stability of the original closed-loop system at the optimal steady-state* (x^*, u^*) *when* $\bar{x} \in \hat{\mathbb{X}}$, $x \in \mathbb{X}$*, and* $w \in \mathbb{W}$*.*

The following theorem expresses the robust stability property of the original closed-loop system.

Theorem 3.5.1 *Let Assumptions 3.3.1 - 3.5.1 hold, then the transformed closed-loop system is ISS in* $\hat{\mathbb{X}}_N$ *for any perturbation* $\bar{g}(\cdot,\cdot,\cdot)$ *such that*

$$\|\bar{g}(\bar{x}, \bar{u}_k), 0\| \leq \frac{r}{L_v}\beta_\infty(\|\bar{x} - 0\|) \tag{3.23}$$

where $r \in \mathbb{R}$ *and* $0 < r < 1$ *is an arbitrary real number. Then from Lemma 3.5.2, the original closed-loop system is ISS at the optimal steady-state* (x^*, u^*)*.*

Proof 3.5.2 *Since the original system has the nominal stability, the inequalities* (3.15) *still holds. With the Lipschitz continuity of* $V_\infty(\cdot)$ *for the transformed system, it can be seen that*

$$\begin{aligned} V_\infty(\bar{h}(\bar{x}_k,\bar{u}_k,w_k)) - V_\infty(\bar{x}_k) &= V_\infty(\bar{h}(\bar{x}_k,\bar{u}_k,w_k)) - V_\infty(\bar{f}(\bar{x}_k,\bar{u}_k)) + V_\infty(\bar{f}(\bar{x}_k,\bar{u}_k)) - V(\bar{x}_k) \\ &\leq L_v\|\bar{g}(\bar{x}_k,\bar{u}_k,w_k)\| - \beta_\infty(\|\bar{x}_k - 0\|), \end{aligned}$$

from (3.20) *and* (3.23),

$$\begin{aligned} V_\infty(\bar{h}(\bar{x}_k,\bar{u}_k,w_k)) - V(\bar{x}_k) &\leq L_v\|\bar{g}(\bar{x}_k,\bar{u}_k,0)\| + L_v l_{\bar{g}}\|w_k\| - \beta_\infty(\|\bar{x}_k - 0\|) \\ &\leq r\beta_\infty(\|\bar{x}_k - 0\|) + L_v l_{\bar{g}}\|w_k\| - \beta_\infty(\|\bar{x}_k - 0\|) \\ &\leq -(1-r)\beta_\infty(\|\bar{x}_k - 0\|) + L_v l_{\bar{g}}\|w_k\| \end{aligned} \tag{3.24}$$

Hence, according to Definition 3.5.3, $V_\infty(\cdot)$ *is an ISS Lyapunov function for the transformed system. Then the transformed system is ISS at* $(0,0)$*. In the view of Lemma 3.5.2, the original system is ISS at the optimal steady-state* (x^*,u^*)

3.6 Conclusion

An econNMPC formulation with a general cost function is presented in this chapter. The economical objective function is modified by adding regularization terms. The regularization terms enforce strong convexity of the stage cost and also force the system to a steady-state. The nominal and robust stability of the econNMPC are proven by considering the value function as a Lyapunov function. More general results of the econNMPC can be found in [69, 74], where the nonlinear systems with cyclic behavior have been considered. The analysis in this Chapter will provide the theoretical basis for the following Chapters 5 and 6 where optimal operation of thermo mechanical pulping processes is performed by using the economically oriented NMPC framework.

Chapter 4

Closed-loop Identification with Constrained MPC

4.1 Summary

In this chapter, two closed-loop identification schemes, which can be applied to a LTI system controlled by a constrained MPC law, are developed. In the first scheme, the *informativity* of the normal operational closed-loop data is analyzed, and a criterion is presented on the closed-loop data set for applying the *direct* identification technique with the Prediction Error Method (PEM). In the second scheme, a joint input-output, the *two-stage method* for closed-loop identification, is discussed. In the first stage of two-stage identification method, the proper component in the control signal is extracted by using the projection method while in the second stage, a model is identified with the use of the PEM. Furthermore, the Long Range Predictive Identification (LRPI) criterion is utilized in the second stage of identification to obtain a better model estimate.

4.2 Introduction

Performance of a closed-loop system with a model based controller mainly depends on the internal model used in the controller; when the accuracy of the process model depreciates, the performance deteriorates greatly [79]. In the case of MPC, the performance mainly depends on the process model to predict the future outputs/states of the process. In practice, the process model is first identified using open-loop identification methods in the commissioning stage, then a stabilizing and well-performing MPC is setup for the process. With time, the performance of the closed-loop gracefully degrades mainly due to a different dynamic behavior of the process, caused by wear and tear or other physical changes in the process [80]. Therefore, to keep the closed-loop system performance at the desired level, it may be necessary to carry out the re-commissioning on a periodic basis [81]. However, these re-commissioning stages can be lengthy and costly; the cost of process modeling is around 75% of the total costs associated with advanced process control projects [79, 82]. Moreover, the open-loop test can not be performed during the operation of a process due to the production commitment. To avoid opening the closed-loop and performing the re-commissioning, closed-loop identification should be applied to the system to identify the process model during the normal operation.

In general, closed-loop identification techniques can be categorized into three main groups, based on assumptions on the feedback mechanism and the type of the controller [83–85]:

1. *Direct identification* uses PEM to identify the open-loop system with the input-output data ignoring any effect of feedback, as in the open-loop case. This approach, when it works, is the simplest and the most attractive one, as it does not need any special identification algorithm.

2. *Indirect identification* consists of two steps: first, identification of either the closed-loop system with the use of measured external independent excitation input (or reference) and output data [86], or sensitivity function with the use of measured input-output data. The open-loop model is then determined using the knowledge of the linear feedback.

3. *Joint input-output identification* assumes that the input is generated using a certain form of the controller, but the exact knowledge of the controller is not necessary. This approach regards both the control and output signals together as the *joint outputs* of the independent *joint inputs* consists of process excitation or reference signal, and the process noise. The joint input-output identification method first extracts the excitation or reference signal component in the control signal, then uses this extracted signal and the output data to fit a process model.

The indirect identification method heavily depends on linearity of the controller though it can be applied to known nonlinear controller with the considerable amount of work [84]. The constrained MPC is usually nonlinear [54]. In this chapter, first an informativity criterion for normal operation data, which is generated by MPC, is analyzed for direct closed-loop identification method. Next, the joint input-output methods, particularly the projection method in which the controller can be nonlinear [87], are studied for closed-loop identification.

4.3 Output Feedback MPC

In this chapter, output feedback MPC for an LTI discrete-time Single-Input Single-Output (SISO) process (4.1) is considered.

$$y_k = G(z)u_k + n_k, \tag{4.1a}$$

$$n_k = H(z)e_k, \quad k \geq 0, \tag{4.1b}$$

where $G(z)$ and $H(z)$ are the process and noise transfer functions, respectively. $u_k \in \mathbb{R}$ and $y_k \in \mathbb{R}$ are the control input and the process output, respectively. $e_k \in \mathbb{R} \sim N(0, \sigma_e^2)$ is a Gaussian white noise signal with the variance σ_e^2. Both $G(z)$ and $H(z)$ are rational and proper functions. Further, $H(z)$ is inversely stable. The internal model, a model of the process (4.1), which is used in the MPC formulation is given by

$$\hat{y}_k = \hat{G}(z)\hat{u}_k + \hat{n}_k, \tag{4.2a}$$

$$\hat{n}_k = \hat{H}(z)\hat{e}_k, \tag{4.2b}$$

where $\hat{G}(z) = z^{-d}\frac{B(z)}{A(z)}$ is the model transfer function. $H(z) = \frac{C(z)}{D(z)}$ is the inversely stable model noise filter. The degrees of the polynomials A, B, C, and D are $deg(A) = deg(B) = n$ and $deg(C) = deg(D) = m$. $\hat{y} \in \mathbb{R}$, $\hat{u} \in \mathbb{R}$ and $\hat{e} \in \mathbb{R}$ are used to denote the model predicted output, calculated control input, and model predicted white noise, respectively. The model delay $d \geq 1$ in $\hat{G}(z)$ is enforced to avoid circulating dependence between $\hat{y}_k$ and $\hat{u}_k$. The dynamic optimization problem is formulated for the MPC at sample time k as follows.

$$\begin{aligned}
\min_{\hat{\mathbf{u}}} \quad & J(y_k, \hat{\mathbf{u}}) \\
& J(y_k, \hat{\mathbf{u}}) = \sum_{i=0}^{N-1} (\hat{y}_{k+i+1} - r_{k+i+1})^2 + \lambda \hat{u}_{k+i}^2, && (4.3a)\\
\text{s. t. :} \quad & A\hat{\mathbf{u}} \leq b, && (4.3b)
\end{aligned}$$

where N is, for simplicity, the length of the horizons in sample times, without differentiating the control and the prediction horizons. $\hat{\mathbf{u}} = \{\hat{u}_k, \hat{u}_{k+1}, \ldots, \hat{u}_{k+N-1}\} \in \mathbb{U}_N(k)$ where $\mathbb{U}_N(k)$ is the set of feasible control moves over the horizon N which satisfy the constraints (4.3b). $r_k \in \mathbb{R}$, the *reference signal*, is the setpoint of the process output y_k. $\lambda \in \mathbb{R}^+$ is a positive real number. $A \in \mathbb{R}^{n_c \times N}$ is the constraint matrix. n_c is the number of linear constraints, and $b \in \mathbb{R}^{n_c}$. The solution of the above constrained optimization problem (4.3) is denoted by $\hat{\mathbf{u}}^* = \{\hat{u}_k^*, \hat{u}_{k+1}^*, \ldots, \hat{u}_{k+N-1}^*\}$. The control input applied to the process is $u_k = \hat{u}_k^*$ according to the receding horizon technique. In the following, the output prediction is described for the MPC formulation.

4.3.1 Output Prediction

The *minimum variance predictor* for $\hat{y}$ can be written as follows [54, 88].

$$\hat{y}_{k+i} = E_i(z)u_{k+i-d} + \left\{ \frac{F_i^d(z)}{C(z)} y_k + \frac{z^{-1}F_i(z)C(z) - z^{-d}F_i^d(z)B(z)}{A(z)C(z)} u_k \right\} \quad (4.4a)$$

$$\hat{d}_{k+i} = \frac{F_i^d(z)}{D(z)} \hat{n}_k, \quad (4.4b)$$

where

$$\hat{n}_k = \hat{H}^{-1}(z)(y_k - \hat{G}(z)u_k)$$

$$\hat{n}_{k+i} = 0, \quad i \geq 1.$$

The polynomials E_i, F_i, E_i^d, and F_i^d in (4.4) are determined by solving the Diophantine equations (4.5).

$$\frac{C(z)}{D(z)} = E_i^d(z) + z^{-i}\frac{F_i^d(z)}{D(z)}, \tag{4.5a}$$

$$\frac{B(z)}{A(z)} = E_i(z) + z^{-(i-d+1)}\frac{F_i(z)}{A(z)} \tag{4.5b}$$

The polynomials E_i, F_i, E_i^d, and F_i^d can be calculated via long division such that degrees of polynomials satisfy $deg(E_i) \leq (i-d)$, $deg(F_i) = (n-1)$, $deg(E_i^d) \leq (i-1)$, and $deg(F_i^d) = (m-1)$. When the delay $d \geq 1$ in (4.4), the predictor $\hat{y}_{k+i}$ can be decomposed into two parts: 1) the first term in (4.4a) is the *future* process behavior which depends on current and future control actions determined by the the optimization problem (4.3) 2) the second term in (4.4a) is the *past* process behavior which is a combination of past control input and process output.

4.3.2 Explicit Solution of MPC

Similar to the MPC formulation with a state space model [56], the constrained optimization problem in the MPC formulation (4.3) with the input output model (4.2a) can be written as a Quadratic Programming (QP) problem [88].

$$\begin{aligned} \min_{\hat{\mathbf{u}}} \quad & \hat{\mathbf{u}}^T M \hat{\mathbf{u}} + 2\mathbf{f}_k^T L \hat{\mathbf{u}}, \\ \text{s. t. :} \quad & A\hat{\mathbf{u}} \leq b, \end{aligned} \tag{4.6}$$

where $M = L^L + \lambda I$, $\mathbf{f}_k^T = (\mathbf{f}_k^y + \mathbf{f}_k^u - \mathbf{r})^T L$. With the predictor (4.4), L, $\mathbf{f}_k^y$, $\mathbf{f}_k^u$, and $\mathbf{r}$ are given in [88] as follows.

$$L = \begin{bmatrix} e_0 & 0 & \dots & 0 & 0 & \dots & 0 \\ e_0 & e_1 & \dots & 0 & 0 & \dots & 0 \\ \vdots & \vdots & \ddots & \vdots & \vdots & \vdots & \vdots \\ e_0 & e_1 & \dots & e_{N-d} & 0 & \dots & 0 \end{bmatrix}, \tag{4.7a}$$

$$E_i(z) = e_0 + e_1 z + \ldots + e_{i-d} z^{-(i-d)} \tag{4.7b}$$

$$\mathbf{f}_k^y = \left[\frac{F_1^d(z)}{C(z)}, \frac{F_2^d(z)}{C(z)}, \ldots, \frac{F_N^d(z)}{C(z)} \right]^T y_k, \tag{4.7c}$$

$$\mathbf{f}_k^u = \begin{bmatrix} \frac{zF_1(z)C(z) - z^{-d} F_1^d(z)B(z)}{A(z)C(z)} \\ \vdots \\ \frac{zF_N(z)C(z) - z^{-d} F_N^d(z)B(z)}{A(z)C(z)} \end{bmatrix} u_k, \tag{4.7d}$$

$$\mathbf{r} = [r_{k+1}, \ldots, r_{k+N}]^T. \tag{4.7e}$$

The above constrained QP problem (4.6) is explicitly solved using KKT conditions for each set of active constraints. The final explicit control law can be written as in [88],

$$u_k = C_p + F_p^y(z) y_k + F_p^r(z) r_k, \tag{4.8}$$

where C_p is a constant, F_p^y is a linear causal filter, and F_p^r is a linear non-causal transfer function. $p = \{p_1, p_2, \ldots, p_q\} \subseteq \{1, \ldots, n_c\}$ is the index set of active constraints q. The regional constraint for p is being active constraint set depends on the free response $(\mathbf{f}_k^y + \mathbf{f}_k^u)$ of the transfer function model (4.2a) while it depends on the current state in the state space formulation [56]. Here, it can be noticed that the constrained MPC law is nonlinear, and it can be represented by a piecewise affine controller with each piece given by (4.8).

4.4 Prediction Error Method (PEM)

Here, a brief description of PEM is given for the parameter estimation problem, and the complete description about PEM including its convergence property can be found in [83, 84]. Consider a particular model in the following model structure $\mathbb{M}$.

$$\mathbb{M}(\theta) : y_k = \bar{G}(z,\theta)u_k + \bar{H}(z,\theta)\bar{e}_k, \tag{4.9}$$

where $\bar{G}$ and $\bar{H}$ are the process and noise model, respectively. $\theta \in \mathbb{D} \subset \mathbb{R}^p$ is the parameter vector with the dimension p, and $\mathbb{D}$ is the parameter set. $\bar{e}$ is the *innovation*. The *one-step-ahead predictor* [84] for (4.9) is given by

$$\bar{y}_{k|k-1} = \bar{H}(z,\theta)^{-1}\bar{G}u_k + \left(I - \bar{H}^{-1}(z,\theta)\right)y_k. \tag{4.10}$$

Then the prediction error for the system (4.9) is given by

$$\varepsilon_k(\theta) = y_k - \bar{y}_{k|k-1} = \bar{H}(z,\theta)^{-1}\left(y_k - \bar{G}(z,\theta)u_k\right) \tag{4.11}$$

With the quadratic error criterion and a data set $Z_{N_d} = \{y_1, u_1, y_2, u_2, \ldots, y_{N_d}, u_{N_d}\}$, the prediction error estimate can be formulated as

$$\bar{\theta} = \arg\min_{\theta \in \mathbb{D}} V_{N_d}(\theta, Z_{N_d}), \tag{4.12a}$$

$$V_{N_d}(\theta, Z_{N_d}) = \frac{1}{N_d}\sum_{k=1}^{N_d} \varepsilon_k(\theta)^2. \tag{4.12b}$$

4.5 Informativity of Closed-loop Data: Direct Method

In this section, direct closed-loop identification with PEM [83–85] is discussed for applying it on a closed-loop data set generated with the constrained MPC. The direct closed-loop identification uses PEM to identify the process using the closed-loop data set as in the open-loop case ignoring any effect of feedback. A consistent estimate of the true process can be obtained using PEM if 1) the data set Z_{N_d} is *informative enough* with respect to a given model set, and 2) the model set contains the true process, i.e. $\bar{G}(z,\theta_0) = G(z)$ and $\bar{H}(z,\theta_0) = H(z)$ for some $\theta_0 \in \mathbb{D}$ for the true process (4.1) and the model (4.9) [84]. The second condition, a *globally identifiable model structure*, is generally assumed in order to achieve the desired global solution, and a model structure has to be carefully selected for unbiased estimation; the disturbance model should be independently parameterized and given enough complexity [84, 87]. The first condition guarantees the uniqueness of the global minimum of PEM with respect to the model structure, and experimental conditions should be applied to ensure that the data set is informative [89]. Since the data set is generated by the true process, these experimental conditions depend on both the true process and the feedback controller for the closed-loop system [89].

A condition, on the closed-loop data set (4.14) generated by the process (4.1) with MPC laws (4.8), for informativity is given in [88]. Here, it is summarized as follows.

Consider a closed-loop data set Z_{N_d} generated by the process (4.1)

$$Z_{N_d} = \{y_1, u_1, y_2, u_2, \ldots, y_{N_d}, u_{N_d}\}, \tag{4.13}$$

with s pieces of active MPC laws (4.8) as

$$u_k^j = C_j + F_j^y(z) y_k^j + F_j^r(z) r_k, \quad j = 1, \ldots, s, \quad \text{and} \quad (u_k, y_k) \in Z_{N_d}. \tag{4.14}$$

Then the prediction error (4.11) corresponding to the data set (4.14) for the model (4.9) can be written as

$$\varepsilon_k^j = \hat{H}^{-1}(z)(y_k^j - \hat{G}(z) u_k^j), \quad j = 1, \ldots, s. \tag{4.15a}$$

Substituting (4.14) in the process (4.1), the prediction error ε_k^j is given by

$$\varepsilon_k^j = \hat{H}^{-1}(z)\left[\left(1 - G(z)F_j^y(z)\right)^{-1} G(z) - \hat{G}(z)\left(I + F_j^y(z)\left(I - G(z)F_j^y(z)\right)^{-1} G(z)\right)\right] \left[\left(C_j + F_j^r(z) r_k\right) + \hat{H}^{-1}(z)\left(1 - \hat{G}(z)F_j^y(z)\right)^{-1} H(z) n_k\right]. \tag{4.15b}$$

It is shown in [88] that the global asymptotic minimum of (4.12b) is achieved when $\varepsilon_k^j = e_k$, and if the matrix

$$\mathscr{F} = \begin{pmatrix} I & \dots & I & 0 & \dots & 0 \\ -F_1^y & \dots & -F_s^y & F_1^r & \dots & F_s^r \end{pmatrix} \tag{4.16a}$$

has full row rank, then

$$\bar{G} = G, \quad \text{and} \quad \bar{H} = H. \tag{4.16b}$$

is unique solution of $\varepsilon_k^j = e_k$. With the criterion (4.16a), the following algorithm can be expressed to identify the models $\bar{G}$ and $\bar{H}$ for the process (4.1).

Algorithm 2 The basic steps of the direct closed-loop identification with constrained MPC

1: Select the model structure $\mathbb{M}$ (4.9).
2: Check the condition (4.16a) for the closed-loop data set Z_{n_d} (4.14).
3: **if** condition (4.16a) is passed, **then**
4: estimate the models $\bar{G}$ and $\bar{H}$ using PEM (4.12).
5: **else**
6: Perform *on-line* experiments to generate an informative data set Z_{n_d}.
7: **end if**

The design and performance of on-line experiments in order to pass the condition (4.16a) are discussed in [88]. These experiments are merely done to activate some pieces of the affine MPC law through the regional constraints. More details can be found in [90] on the idea of the Algorithm 2 under the topic of *least costly identification*; first, identify models based on the operation closed-loop data, and if necessary, design and perform the least disturbing experiment in the closed-loop.

4.5.1 Example

The objective of this example is to study several cases to show the effect of complexity of MPC for consistent estimates. Consider the following process,

$$y_k = G(z)u_k + H(z)e_k, \tag{4.17a}$$
$$G(z) = \frac{0.6z^{-1}}{1-1.6z^{-1}+0.7z^{-2}}, \quad H(z) = \frac{1+0.8z^{-1}}{1-1.2z^{-1}+0.2z^{-2}}, \tag{4.17b}$$

where $e \sim N(0, 0.01)$. For the MPC formulation, the model described in 4.18 is used as its internal model.

$$\hat{y}_k = \hat{G}(z)u_k + \hat{H}(z)\hat{e}_k, \tag{4.18a}$$
$$\hat{G}(z) = \frac{0.5z^{-1}}{1-0.9z^{-1}}, \quad \hat{H}(z) = \frac{1+0.5z^{-1}}{1-z^{-1}}. \tag{4.18b}$$

Then the constrained optimization problem in the MPC can be written as

$$\min_{\hat{\mathbf{u}}} \quad J(y_k, \hat{\mathbf{u}}) = \sum_{i=0}^{N-1} (\hat{y}_{k+i+1} - r_{k+i+1})^2 + \lambda \hat{u}_{k+i}^2, \tag{4.19a}$$
$$\text{s. t}: \quad \hat{u}_{k+i} \leq 1, \quad \forall\, i = 0, \ldots, N-1. \tag{4.19b}$$

Then for the prediction horizon $N = 2$ and the controller weighing $\lambda = 0.01$, MPC laws are given as follows.

For no being active constraints,

$$u(k) = F_1^y(z)y_k + F_1^r(z)r_k, \tag{4.20a}$$
$$F_1^y(z) = \frac{-0.754+0.6786z^{-1}}{1-0.4054z^{-1}-0.2642z^{-2}}, \tag{4.20b}$$
$$F_1^r(z) = \frac{-3.232z^2+5.027z-0.0395-1.68z^{-1}}{1-0.4054z^{-1}-0.2642z^{-2}}. \tag{4.20c}$$

For second constraint being active i.e. $u_{k+1} = 1$,

$$u(k) = F_2^y(z)y_k + F_2^r(z)r_k + 1.0465, \tag{4.21a}$$

$$F_2^y(z) = \frac{-3.081 + 2.773z^{-1}}{1 - 1.06z^{-1} - 0.00973z^{-2}}, \tag{4.21b}$$

$$F_2^r(z) = \frac{0.973z^2 + 0.6919z - 0.8703 - 0.4865z^{-1}}{1 - 1.06z^{-1} - 0.00973z^{-2}}. \tag{4.21c}$$

For first constraint being active,

$$u_k = 1. \tag{4.22}$$

The closed-loop is simulated in MATLAB, and 2.4×10^4 samples were collected for experiments. Box-Jenkins (BJ) model structure was selected, and identification task was performed via MATLAB command **bj**. Here, for simplicity, order of numerator polynomials for both the estimates $\hat{G}$ and $\hat{H}$ are assumed the same as the true process 4.17. Following cases are studied.

Case	r	Constraint	Control law
A	$r = 0$	Unconstrained	$u_k = F_1^y(z)y_k$
B	$r \sim N(0, 0.01)$	Unconstrained	$u_k = F_1^y(z)y_k + F_1^r(z)r_k$
C	$r = 0$	Constrained	$u_k = \begin{cases} F_1^y(z)y_k & \text{or} \\ F_2^y(z)y_k + 1.0465 & \text{or} \\ 1 \end{cases}$

Table 4.1: Three different case studies and respective control laws for Example 4.5.1

The complexity criterion (4.16a) discussed for direct closed-loop identification are given in Table 4.2. Note that consistent estimates are expected when $\mathscr{F}$ has full raw rank 2. For the case A, the rank of $\mathscr{F}$ is 1. Therefore, the estimates are quite biased as shown in Fig. 4.1 and Fig. 4.2. For the each case B and C, the rank of $\mathscr{F}$ is 2, and the estimates are consistent with the true process as shown in Fig. 4.1 and Fig. 4.2.

Case	Complexity criterion $\mathscr{F}$	Rank of $\mathscr{F}$
A	$\mathscr{F}_A = (1 \quad F_1^y)^T$	1
B	$\mathscr{F}_B = \begin{pmatrix} 1 & 0 \\ F_1^y & F_1^r \end{pmatrix}$	2
C	$\mathscr{F}_C = \begin{pmatrix} 1 & 1 \\ F_1^y & F_2^y \end{pmatrix}$	2

Table 4.2: The complexity criterion $\mathscr{F}$ for the cases listed in Table 4.1 of Example 4.5.1

Case	$\hat{G}$	$\hat{H}$
A	$\bar{G}_A = \frac{-2.369z^{-1}+2.014z^{-2}}{1-0.1165z^{-1}-0.802z^{-2}}$	$\bar{H}_A = \frac{1-0.6437z^{-1}}{-0.4329z^{-1}-0.5408z^{-2}}$
B	$\bar{G}_B = \frac{0.6023z^{-1}+0.001607z-2}{1-1.601z^{-1}+0.6986z^{-2}}$	$\bar{H}_B = \frac{1+0.7978z-1}{1-1.196z^{-1}+0.1965z^{-2}}$
C	$\bar{G}_C = \frac{0.6001z^{-1}-0.0003913z^{-2}}{1-1.602z^{-1}+0.7014z^{-2}}$	$\bar{H}_C = \frac{1+0.8014z^{-1}}{1-1.198z^{-1}+0.1978z^{-2}}$

Table 4.3: Model estimates for the cases listed in Table 4.1 of Example 4.5.1

4.6 Joint Input-Output Method

In this section, a joint input-output closed-loop identification method is described for the closed-loop data set Z_{N_d}(4.14). The identification task is to estimate the models $\bar{G}$ and $\bar{H}$ (4.9) for the process (4.1). The basic idea of joint input-output closed-loop identification [83] is to consider the control input signal u and the process output y together as the *joint outputs* (u,y) of the *joint inputs* (r,e), which consists of the process reference signal r and underlying process disturbance e. The two input signals (r,e) are typically independent. Therefore, the joint outputs (u,y) can be separated as two independent parts: one due to r and one due to e.

$$u_k = u_k^r + u_k^e, \tag{4.23a}$$

$$\begin{aligned} y_k &= y_k^r + y_k^e \\ &= G(z)u_k^r + H_* \circ e_k, \quad H_* \circ e_k = \{G(z)u_k^e + H(z)e_k\}, \end{aligned} \tag{4.23b}$$

where u^r and u^e are input signal components due to reference signal r and process disturbance e, respectively. y^r and y^e are corresponding components of process output y. $(y^r,u^r)\perp(y^e,u^e)$, and $H_* \circ e$ represents the noise portion of y. Then if

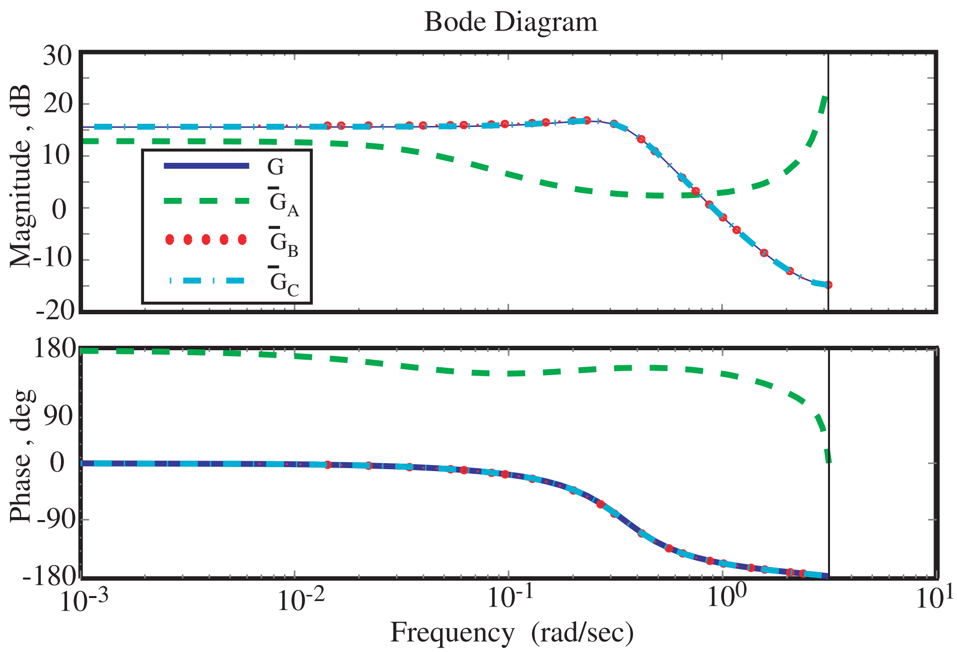

Figure 4.1: The Bode plots of the true process G, and its estimated process models $\bar{G}_A$, $\bar{G}_B$, and $\bar{G}_C$ for the case studies A, B, C, respectively in Example 4.5.1

one can separate (y^r, u^r) from (y, u) based on measured (u, y, r), a model $\bar{G}$ can be fit between u^r and y. In this work, the *two-stage* method is considered, i.e. first separate u^r from u, then fit a model $\bar{G}$ between u^r and y.

4.6.1 Two-stage Method

Here, the two-stage method [91] is briefly described to identify the model $\bar{G}$ from closed-loop data. If the feedback is a linear causal relation, for instance $u_k = -\kappa(z^{-1})y_k$, then $H_* \circ e_k$ in (4.23b) simply becomes $H_* e_k$, and H_* is the sensitivity not the disturbance model H. In this case

$$y_k = G(z)S_{ur}(z)r_k + S_{ye}(z)e_k, \quad (4.24a)$$

$$u_k = S_{ur}(z)r_k + S_{ue}(z)e_k, \quad (4.24b)$$

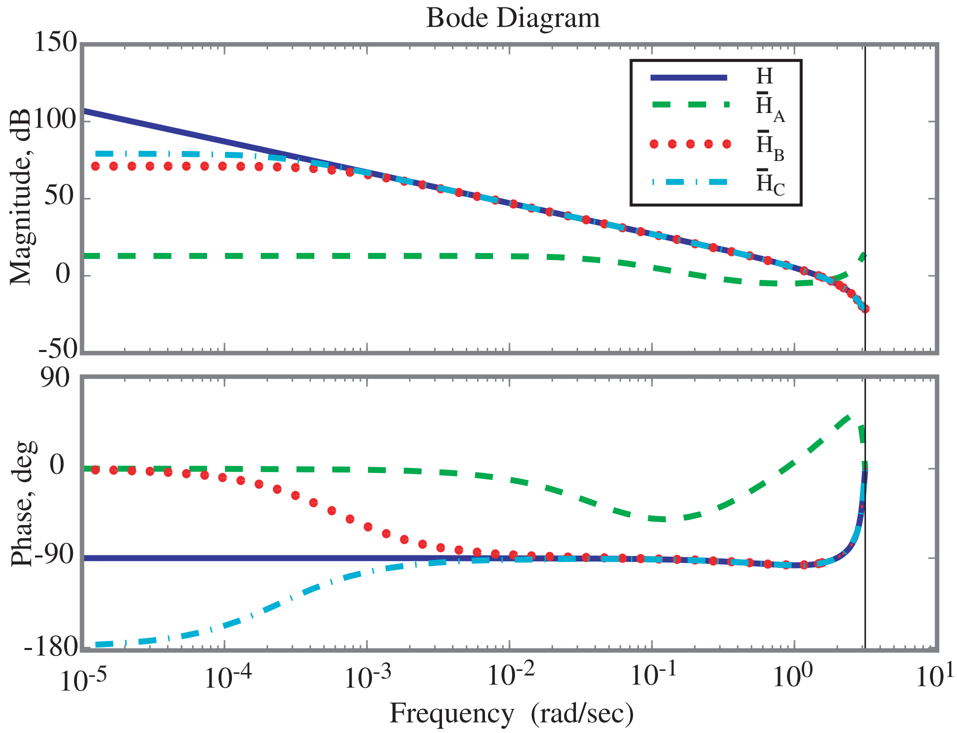

Figure 4.2: The Bode plots of the true noise process H, and its estimated process models $\bar{H}_A$, $\bar{H}_B$, and $\bar{H}_C$ for the case studies A, B, C, respectively in Example 4.5.1

and the optimal separation of u^r from u is to know the exact S_{ur}, i.e. $u^r = S_{ur}r$. Then two-stage method can be summarized as in the Algorithm 3.

In the first stage, causal high-order models, for example Finite Impulse Response (FIR) or Auto-Regressive Exogenous (ARX), are used for $\bar{S}_{ur}$[84, 87, 91] while in the second stage, PEM can be used to identify the model $\bar{G}$.

4.6.2 First Stage: Projection Method

A more general method of joint input-output identification is the projection method [87], in which the controller is possibly nonlinear while the process (G,H) is still linear. In this case, the separation of u^r from u is done via fitting a non-causal model between u and r. If infinite impulse model were allowed, then the optimal

Algorithm 3 The basic steps of two-stage method for closed-loop identification.

1: First stage: Estimate $\bar{S}_{ur}$ for S_{ur} in (4.24b), based on the data (u,r). Then, calculate u_r via $\bar{u}^r = \bar{S}_{ur} r$.

2: Second stage: Using the data $(\bar{u}^r, y)$, identify a model $\bar{G}$ of G in (4.24a) with the following structure.

$$y_k = \bar{G}(z,\theta)\bar{u}^r_k + \bar{H}_*(z)e_k \tag{4.25}$$

solution of

$$\min_{s_k} \| u_k - \sum_{k=-\infty}^{\infty} s_k r_k \|^2, \tag{4.26}$$

s^*_k would give $\bar{u}^r_k = \sum_{k=-\infty}^{\infty} s^*_k r_k$, and the residue $\bar{u}^e_k = u_k - \bar{u}^r_k$ is orthogonal to r. For practical reasons, a high order non-causal FIR is used, then $\bar{u}^r_k = \sum_{k=-M_1}^{M_2} s^*_k r_k$ [92]. Once $\bar{u}^r$ is generated, PEM is often used to fit the model between $\hat{u}^r$ and y. Then the prediction error for (4.23b) is

$$\varepsilon_k(\theta) = \bar{H}_*^{-1}(z)\left(y_k - \bar{G}(z,\theta)\bar{u}^r_k\right). \tag{4.27}$$

The PEM minimizes the cost function $V_{N_d}(\theta)$ (4.28) with respect to θ.

$$V_{N_d}(\theta) = \frac{1}{N_d}\sum_{k=1}^{N_d} \varepsilon_k^2 \tag{4.28}$$

Then w.p.1 as $N_d \to \infty$ and using Parseval's theorem, the estimation problem becomes [87]

$$\arg\min_{\theta\in\mathbb{D}} \int_{-\pi}^{\pi} |\, G - \bar{G} - \bar{B}\,|^2 \frac{\Phi_{\bar{u}^r}}{|\, H_*\,|^2} d\omega, \tag{4.29}$$

where $\Phi_{\bar{u}^r}$ is the spectrum of $\bar{u}^r$, and $\bar{B} = \frac{G\Phi_{\bar{u}^e\bar{u}^r}}{\Phi_{\bar{u}^r}}$ is the bias term. Thus the consistent estimation of G can be archived when $\Phi_{\bar{u}^e\bar{u}^r} = 0$, i.e. optimum projection of u onto r. Hence this estimation problem fits into the class of open-loop identification for the model described by (4.23b) with fixed $\bar{H}_*$.

The above only presents an overview of the method. Detailed discussion about joint input-output identification and projection method can be found in [83, 87, 92]. The important features of the projection method are: 1) consistent estimate of G can be achieved even though controller is non-linear, provided that u^r and u^e are uncorrelated, and 2) it allows fitting the model to the data with arbitrary frequency weighting in PEM.

4.6.3 Example

In this section, the joint input-output identification method is applied to closed-loop data generated by a constrained MPC, where the first stage uses the projection method to obtain excitation and noise contents separation followed by a standard PEM in the second stage. With MPC in the loop, $H_* \circ e_k$ is not a linearly filtered process. As the unbiasedness of $\bar{G}$ does not rely on the knowledge of the noise portion but the de-correlation between u^r and u^e, a linear approximation $\bar{H}_* e_k$ for the noise portion can be used. In that case, $\bar{H}_*$ serves as a data filter that can be chosen arbitrarily.

Consider the following process with input constraint,

$$y_k = G(z)u_k + H(z)e_k, \tag{4.30a}$$

$$G(z) = \frac{0.6z^{-1} + 0.45z^{-2}}{1 - 2.5z^{-1} + 2.14z^{-2} - 0.63z^{-3}}, \quad H(z) = \frac{1 + 0.5z^{-1}}{1 - z^{-1}},$$

$$u_k \leq 1, \quad \forall k \geq 0, \tag{4.30b}$$

and the process noise is $e_k \sim N(0, 0.1)$. The constrained MPC is formulated for (4.30) with the following initial model.

$$\hat{G}_{init}(z) = \frac{-0.1011z^{-1} + 0.7689z^{-2}}{1 - 1.702z^{-1} + 0.8593z^{-2}}, \quad \hat{H}_{init}(z) = \frac{1 + 0.5z^{-1}}{1 - z^{-1}}. \tag{4.31}$$

Then for the prediction horizon $N = 5$ and the controller weighting $\lambda = 0.03$, the MPC problem (4.3) can written as

$$\min_{\hat{\mathbf{u}}} \quad J(y_k, \hat{\mathbf{u}}) = \sum_{i=0}^{N-1} (\hat{y}_{k+i+1} - r_{k+i+1})^2 + \lambda \hat{u}_{k+i}^2 \tag{4.32a}$$

$$\text{s. t :} \quad \hat{u}_{k+i} \leq 1, \quad \forall i = 0, \ldots, N-1. \tag{4.32b}$$

The objective of the MPC is to improve the loop performance, and the achieved performance is measured by the cost function defined as

$$V_p(y,u,N) = \frac{1}{N}\sum_{k=1}^{N}[y_k^2 + u_k^2]. \tag{4.33}$$

For the above set-up, the cost (4.33) was 1.6978 from 16384 samples simulation, and the major active controller modes were 55.10% from unconstrained case and 38.28% from $u = 1$. The objective of this simulation is to identify an improved, but still reduced-order (second order) model $\bar{G}$. The closed-loop experiment data was generated from a 8192 sample experiment with extra excitation $r_k \sim N(0, 0.36)$. The non-causal model used in the first stage is given by

$$\bar{u}_r = \sum_{j=-29}^{11} s_j r_{k+j}.$$

Then in the second stage, the process model $\bar{G}_1$

$$\bar{G}_1(z) = \frac{0.4472z^{-1} + 0.3871z^{-2}}{1 - 1.821z^{-1} + 0.8859z^{-2}} \tag{4.34}$$

was determined via MATLAB routine $bj()$ with the freedom to choose H_* among 4th order transfer functions. Next, the closed-loop was simulated with the updated models $(\bar{G}_1, \hat{H})$ in the MPC with the same prediction horizon N and weighting λ. Then the achieved cost was reduced to 0.2650 where the unconstrained controller mode accounted for 96.73% samples while the saturated mode accounted for only 2.48%.

4.6.4 Second Stage: Long Range Predictive Identification

In the *identification for control* context [79], an identification criterion for model estimate bears control performance goals, especially when modeling error is unavoidable such as the under modeling case, and often can be transformed into standard PEM with special data filters/noise models. Since MPC techniques determine the control action based on predicted future process outputs over a horizon and the performance of an MPC technique largely depends on the model's prediction ability, one may question the use of models which only minimize one-step ahead prediction errors (4.10) in MPC techniques. In [93], it is shown that the combination of the pure Recursive Least Square (RLS) and GPC does not produce a good results. Alternatively, the LRPI method which is used to minimize the averaged prediction error throughout the MPC horizon is introduced in [93]. Good discussion about MPC relevant identification methods and LRPI can be found in [94, 95]. In this section, the LRPI is adopted as a MPC relevant criterion in the second stage of identification in the joint input-output identification method.

The LRPI criterion for the second stage identification is given by

$$J_{LRPI} = \lim_{N_d \to \infty} \frac{1}{N_d} \sum_{k=1}^{N_d - N} \frac{1}{N} \sum_{i=1}^{N} (y_{k+i} - \bar{y}_{k+i|k})^2, \tag{4.35}$$

where $\bar{y}_{i+1|k}$ is the predicted output from data $\{y_{0,\ldots,k}, \bar{u}^r_{0,\ldots,k+N}\}$ with the model (4.40). It is shown in [93] that the criterion (4.35) is equivalent to PEM with a data filter that depends on the noise model parameters. Though the original formula was derived for an ARX model, it can be extended for general models $(\bar{G}, \bar{H}_*)$ as follows.

For simplicity, suppose that

$$\bar{H}_* = \bar{H}_0 = \frac{\bar{C}(z)}{D(z)} \tag{4.36}$$

is known. Then the output prediction, similar to (4.4), can be written as

$$\bar{y}_{k+i|k} = \bar{G}(z) u^r_{k+i} + z^{-i} \frac{\bar{F}^d_i(z)}{C(z)} (y_{k+i} - \bar{G}(z) u^r_{k+i}), \tag{4.37a}$$

$$\frac{\bar{C}(z)}{D(z)} = \bar{E}^d_i(z) + z^{-i} \frac{\bar{F}^d_i(z)}{D(z)}, \tag{4.37b}$$

where the degrees of the polynomials are $deg(E^d_i) \leq (i-1)$ and $deg(F^d_i) = deg(C) -$

1. Thus the prediction error is

$$y_{k+i} - \bar{y}_{k+i|k} = \left(1 - z^{-i}\frac{\bar{F}_i^d(z)}{C(z)}\right)\left(y_{k+i} - \bar{G}(z)u_{k+i}^r\right), \\ = \bar{E}_i^d \bar{H}_0^{-1}\left(y_{k+i} - \bar{G}(z)u_{k+i}^r\right). \tag{4.38}$$

Therefore, by Parseval's theorem, the LRPI criterion (4.35) becomes

$$J_{LRPI} = \lim_{N_d \to \infty} \frac{1}{N_d}\sum_{k=1}^{N_d}(\varepsilon_k^f(\theta))^2, \tag{4.39}$$

$$\varepsilon_k^f(\theta) = L(z)\left[\bar{H}_0^{-1}(y_k - \bar{G}u_k^r)\right],$$

$$L(z)L^*(z^{-1}) = \frac{1}{N}\sum_{i=1}^{N} \mid \bar{E}_i^d(z) \mid^2 .$$

Since the noise model $\bar{H}_0$ is assumed to be known, this is a simple filtered PEM problem. Otherwise, in the iterative approaches of seeking better models and control, the current noise model $\bar{H}$ can be used to simplify matters.

The two-stage method with the projection method and the LRPI criterion can be summarized as in Algorithm 4.

Algorithm 4 The basic steps of the two-stage method with the projection method and the LRPI criterion for closed-loop identification.

1: First stage: Estimate $\bar{S}_{ur}$ for S_{ur} in (4.24b) based on the data (u, r), using the following non-causal FIR model structure.

$$\bar{S}_{ur}: \quad \bar{u}_k^r = \sum_{k=-M_1}^{M_2} s_k^* r_k$$

Then, calculate u_r via $\bar{u}^r = \bar{S}_{ur} r$.

2: Second stage: Using the PEM with LRPI (4.39) as the identification criterion, identify a model $\bar{G}$ of G in (4.24a) based on the data $(\bar{u}^r, y)$, with the following structure.

$$y_k = \bar{G}(z,\theta)\bar{u}_k^r + \bar{H}_*(z)e_k \tag{4.40}$$

4.6.5 Example

Here, Example 4.6.3 is continued to illustrate the Algorithm 4. In the second stage, the following first order LRPI filter is used.

$$L = \frac{1.605 + 0.3879z^{-1}}{1 - 0.6083z^{-1}} \tag{4.41}$$

Then a model $\bar{G}_{LRPI}$ is identified using the PEM with the LRPI filer.

$$\bar{G}_{LRPI} = \frac{0.4323z^{-1} + 0.3671z^{-2}}{1 - 1.827z^{-1} + 0.9658z^{-2}}. \tag{4.42}$$

For the same initial conditions and noise process used in Example 4.6.3, the achieved cost (4.33) of the new MPC based on $\bar{G}_{LRPI}$ is 0.2504, slightly better than $\bar{G}_1$, where the unconstrained controller mode accounted for 96.82% samples and the saturated mode accounted for only 1.93%. The Bode plots of the true, the initial model, and estimated process models are shown in Fig. 4.3.

4.7 Conclusion

In this chapter, two closed-loop identification schemes are discussed to apply on the input output data set generated with a constrained MPC in the loop. In the first scheme, the direct closed-loop identification method is investigated, and the informativity criterion, which ensure that the constrained MPC law is complex enough, is presented on the normal operational data set. One would first check this criterion, and if it passes, then estimate models using PEM directly with the closed-loop data. Otherwise, on-line experiments have to be conducted to achieve informative data in order to have consistent model estimates. Although the informativity criterion is originally presented to the SISO input output process, it can be extended to Multi-Input Multi-Output (MIMO) state space processes.

In the second scheme, the joint input-output method is discussed. The projection method is applied in the first stage to fit a non-causal FIR model. A successful first stage then gives the freedom of choosing frequency weighting arbitrarily in the identification criterion during the second stage. In particular, in the case of un-

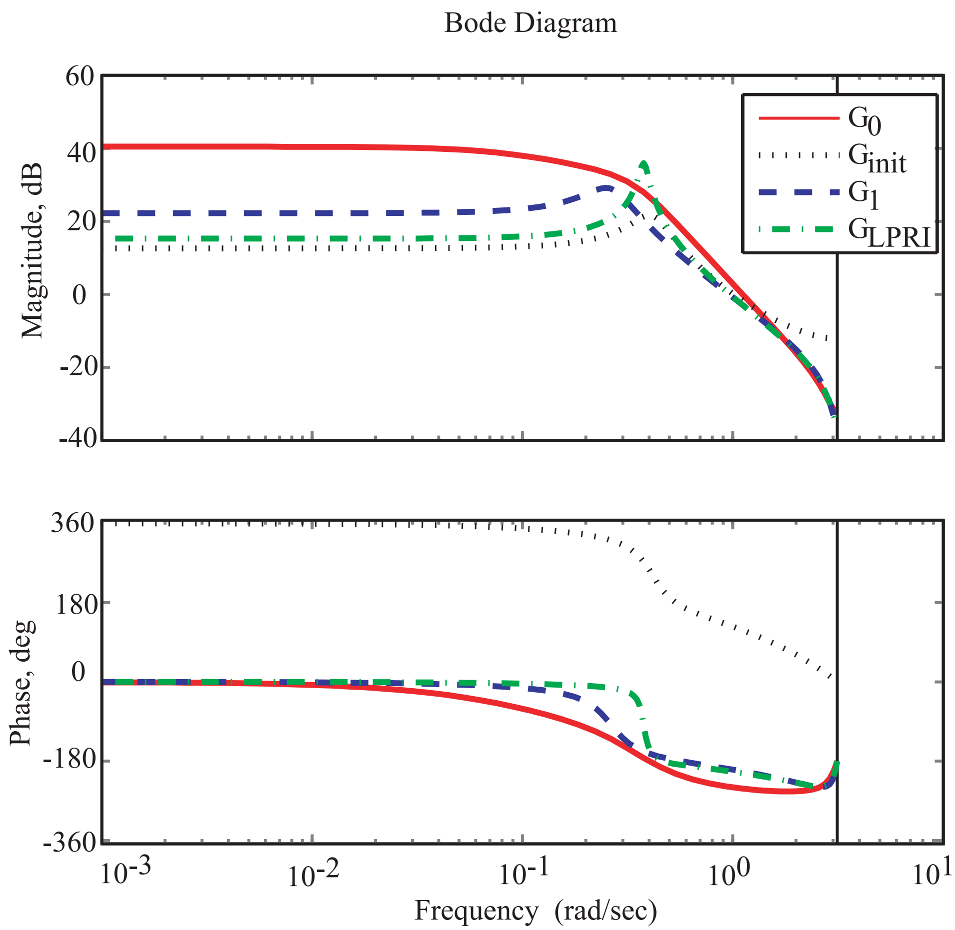

Figure 4.3: The Bode plots of the true process G_0, the initial model G_{init}, the estimated transfer functions G_1 and G_{LRPI} in Example 4.6.3 and 4.6.5, respectively

der modeling, meaningful MPC-relevant identification criterion, such as the LRPI, become viable so that the resultant MPC may give satisfying performance with low controller complexity. Moreover, the projection method might require a large number of parameters in the non-causal FIR model to achieve a better separation of the input signal. One could utilize the explicit piece-wise MPC law in the constrained MPC to revise the first stage that requires less parameters.

Chapter 5

Control and Optimization of Two-stage Thermo Mechanical Pulping (TMP) Processes

5.1 Summary

In this chapter, NMPC techniques are presented to control and optimize for TMP processes. The TMP process considered in this chapter has two-stages of refining with a primary and a secondary refiners. In the first part of this work, a setpoint tracking problem is formulated with the NMPC technique for the TMP process. Then the performances of *ideal*-NMPC described in Section 2.3 and asNMPC described in Section 2.6.2 are compared in a simulation study. In the second part, an econNMPC is formulated for the TMP process. In econNMPC, a dynamic optimization problem is formulated to simultaneously regulate and optimize the TMP process in the presence of disturbances. In a simulation study, potential economical benefits of the proposed econNMPC method are demonstrated, through a reduction in total specific energy. The computational burden of the resulting NLP problems in NMPC formulations are handled with the IPOPT solver described in Section 2.6.1.

5.2 Introduction

MPC has been applied to control and optimize chemical processes [68], [65]. One of the main advantages of MPC is its ability to cope with hard constraints on control and state variables. Therefore, MPC has attracted considerable research effort, and has been widely applied in process industries for low-level regulatory control under constraints [96], [45]. The main issues with the applications of NMPC with detailed nonlinear models were due to computational burden and lack of theoretical support for stability [63, 64]. However, with the improvement of today's computational power and development of efficient NLP solvers [59] and tailored algorithms [58], there is growing tendency to use NMPC in the optimization layer of the decision making hierarchy, with detailed nonlinear dynamic models [65, 67, 68].

Computer control of wood-chip refiners has been studied in literature and industry for a long time [10], and there have been a few attempts to control and optimize TMP processes using MPC strategy. Ruscio [97] [7] demonstrated a linear MPC control technique for a TMP process. The objective of that work was to control specific energy and consistency of the TMP process using screw speed, dilution flow and plate gap. First, a subspace identification technique was presented, and then a linear state-space model was identified with time series data to use for MPC. Du et al. [98] presented a GPC algorithm based on a nonlinear Laguerre model to control motor load and consistency of a TMP process. In addition, there are few applications reported to control pulp quality and reject refining process using MPC [3], [99]. Recently, Sidhu et al. [8] applied MPC strategy to an industrial two-stage TMP process. They presented a two-level control strategy in order to control motor loads and consistencies, and to improve pulp quality. The strategy was to first decouple the control variables according to their bandwidths, and then to formulate linear stabilizing and quality controllers. However, the separation was merely due to the placement of the pulp quality sensor after the latency tank, but not due to the dynamics of the refiners. The coordination between the quality controller and the stabilizing controller was performed in steady-state.

In contrast to the above developments, a general NMPC framework to control and optimize a two-stage TMP process is considered in this chapter. First, NMPC for setpoint tracking problem is designed, and then an economical objective is integrated in the NMPC formulation. The economical benefit is realized through a reduction in specific energy consumption of the TMP process. The resulting NLP problems are solved using the IPOPT solver described in Section 2.6.1. in order to handle the computational burden. Further, the computational issue is improved with asNMPC controller concept described in Section 2.6.2.

5.2.1 TMP Process Modeling

TMP processes are, inherently, MIMO processes with complex dynamics and severe interactions among process variables. Modeling of TMP is challenging due to complex conditions inside the pulp refiners. It is not yet clearly understood what the desired mechanism for efficient fiber development is and how energy transforms into the pulp inside the refiners [100]. In this chapter, the following models are used for the process variables to develop a discrete-time nonlinear model for the TMP process.

Production Rate

Production rate or throughput of the TMP process is proportional to chip-transfer screw speed and is simply calculated by multiplying the chip-transfer screw speed by a constant in most industrial processes [12]. Changes in chip bulk density and chip solid content are considered as more dominant disturbances in TMP processes. In order to consider these variations, here the following model is used for the production rate, P $(tonnes/day)$ [6].

$$P = 1.44 k_p s_c d_c R, \tag{5.1}$$

where k_p (m^3/rev) is proportional constant, s_c $(\%)$ is chip solid content, d_c (kg/m^3) is chip bulk density, and R (rpm) is chip-transfer screw speed, respectively.

Motor Loads

The plate gap, which determines refining zone surface area to volume ratio, is a key variable for modeling the motor load [6], [11]. The number of wood fibers per unit volume entering the refiner, which is a function of production rate and dilution water flow rate, is another variable which determines the motor load. In this work, the following model[1] is used to describe motor load as a function of the production rate, plate gap, and dilution flow rate.

[1] This model has been used in the case study of MPC Supervisory Control of a Two Stage Thermo-Mechanical Pulping Process, Model Predictive Control Toolbox DEMOS, MATLAB 7.8.0 (R2009a).

$$M_i = \frac{km_i P}{D_i} \left(1 - \exp(-10G_i)\right)(a_i - b_i G_i), \tag{5.2}$$

where M_i (MW) is the motor load, D_i (l/min) is the dilution water flow rate, G_i (mm) is the gap, and km_i, a_i and b_i are parameters of the refiner. The subscript index $i = p, s$ represent the primary and secondary refiners, respectively.

Consistencies

Refining consistency is defined as the ratio of dry fiber flow rate to fiber and water flow rate. The refining consistency of each refining process changes with production rate, motor load, and dilution flow rate and can be derived using mass balance [7], [6]. In this work, it is assumed that water and energy losses in the refiners are negligible, and back-flow of steam is a function of motor load for each refiner. Then outlet consistencies of the primary and secondary refiners can be expressed as

$$C_p = \frac{100P}{P + 1.44D_p - ke_p M_p}, \tag{5.3a}$$

$$C_s = \frac{100P}{(P/(0.01C_p) + 1.44D_s - ke_s M_s)}, \tag{5.3b}$$

where ke_p and ke_s are parameters for the primary and secondary refiners, respectively.

Pulp Quality Variables

In this work, pulp quality variables such as Canadian Standard Freeness (CSF), Long Fiber Content (LFC), and Shive Content (SC) are considered after the secondary refining process, as the target pulp quality variables. For the pulp quality variables, the nonlinear model developed in [101] in terms of specific energy and specific refining power is used. The specific energy and specific refining power are implicit functions of the production rate, motor loads and consistencies of the both primary and secondary refiners. Therefore, for simplicity, the relationship between pulp quality variables and the production rate, motor loads and consistencies is expressed as a general nonlinear implicit function g_{tmp} as follows.

$$0 = g_{tmp}(CSF, LFC, SC, P, M_P, C_p, M_s, C_s) \tag{5.4}$$

Here, the aim is to form a nonlinear discrete-time model for the TMP refining process; both primary and secondary refiners are considered together as a single process model. The production rate, primary motor load, primary consistency, secondary motor load, and secondary consistency are considered as the discretized differential state variables while the pulp quality variables: CSF, LFC, and SC, are considered as the discretized algebraic state variables of the TMP refining process model. Manipulated variables are chip-transfer screw speed, plate gap and dilution water flow rates of the both primary and secondary refiners. By introducing linear dynamics for the discretized differential state variables and superimposing it on the steady-state relationships (5.1)-(5.3), a Wiener type discrete-time nonlinear model for this TMP refining process can be formulated at sample time k as follows.

$$z_{k+1} = A_{tmp} z_k + h_{tmp}(z_k, v_k) \tag{5.5a}$$

$$0 = g_{tmp}(z_k, y_k) \tag{5.5b}$$

where $z_k \in \mathbb{R}^{n_z}$, $y_k \in \mathbb{R}^{n_y}$, and $v_k \in \mathbb{R}^{n_v}$ denote the vectors of discretized differential state, algebraic state, and manipulated variables of the TMP refining model. n_z, n_y, and n_v are dimensions of the variables z, y, and v, respectively. Then

$$z = \begin{bmatrix} \text{Production rate} \\ \text{Primary refiner motor load} \\ \text{Primary refiner consistency} \\ \text{Secondary refiner motor load} \\ \text{Secondary refiner consistency} \end{bmatrix}, \; y = \begin{bmatrix} \text{CSF after primary refining} \\ \text{LFC after primary refining} \\ \text{SC after primary refining} \\ \text{CSF after secondary refining} \\ \text{LFC after secondary refining} \\ \text{SC after secondary refining} \end{bmatrix}, \text{ and}$$

$$v = \begin{bmatrix} \text{Chip-transfer screw speed} \\ \text{Primary refiner plate gap} \\ \text{Primary refiner dilution water flow rate} \\ \text{Secondary refiner plate gap} \\ \text{Secondary refiner dilution water flow rate} \end{bmatrix}. \tag{5.6}$$

$A_{tmp} \in R^{n_z \times n_z}$ is the dynamic matrix which can be identified for the TMP process by using any linear system identification method. On the other hand, for simplicity, one can use the time constant and time delay information of each subprocesses to form A_{tmp} as follows.

$$\bar{A}_{tmp}(z) = \begin{bmatrix} g_{ps}(z) & 0 & 0 & 0 & 0 \\ 0 & g_{pmpg}(z) & 0 & 0 & 0 \\ 0 & 0 & g_{pcpd}(z) & 0 & 0 \\ 0 & 0 & 0 & g_{smsg}(z) & 0 \\ 0 & 0 & 0 & 0 & g_{scsd}(z) \end{bmatrix} \tag{5.7}$$

where $\bar{A}_{tmp}(z)$ is the dynamic transfer function matrix of the TMP process. $g_{ps}(z)$ is the transfer function between production rate and chip-transfer screw speed. $g_{pmpg}(z)$ is the transfer function between primary refiner motor load and primary refiner gap. $g_{pcpc}(z)$ is the transfer function between primary refiner consistency and primary refiner dilution water flow rate. $g_{smsg}(z)$ is the transfer function between secondary refiner motor load and secondary refiner plate gap. $g_{scsd}(z)$ is the transfer function between secondary refiner consistency and secondary refiner dilution water flow rate. The transfer functions of the subprocesses have following form.

$$g_{ps} = \frac{b_1 z^{-d_1}}{z - a_1} \tag{5.8}$$

$$g_{pmpg} = \frac{b_2 z^{-d_2}}{z - a_2} \tag{5.9}$$

$$g_{pcpd} = \frac{b_3 z^{-d_3}}{z - a_3} \tag{5.10}$$

$$g_{smsg} = \frac{b_4 z^{-d_4}}{z - a_4} \tag{5.11}$$

$$g_{scsd} = \frac{b_5 z^{-d_5}}{z - a_5} \tag{5.12}$$

where a_i and d_i for $i = 1 \dots 5$ are the poles and time delays of the subprocess, respectively. b_i for $i = 1 \dots 5$ are parameters, and can be found as $b_i = 1 - a_i$, for unity dynamic gains of the each subprocesses. Then the dynamic matrix can be expressed as

$$A_{tmp} = diag([a_1, a_2, a_3, a_4, a_5]^T). \tag{5.13}$$

The nonlinear state function, $h_{tmp} : \mathbb{R}^{n_z + n_v} \mapsto \mathbb{R}^{n_z}$, and $h_{tmp} = (I - A_{tmp})H_{tmp}$ where H_{tmp} maps steady-state control input variables to steady-state differential state variables of the TMP refining model. Note that the time delay information is represented in the the state function h_{tmp} as $h_{tmp}(z_k, v_{k-d})$ where $d = [d_1, d_2, d_3, d_4, d_5]^T$ is the time delay vector in sample times. In this work, we assigned time constants and time delays of subprocesses as given in Table 5.1, and then a_i and b_i are calculated.

Subprocess	Time constant (s)	Time delay, d	a	b
g_{ps}	2	2	0.6065	0.3935
g_{pmpg}	2	1	0.6065	0.3935
g_{pcpd}	2	0	0.6065	0.3935
g_{smsg}	2	1	0.6065	0.3935
g_{scsd}	2	0	0.6065	0.3935

Table 5.1: Time constants and time delays of subprocesses of the TMP process

For simplicity, a general form of state equation for (5.5a) is considered in following NMPC formulations.

$$z_{k+1} = f_{tmp}(z_k, v_k) \tag{5.14}$$

Note that in the remainder of this chapter, the TMP process is simulated up to the secondary refiner, assuming the pulp quality measurements are available at that point. The following section describes the NMPC strategy for setpoint tracking problem for the TMP process.

5.3 NMPC for Setpoint Tracking

Using the current process state x_k, the dynamic optimization problem is formulated for the NMPC at sample time k as follows.

$$\min_{\mathbf{v}} \quad J_{spt}, \quad J_{spt} := \sum_{i=1}^{N} \|\xi_i - \xi_{k+i}^s\|_{Q_\xi}^2 + \|v_i - u_{k+i-1}^s\|_{Q_v}^2 \tag{5.15a}$$

$$\text{s. t.}: \quad z_0 = x_k, \tag{5.15b}$$

$$z_i = f_{tmp}(z_{i-1}, v_{i-1}), \tag{5.15c}$$

$$0 = g_{tmp}(z_{i-1}, y_{i-1}), \tag{5.15d}$$

$$z_{min} \le z_i \le z_{max}, \tag{5.15e}$$

$$y_{min} \le y_i \le y_{max}, \tag{5.15f}$$

$$u_{min} \le v_{i-1} \le u_{max}, \quad i = 1, \ldots, N \tag{5.15g}$$

where N is the length of the prediction horizon in sample times. $\mathbf{v} = \{v_0, v_1, \ldots, v_{N-1}\}$ a feasible control moves which satisfy the constraints (5.15b)-(5.15g). z_{min} and z_{max}, y_{min} and y_{max}, and u_{min} and u_{max} are lower and upper bound vectors of differential and algebraic state, and manipulated variables of the TMP process, respectively. $\xi \in \mathbb{R}^{n_\xi} \subset \mathbb{R}^{n_z+n_y}$ is a vector of controlled variables. With the TMP process, the discretized differential variables - production rate, motor loads and consistencies of both primary and secondary refiners - are the controlled variables, i.e. $\xi \equiv z$, while the discretized algebraic state variables: CSF, LFC, SC are controlled within a desired range given in (5.15f). The diagonal matrices Q_ξ and Q_v are weights for controlled state variables and input variables, respectively. ξ^s is the optimum setpoint vector, obtained normally solving a steady-state optimization, for controlled variables, and u^s is the corresponding reference input vector for the control variables. Although the use of reference input vector u^s is not necessary if there is no degree of freedom in the controller i.e. $n_\xi = n_v$, this information might be useful when changing the operating conditions especially for nonlinear processes [27].

5.3.1 Example 1

In this study, the closed-loop is simulated for the TMP process for the setpoint tracking with the NMPC technique. The simulation was set-up so that there was no process/model mismatch and disturbances. In the beginning of the simulation, the production rate, primary motor load and consistency, and secondary motor load and consistency are set to 208 tonnes/day, 10.5 MW and 50 %, and 4.75 MW and 43%, respectively. At time 50s, new target setpoints are introduced as 250 tonnes/day, 8.8 MW, 44 %, 4.82 MW and 37.2%, respectively, along with the new reference input vector, for the setpoint tracking NMPC formulation. The sampling time is 1 s, and the control and prediction horizons are set to 10 s. The controlled and manipulated weighting matrices are kept as $Q_\xi = diag([0.01\ 1\ 1\ 1\ 1]^T)$ and $Q_v = diag([0.8\ 8\ 0.8\ 8\ 0.8]^T \times 10^{-3})$. First, the resulting NLP problem was solved using *fmincon* solver in MATLAB with interior-point option. In this case, it took $5-15$ s CPU seconds to find the optimum solution. In contrast, the IPOPT solver took $0.02-0.04$ s to find the optimum solution. The simulation studies were performed with Intel Core 2 CPU with 2.4 GHz PC.

The computational delay for NMPC optimization introduces feedback delay in the system. This feedback delay may cause poor performance and deterioration of the stability of the system [102], [103]. The computational burden is one of main drawbacks of NMPC techniques when applied to real systems. In [103, 104], it showed how this computational delay can be explicitly included in the NMPC algorithm to ensure minimal degradation of the performance, and moreover, discussed the conditions under which the stability of the closed-loop can be guaranteed. In this chapter, it is assumed that states can be directly measured for the TMP process. However in practice, all states of the TMP process, for example outlet consistencies of the refiners, are not measured, but need to be estimated. Incorporation of a state estimation technique to NMPC formulation would increase the computational burden of the overall problem.

In the following example, the closed-loop simulation was performed to demonstrate the performance of the asNMPC technique described in Section 2.6.2 as a way to reduce on-line computational time, along with the ideal-NMPC technique described in Section 2.3 for the setpoint tracking problem of the TMP process.

5.3.2 Example 2

This simulation study considers the presence of random disturbances on the state variables of the TMP process to illustrate the performance of asNMPC technique. The asNMPC technique computes approximate solution to the resulting NLP problem of NMPC quickly. The ideal NMPC and asNMPC have identical performance under nominal conditions. The difference between the solution of ideal-NMPC and its approximation through asNMPC is identified by the second order effects of model/process mismatch and disturbances [58], which in turn leads to prediction error of the states of the process. As in the first simulation study 5.3.1, the asNMPC and ideal-NMPC techniques are given new setpoint targets, along with the corresponding reference manipulated inputs vector, at time 50s. At 100s, the targets are set back to their original values. The tuning parameters, N, Q_{ξ}, and Q_{v}, are the same as in Example 5.3.1. The IPOPT solver took 0.02 s to solve the NLP problem in ideal-NMPC while the on-line computational time of asNMPC was 0.004s. By providing the values of the variables of the previous solution, the warm-start strategy was used in the both cases. The simulation results are shown in Fig. 5.1 and Fig. 5.2. The simulation results illustrate that the asNMPC technique was able to track the setpoints, similar to the ideal-NMPC technique, in the presence of disturbances.

5.4 NMPC for Economical Operation

As discussed in Section 3.2, the conventional two-layer architecture for advanced control systems has several drawbacks, mainly due to 1) low frequency of opera-

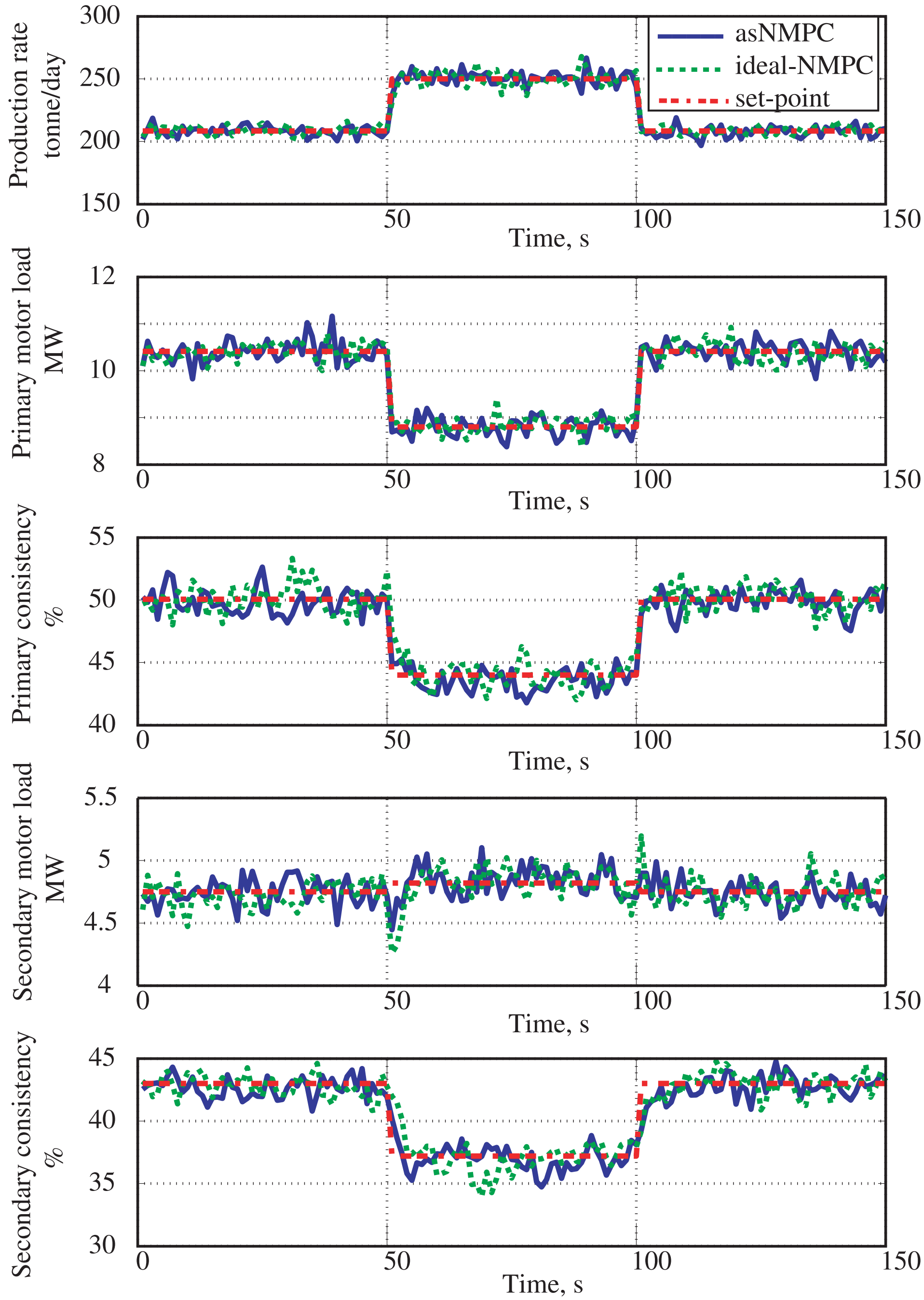

Figure 5.1: Controlled variables of the TMP process: Performance comparison of asNMPC and ideal-NMPC techniques for setpoint tracking problem.

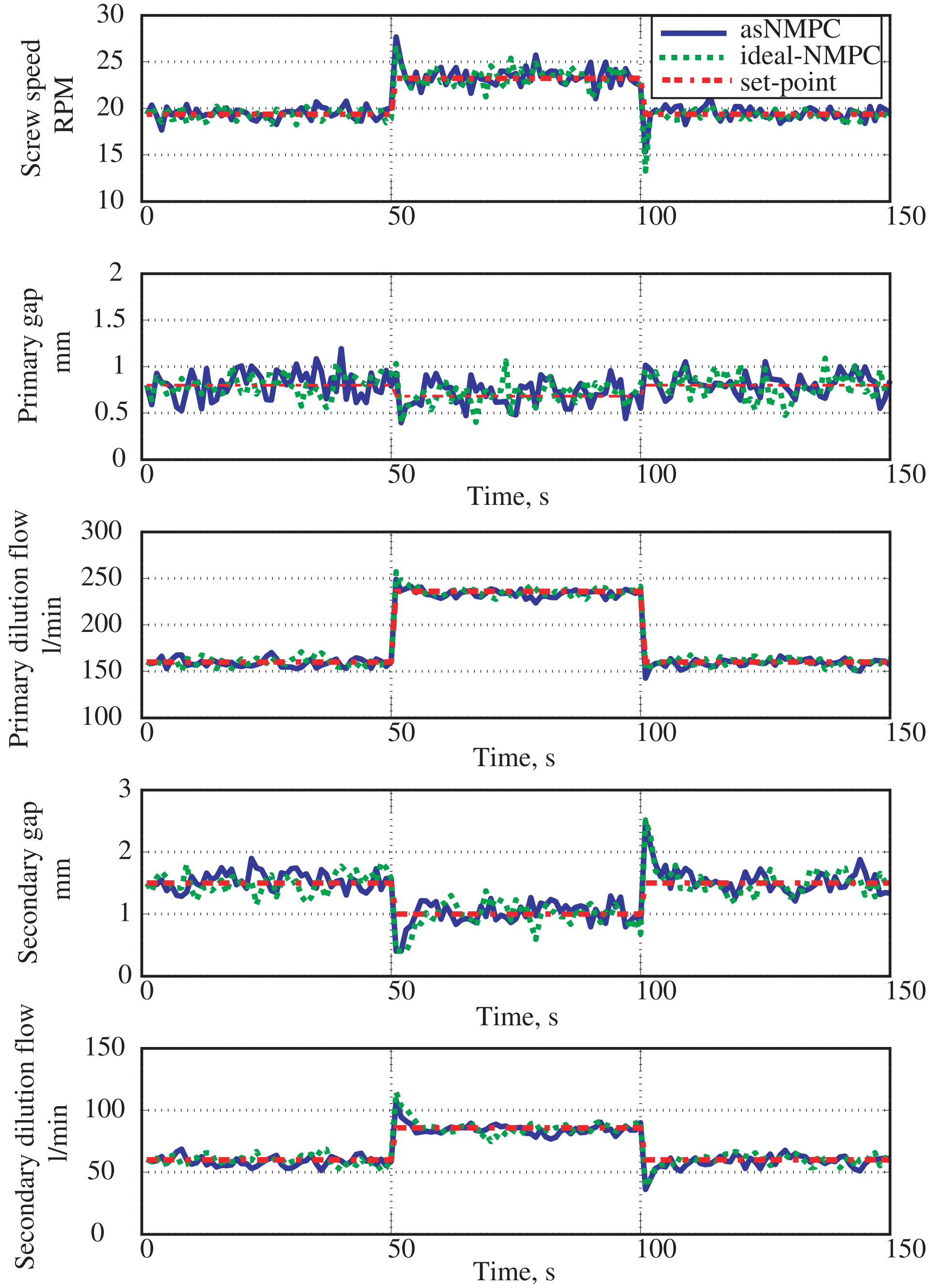

Figure 5.2: Manipulated inputs of the TMP process: Performance comparison of asNMPC and ideal-NMPC techniques for setpoint tracking problem.

tion of the RTO layer, and 2) assumption of slow variation of the disturbances on the process. In particular, disturbances in wood chip species, chip size distribution, the chip solid content, and the chip bulk density are rapidly changing in the TMP process. The consequences of the slow operation of the RTO layer and the disturbances are that the operating setpoints will be sub-optimal and also the economical optimum may not even be at steady-state.

In this section, the economical objective is integrated with the setpoint tracking objective in the formulation of NMPC technique, as discussed in 3.3 and compare the economical benefits with the setpoint tracking NMPC technique when disturbances are present in the TMP process. The simulation studies are performed with the asNMPC control strategy along with IPOPT solver. The specific energy, defined as in Section (5.16), is considered as the economical indicator for the TMP process. The overall economical objective is to minimize the total specific energy while keeping the pulp quality variables within a specific range.

$$\begin{aligned}\text{Specific Energy} &= \frac{\text{Total motor load}}{\text{Production rate}} \quad \text{MW/(tonnes/day)} \\ &= \frac{\text{Primary motor load + Secondary motor load}}{\text{Production rate}}.\end{aligned} \tag{5.16}$$

Thus the objective function for economically-oriented NMPC formulation (econNMPC) is described by

$$J_{econ} = \alpha_{tmp} \sum_{i=1}^{N} \text{Specific Energy} + \beta_{tmp} \sum_{i=0}^{N} \|\xi_i - \xi_{k+i}^s\|_{Q_\xi}^2 + \|v_{i-1} - u_{k+i-1}^s\|_{Q_v}^2. \tag{5.17}$$

The α_{tmp} and β_{tmp} are positive weights for the specific energy and the tracking objectives, respectively. Throughout the rest of this chapter, sptNMPC and econNMPC denote for the NMPC formulations (5.15) with setpoint tracking objective function (5.15a), and with the economically-oriented objective function (5.17), respectively. With the objective function (5.17), the econNMPC technique tries to minimize the specific energy consumption and simultaneously tries to minimize transition time to reach the target setpoint from the current state. Note that first, it was to try to use only the economic objective to formulate the NMPC, i.e. $\beta_{tmp} = 0$ in (5.17) because the overall objective is to minimize the total specific energy consumption while respecting the process constraints. However, as noted by several researchers [65] [105], the difficulty in solving the resulting NLP problem was experienced. This is simply because with $\beta_{tmp} = 0$ it cannot be guaranteed the uniqueness of the solution of the resulting NLP problem, the second order optimality conditions might not hold, and it may lead to ill-posed search directions in the IPOPT solver which makes the NMPC problems difficult to solve [65]. By adding the setpoint tracking objective to the econNMPC formulation in (5.17), the objective function is regularized. In this case, it is necessary to set α_{tmp} and β_{tmp} as 86 and 1, respectively. The following closed-loop simulation studies demonstrate the potential economical benefits of the econNMPC formulation against the sptNMPC formulation when the disturbances are present in the TMP process.

5.4.1 Example 1

In this study, changes in the chip bulk density are considered as a disturbance to the TMP process; variation in the chip bulk density is considered as the main cause of disturbances in this process [6]. Changes in the chip bulk density d_c in (5.1) in turn cause some variations in the production rate (5.1), motor loads (5.2) and consistencies (5.3) instantaneously and hence in specific energy (5.16). This is mainly because the TMP refiners operate based on mass throughput [8]. First, the chip bulk density is set to 90% of its nominal value until 60s of the simulation. Then, the chip bulk density is increased up to 110% of it nominal value for the period of 1 min. Then it is set back to 90% of the nominal value at 120s. Random disturbances on state variables were not considered in order to demonstrate the main effects of the chip bulk density changes. The sampling time is 1s, and the prediction and control horizons are set to 10s for the both sptNMPC and econNMPC techniques. Since the overall economical objective is to minimize the specific energy of the TMP process, the controllers are tuned so that there is some freedom to optimize the specific energy, rather than being constrained by tightly controlled the production rate, motor loads [8].

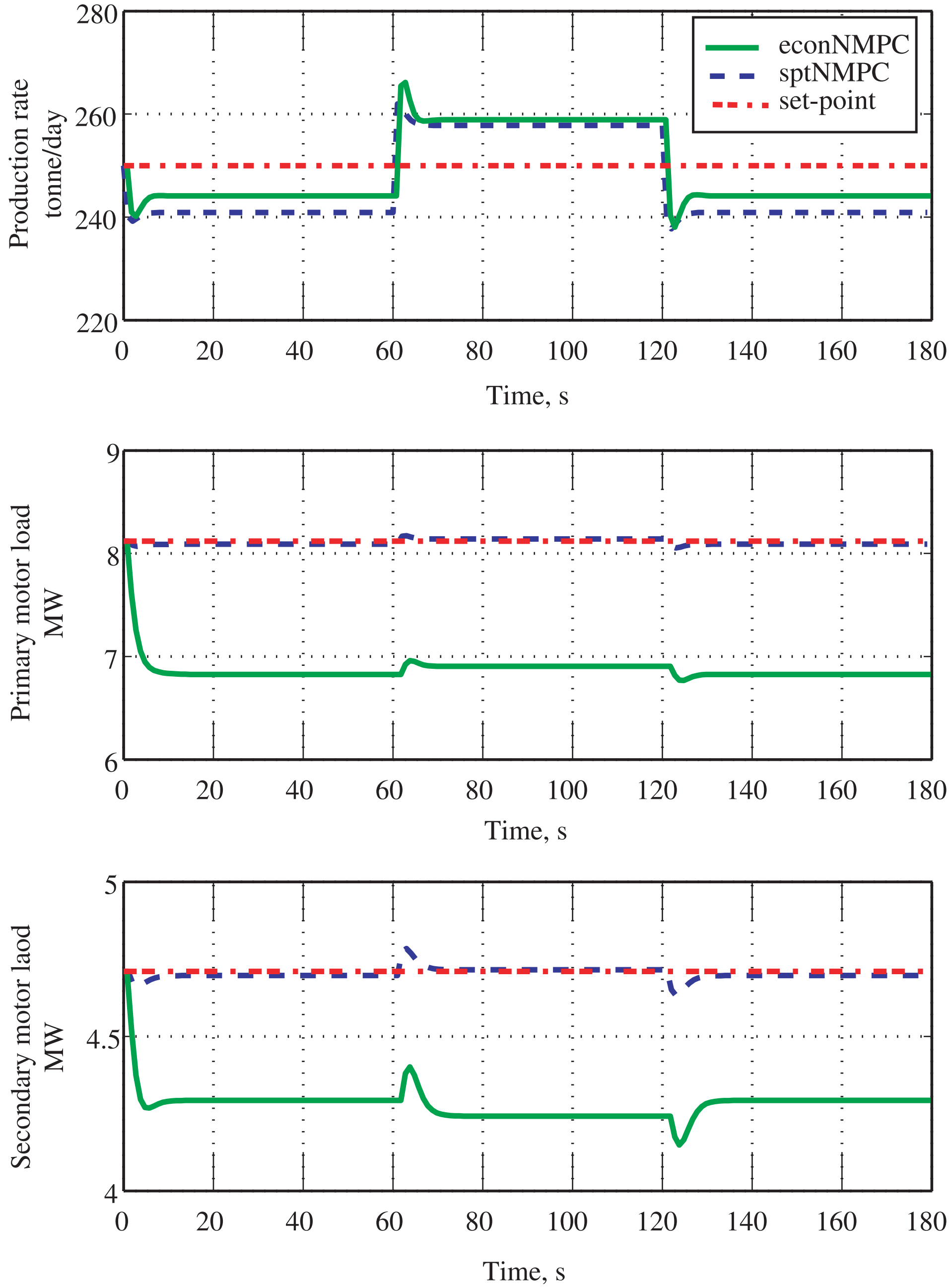

Figure 5.3: The production rate, and motor load responses of the TMP process to the change of the chip bulk density

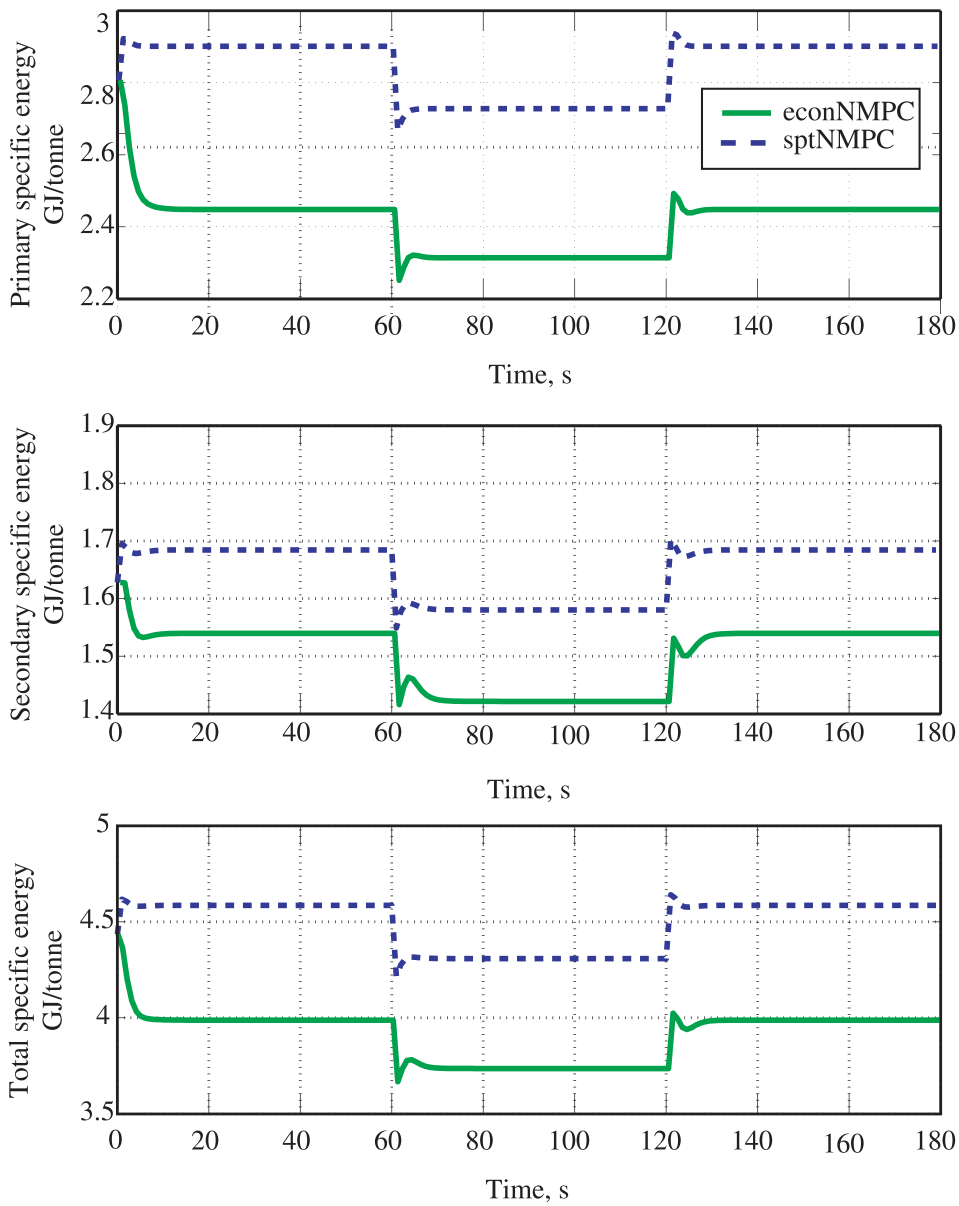

Figure 5.4: The specific energies of the both primary and secondary TMP process: performance comparison of the sptNMPC with econNMPC techniques to the change of the chip bulk density

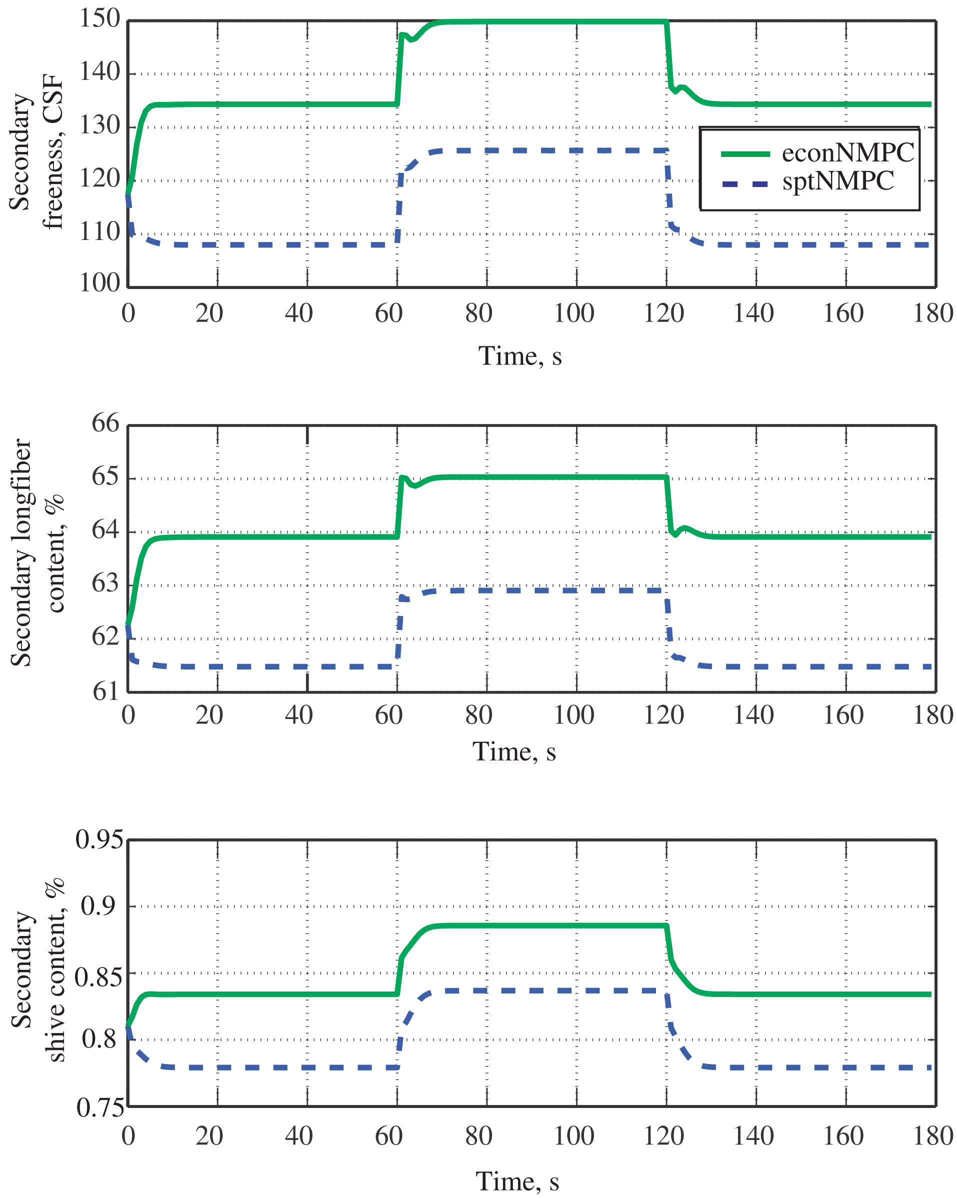

Figure 5.5: The freeness, long fiber content and shive content responses of the TMP process to the change of the chip bulk density.

The closed-loop responses are shown in Fig. 5.3 - 5.5. Fig. 5.3 shows the production rate, primary motor load and secondary motor load responses while Fig. 5.4 shows the specific energy changes during the simulation. As shown in Fig. 5.5, the both asNMPC and econNMPC techniques were able to keep the pulp quality variables: freeness, long fiber content, and shive content, within the operating limits of $(0-175)$ CSF, $(50-70\%)$, and $(0-1.2\%)$, respectively. As it is clear from the simulation results, there is a potential reduction, about 13%, in total specific energy in the system with the econNMPC technique, in contrast to the system with the sptNMPC technique. The changes in the chip bulk density and the chip solid content are considered as disturbances in Example 5.4.2, where the closed-loops are simulated with some random disturbances on the state variables.

5.4.2 Example 2

The objective of this simulation study is to show the economic benefits of the econNMPC technique with the presence of state disturbances. The simulation set-up is same as Example 5.4.1. Here, changes in the chip solid content is considered as an additional disturbance from 180s to 300s of the simulation. The variation in the chip solid content s_c in (5.1) or chip moisture content is also a key disturbance, which causes production rate (5.1), motor loads (5.2), and consistencies (5.3) to change in the TMP process. Up to 180 s the chip bulk density changes are the same as in Example 5.4.1. After that, from 180s to 240s the chip solid content is set to increase to 110% and decrease to 90% of its nominal value at 240s, while keeping the chip bulk density as 90% of its nominal value. The closed-loop simulation results are shown in Fig. 5.6 - 5.8. Fig. 5.6 shows the production rate, motor loads and consistencies for the both primary and secondary refiners. As it is clearly seen from Fig. 5.7, there is still reduction in specific energy, of about 12%, in the TMP process, even with some random disturbances on the state variables. The both asNMPC and econNMPC techniques were able to keep the pulp quality variables: freeness, long fiber content, and shive content, within the operating limits of $(0-175)$ CSF, $(50-70\%)$, and $(0-1.2\%)$, respectively. Here the pulp quality variables are considered being measured once a second just after the secondary refiner.

5.5 Conclusion

In this chapter, an NMPC strategy for the setpoint tracking problem, described in Section 2.3, for the TMP refiner process is first presented. The burden of computational delay for NMPC was handled by using the asNMPC concept, described in Section 2.3, with the IPOPT solver described in Section 2.6.2. The performances were the same as the system with ideal NMPC strategy 2.3. Next, an economical objective was integrated to the NMPC formulation to dynamically optimize the TMP process with the presence of disturbances. A potential economic benefit was realized through reductions, of about 13%, in the total specific energy of the TMP process when chip bulk density changes with time, compared to the closed-loop system with the setpoint tracking NMPC technique. In the final simulation study, it was realized approximately 12% reduction in the total specific energy when the TMP process undergoes the both chip bulk density and chip solid content changes, and some random disturbances on the state variables.

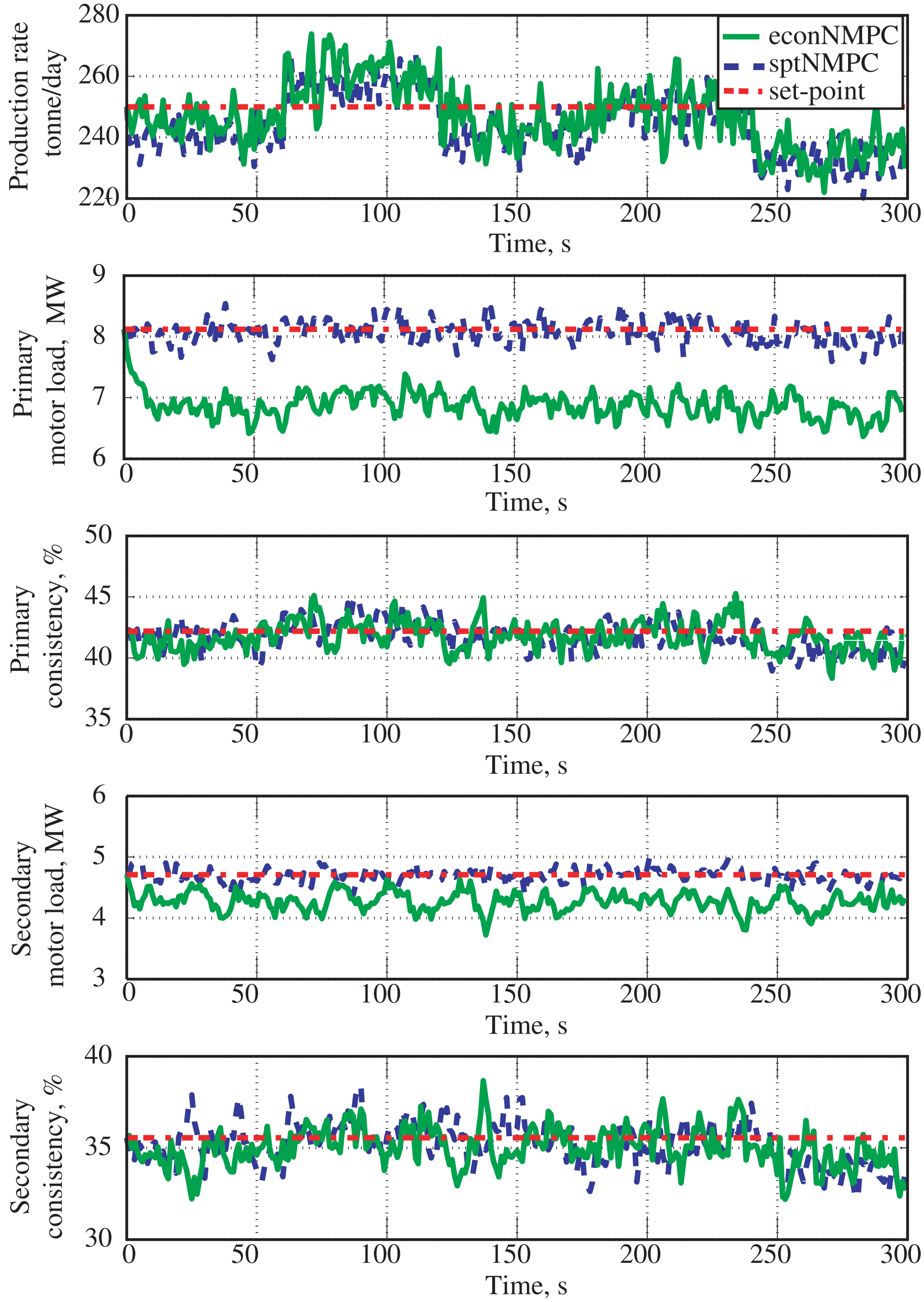

Figure 5.6: The production rate, consistencies and motor loads responses of the TMP process to the change of the chip bulk density and chip solid content, with random disturbances on the state variables

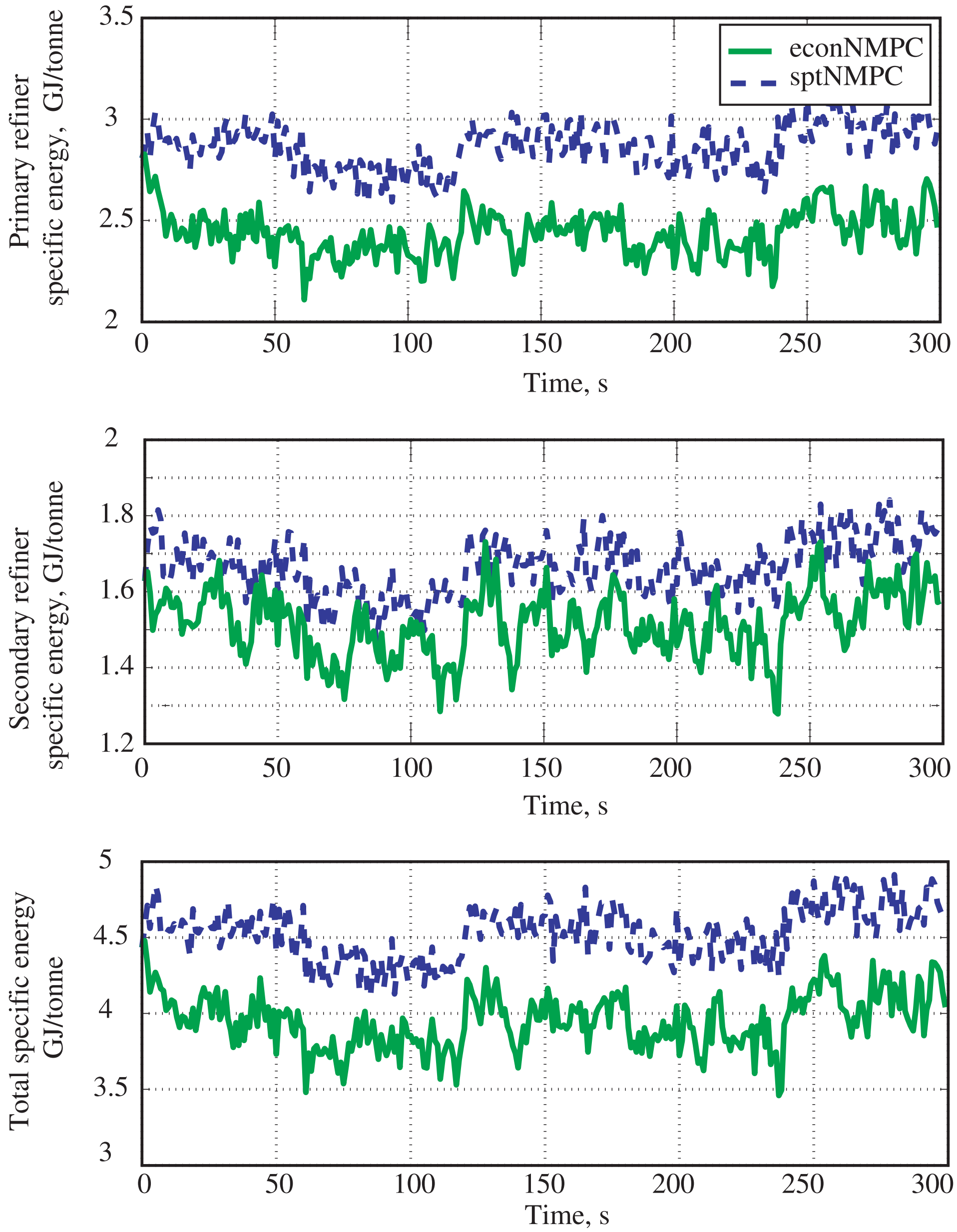

Figure 5.7: The specific energies of the both primary and secondary the TMP process: performance comparison of the sptNMPC and econNMPC techniques to the change of the chip bulk density and chip solid content, with random disturbances on the state variables

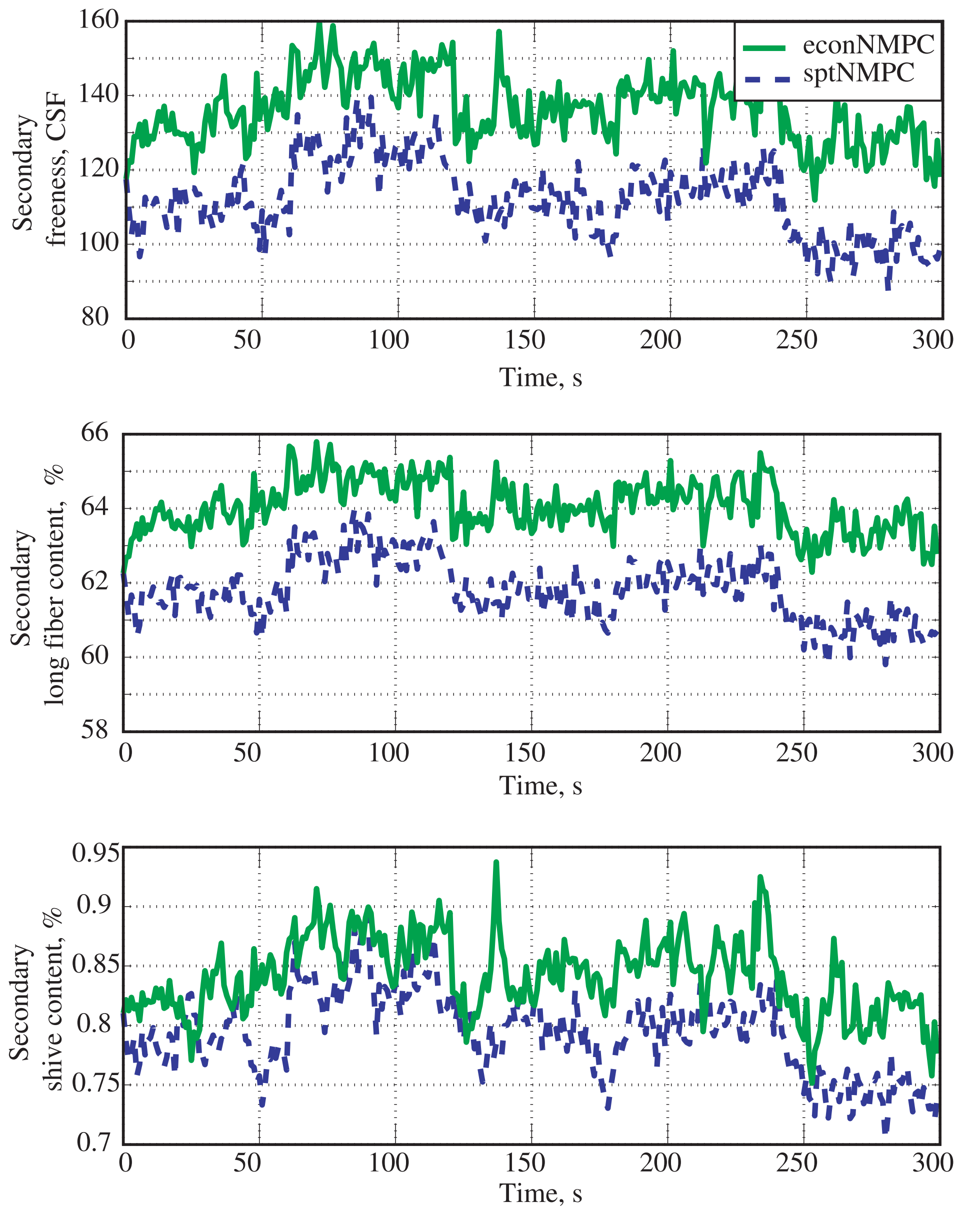

Figure 5.8: The freeness, long fiber content and shive content responses of the TMP process to the change of the chip bulk density and chip solid content, with random disturbances on the state variables.

Chapter 6

Control and Optimization of TMP Processes with Multi-stage Low Consistency Refining

6.1 Summary

In this chapter, nonlinear model based dynamic optimization approaches for optimal control for TMP processes are presented. Two types of TMP refining processes are considered. The first TMP process is a conventional refining process with two-stages of HC refining with a primary and a secondary refiners followed by a latency chest and a third-stage LC refiner, while the second TMP process has only a HC primary refiner, and the secondary stage HC refiner is replaced by multiple-stages of LC refiners after the latency test. Both TMP plants are dynamically optimized against disturbances to produce the same target final pulp qualities while minimizing specific energy consumptions of the processes. In this work, a NMPC technique with an economic objective function is considered. The simulations result shows the potential economical benefits of an improved TMP process, the TMP process with multi-stage LC refining, through a reduction in total specific energy, compared to a conventional TMP process. The NMPC controller is implemented with the asNMPC concept described in Section 2.6.2, and by using the IPOPT described in Section 2.6.1.

6.2 Introduction

The advanced control of TMP processes, which aims at optimal operation of the process, has become of prime important [5, 8, 14, 67]. The primary objective of these advanced control systems is to minimize energy consumption while reducing variability in pulp quality against inevitable disturbances. Most of the industrial implementations of advanced TMP control systems has been considered for main line primary and secondary refiners and, in some instances, for main line reject refiners and screening processes [8, 106]. The mainline refiners are, however, high energy-consuming; approximately 60% of total energy in the TMP process is consumed by these refiners as they operate at HC [1]. Therefore, in recent years, researchers have leaned toward developing LC refining technology, which would be more energy efficient than conventional HC refining [1, 18]. At the same time, the pulping industry tends to install LC refiners in the main line, most commonly following the latency chest and before the screening process [18, 107, 108]. The inclusion of the third stage LC refiner in the mainline has led to the reconsideration of advanced control system to optimally coordinate the HC and LC refiners.

In this chapter, the econNMPC framework is investigated for two TMP processes to dynamically optimize the processes when the inevitable disturbances present. In Scheme A, a conventional TMP refining process is considered, where it has two-stages of HC refining with a primary and a secondary refiners followed by a latency chest and a third-stage LC refiner. In Scheme B, the improved TMP process [1] only has one HC primary refiner, and the secondary stage HC refiner is replaced by multiple-stages of LC refiners after the latency test. Both the schemes are compared with setpoint tracking NMPC and econNMPC techniques. In this work, the resulting NLP problem is solved using the IPOPT solver, described in Section 2.6.1, in order to handle the computational burden. The feedback computational is further improved with the asNMPC concept, described in Section 2.6.2. To the best of author's knowledge to date, this work is one of the first contributions that investigates dynamic optimization of TMP processes with multi-stage LC refining using an economically oriented NMPC framework.

6.3 Process Description and Modeling

In this work, the HC refiners are modeled as described in Section 5.2.1. In the latency chest, latency removal is characterized by freeness drop, and LFC and SC are assumed remain unchanged. The model for latency chest freeness presented in [109] is used in this work. For LC refiners, recently developed steady state models in [1] are used.

6.3.1 Latency Chest Modeling

Consistency in the latency chest can be modeled using mass balance. Assuming water and energy losses are negligible, the following model can be expressed, similar to the model described in (5.2.1).

$$C_l = \frac{100P}{(P/(0.01C_s) + 1.44D_l)}, \tag{6.1a}$$

where $C_l(\%)$ is latency chest consistency, $P(tonne/day)$ production rate, $C_s(\%)$ secondary refiner consistency, and $D_l(l/min)$ latency chest dilution water flow rate. The model presented in [109] for CSF in the latency chest is adapted for steady state modeling as follows.

$$CSF_l^{out} = CSF_l^{in}\left\{1 - \frac{1}{\left(1 + a_l \exp^{-(\frac{b_l}{T_l})}\right)}\right\}, \tag{6.1b}$$

where CSF_l^{out} and CSF_l^{in} are freeness of the pulp after and before the latency chest, respectively. $T_l(^\circ C)$ is the temperature of the latency chest. a_l and b_l are parameters.

6.3.2 LC Refiner Modeling

In a most recent work [1], the following models are presented for motor load, LFC, and CSF for LC refiners, respectively.

$$M_t = km_t \left(\frac{D_t}{G_t}\right)^{a_t} \left(\frac{FL_{in}}{D_t}\right)^{b_t}, \tag{6.2a}$$

where $M_t(MW)$ is the LC refiner motor load, $D_t(m)$ is the diameter of the LC refiner, $G_t(mm)$ is the gap, $FL_{in}(mm)$ is the length of the incoming fiber to the LC refiner. km_t, a_t, and b_t are parameters for a given LC refiner.

$$CSF_t^{out} = CSF_t^{in} \exp^{\left(\frac{CSF_t^{in}}{D_t^3}\right)^{-c_t} \left(\frac{D_t}{G_t}\right)^{d_t} \frac{NSE_t}{\omega^2 D_t^2}} \tag{6.2b}$$

where $CSF_t^{out}(CSF)$, and $CSF_t^{in}(CSF)$ are the freeness of the pulp before and after the LC refining, respectively. $NSE_t(kWh/t)$ is the net specific energy, and $\omega(1/s)$ is the LC refiner rotational speed. c_t and d_t are parameters for a given LC refiner.

$$LFC_t^{out} = \begin{cases} a_{lfc} LFC_t^{in} & \text{if } G_t \geq G_{crit}; \\ \left(h_{lfc} \ln\left(\frac{G_t}{G_{crit}}\right) + a_{lfc}\right) LFC_t^{in} & \text{if } G_t < G_{crit}, \end{cases} \tag{6.2c}$$

where $LFC_t^{out}(\%)$ and $LFC_{in}(\%)$ are LFC after and before LC refining, respectively. $G_{crit}(mm)$ is the critical gap. a_{lfc} and h_{lfc} are parameters.

6.4 Scheme A: Conventional TMP Process with a Third-stage LC Refiner

Two-stage TMP processes are most common in pulp and paper industry, and have extensively been studied for optimal operation [8, 67]. However, with the introduction of more energy efficient LC refining technology, a third stage LC refiner is installed just after the latency chest as shown in Fig. 6.1. The precise physical mechanism for the increased efficiency of LC refining is not yet clearly understood [1]. Despite the lack of a theoretical understanding of LC refining, LC refiners are being applied in the pulp and paper industry, and significant energy savings

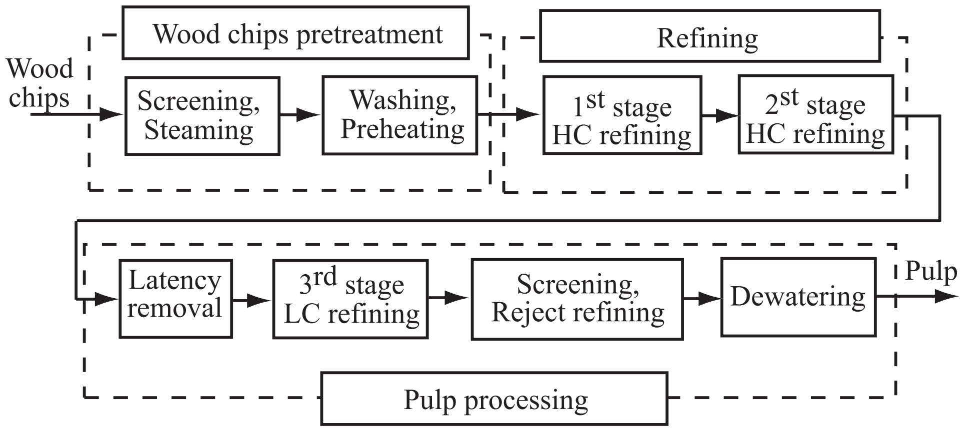

Figure 6.1: Scheme A: basic schematic of a conventional TMP process with a third stage LC refiner

are reported [108]. In this work, a Wiener type discrete-time nonlinear model for this TMP refining process is used in the NMPC formulation, similar to the model described in Section 5.5.

$$z_{k+1} = A^A_{tmp} z_k + h^A_{tmp}(z_k, v_k) \tag{6.3a}$$

$$0 = g^A_{tmp}(z_k, y_k), \tag{6.3b}$$

where $(\cdot)^A$ denotes Scheme A, $z_k \in \mathbb{R}^{n_z}$, $y_k \in \mathbb{R}^{n_y}$, and $v_k \in \mathbb{R}^{n_v}$ denote the vectors of discretized differential state, algebraic state, and manipulated variables of the TMP refining model. n_z, n_y, and n_v are dimensions of the variables z, y, and v, respectively. Then

$$z = \begin{bmatrix} \text{Production rate} \\ \text{Primary refiner motor load} \\ \text{Primary refiner consistency} \\ \text{Secondary refiner motor load} \\ \text{Secondary refiner consistency} \\ \text{Consistency after latency chest} \\ \text{CSF after latency chest} \\ \text{Tertiary refiner motor load} \\ \text{CSF after tertiary refiner} \end{bmatrix}, \; y = \begin{bmatrix} \text{CSF after primary refining} \\ \text{LFC after primary refining} \\ \text{SC after primary refining} \\ \text{CSF after secondary refining} \\ \text{LFC after secondary refining} \\ \text{SC after secondary refining} \\ \text{LFC after latency chest} \\ \text{SC after latency chest} \\ \text{LFC after tertiary refiner} \\ \text{SC after tertiary refiner} \end{bmatrix}, \text{ and}$$

$$v = \begin{bmatrix} \text{Chip-transfer screw speed} \\ \text{Primary refiner plate gap} \\ \text{Primary refiner dilution water flow rate} \\ \text{Secondary refiner plate gap} \\ \text{Secondary refiner dilution water flow rate} \\ \text{Latency chest temperature} \\ \text{Latency chest dilution water flow rate} \\ \text{Tertiary refiner plate gap} \end{bmatrix}. \tag{6.4}$$

$A^A_{tmp} \in R^{n_z \times n_z}$ is the dynamic matrix, and the nonlinear state function, $h^A_{tmp} : \mathbb{R}^{n_z+n_v} \mapsto \mathbb{R}^{n_z}$, maps steady-state control input variables to steady-state differential state variables of the TMP refining model. g^A_{tmp} is the nonlinear implicit function of variables z and y. For simplicity, a general form of state equation for (6.3a) is considered in following NMPC formulations.

$$z_{k+1} = f^A_{tmp}(z_k, v_k) \tag{6.5}$$

Note that in Scheme A, the TMP process is simulated up to the tertiary LC refiner, assuming the pulp quality measurements are available at that point. The following section describes the NMPC strategy for setpoint tracking problem for the TMP process 6.1.

6.4.1 NMPC for Setpoint Tracking and Economical Operation

Similar to Section 5.3, using current process state x_k, the dynamic optimization problem is formulated for the NMPC at sample time k as follows.

$$\min_{\mathbf{v}} \quad J^A_{spt}, \quad J^A_{spt} := \sum_{i=1}^{N^A} \|\xi_i^A - \xi^{A_s}_{k+i}\|^2_{Q_{\xi^A}} + \|v_{i-1} - u^{A_s}_{k+i-1}\|^2_{Q_{v^A}} \tag{6.6a}$$

$$\text{s. t.}: \quad z_0 = x_k, \tag{6.6b}$$

$$z_i = f^A_{tmp}(z_{i-1}, v_{i-1}), \tag{6.6c}$$

$$0 = g^A_{tmp}(z_{i-1}, y_{i-1}), \tag{6.6d}$$

$$z_{min} \le z_i \le z_{max}, \tag{6.6e}$$

$$y_{min} \le y_i \le y_{max}, \tag{6.6f}$$

$$u_{min} \le v_{i-1} \le u_{max}, \quad i = 1, \ldots, N^A \tag{6.6g}$$

where N^A is the length of the prediction horizon in sample times. $\mathbf{v} = \{v_0, v_1, \ldots, v_{N^A-1}\}$ a feasible control moves which satisfy the constraints (6.6b)-(6.6g). z_{min} and z_{max}, y_{min} and y_{max}, and u_{min} and u_{max} are lower and upper bound vectors of differential and algebraic state, and manipulated variables of the TMP process (6.1), respectively. $\xi^A \in \mathbb{R}^{n_\xi} \subset \mathbb{R}^{n_z+n_y}$ is a vector of controlled variables. For Scheme A, $\xi^A \equiv z$. Since the final freeness, after the tertiary LC refiner, is controlled to a desired value, it is considered as a controlled variable in this formulation. The diagonal matrices Q_{ξ^A} and Q_{v^A} are weights for the controlled state variables and input variables, respectively. ξ^{A_s} is the optimum setpoint vector, obtained solving a steady-state optimization, for controlled variables, and u^{A_s} is the corresponding reference input vector for the control variables. In the econNMPC formulation, the following objective function (6.7) is minimized whereas in the NMPC optimization (6.6), J^A_{spt} is minimized.

$$J^A_{econ} = \alpha^A_{tmp} \sum_{i=1}^{N^A} \text{Specific Energy} + \beta^A_{tmp} \sum_{i=1}^{N^A} \|\xi_i - \xi_{i+1}\|^2_{Q_{\xi^A}} + \|v_{i-1} - v_i\|^2_{Q_{v^A}}, \tag{6.7}$$

where Specific Energy is defined as

$$\begin{aligned}\text{Specific Energy} &= \frac{\text{Total motor load}}{\text{Production rate}} \quad \text{MW/(tonnes/day)} \\ &= \frac{\text{Primary motor load + Secondary motor load + Tertiary motor load}}{\text{Production rate}}.\end{aligned} \tag{6.8}$$

α^A_{tmp} and β^A_{tmp} are positive weights for the specific energy and the tracking objectives, respectively. Similar to the description in Section 5.3, with this objective function (6.7), the econNMPC technique tries to minimize the specific energy consumption and simultaneously tries to minimize transition time to reach a steady state from the current state. Throughout this chapter, sptNMPC and econNMPC denote for the NMPC formulations (6.6), with setpoint tracking objective function (6.6a), and with the economically-oriented objective function (6.7), respectively.

6.4.2 Closed-loop Simulation

The objective of this simulation study is to show the economical benefits of the econNMPC technique with the presence of disturbances. Changes in the chip bulk density and chip solid content are considered as the main disturbances, and additionally, random disturbances on the state variables are also considered in the the TMP process (6.1). As discussed in Example 5.4.1, changes in the chip bulk density d_c and chip solid content s_c in (5.1) in turn cause some variations in the production rate, motor loads, consistencies and specific energy (6.8). Table 6.1 shows the values of the chip bulk density and chip solid content from their nominal values during the closed-loop simulation.

Time, s	0 -60	60 - 120	120 - 180	180 - 240	240 - 300
Chip bulk density	95%	110%	100%	110%	90%
Chip solid content	100%	100 %	90 %	90%	90%

Table 6.1: The chip bulk density and chip solid content changes during the closed-loop simulation of the TMP process in Scheme A

The sptNMPC and econNMPC techniques are both implemented with the same set of disturbances. The sampling time is 1s, and the prediction and control horizons are set as $N^A = 30$ for both the sptNMPC and econNMPC techniques. The controlled and manipulated weighting matrices are kept as $Q_{\xi^A} = diag([0.01\ 0.5\ 1\ 0.5\ 1\ 1\ 1\ 0.5\ 1]^T \times 10^{-1})$ and $Q_{v^A} = diag([0.8\ 8\ 0.8\ 8\ 0.8\ 0.8\ 0.8\ 8]^T \times 10^{-1})$. $\alpha^A_{tmp} = 1000$ and $\beta^A_{tmp} = 1$. The closed-loop simulation results are shown in Fig. 6.2 - 6.5. As evident from the result in Fig. 6.4, there is 188 kWh/tonne reduction in average specific energy, i.e. about 13%, in the system with econNMPC technique when disturbances are present, compared to the system with sptNMPC technique. Both sptNMPC and econNMPC techniques were able to keep the pulp quality variables: long fiber content, and shive content, within the operating limits of $(50-75\%)$, and $(0-2.5\%)$, respectively, while keeping final freeness after the tertiary LC refining at the desired value of 106.5 (CSF). Here, the pulp quality variables are considered being measured once every second just after the tertiary LC refiner.

6.5 Scheme B: Improved TMP Process with Single-stage of HC and Multi-stage LC Refiners

In this section, an improved TMP process presented in [1] is studied for optimal operation, where the secondary stage refining in the conventional TMP process, see Fig. 6.1, is replaced by multi-stages of LC refining after the latency chest as shown in Fig. 6.6. The process is dynamically optimized when the disturbances are present. As discussed in Section 6.3, the improved TMP process is modeled for the NMPC formulation. In Scheme B, the two-stages of LC refining are found to be optimal at steady state to replace the secondary stage HC refiner of the TMP process discussed in Scheme A [1]. Hence in this work, two LC refiners are placed after the latency chest as shown in Fig. 6.6. For this process, the following general nonlinear model can be expressed.

$$z_{k+1} = f^B_{tmp} = A^B z_k + h^B(z_k, v_k) \tag{6.9a}$$

$$0 = g^B(z_k, y_k) \tag{6.9b}$$

where z, y, and v can be given by

$$z = \begin{bmatrix} \text{Production rate} \\ \text{Primary refiner motor load} \\ \text{Primary refiner consistency} \\ \text{Consistency after latency chest} \\ \text{CSF after latency chest} \\ \text{Tertiary refiner 1 motor load} \\ \text{CSF after tertiary refiner 1} \\ \text{Tertiary refiner 2 motor load} \\ \text{CSF after tertiary refiner 2} \end{bmatrix}, \; y = \begin{bmatrix} \text{CSF after primary refining} \\ \text{LFC after primary refining} \\ \text{SC after primary refining} \\ \text{LFC after latency chest} \\ \text{SC after latency chest} \\ \text{LFC after tertiary refiner 1} \\ \text{SC after tertiary refiner 1} \\ \text{LFC after tertiary refiner 2} \\ \text{SC after tertiary refiner 2} \end{bmatrix}, \text{ and}$$

$$v = \begin{bmatrix} \text{Chip-transfer screw speed} \\ \text{Primary refiner plate gap} \\ \text{Primary refiner dilution water flow rate} \\ \text{Latency chest temperature} \\ \text{Latency chest dilution water flow rate} \\ \text{Tertiary refiner 1 plate gap} \\ \text{Tertiary refiner 2 plate gap} \end{bmatrix}. \qquad (6.10)$$

6.5.1 NMPC for Setpoint Tracking and Economical Operation

Similar to the optimization problem in Scheme A, the dynamic optimization problem is formulated for the NMPC at sample time k (6.11). Here all the variables are corresponding to the TMP process in Scheme B, and have been defined similar to Scheme A. First, the setpoint tracking problem is solved. Then econNMPC is formulated with the economic objective function 6.12. For Scheme B, $\xi^B \equiv z$. In oder to compare performances and specific energy savings of the TMP processes in Schemes A and B, the final freeness after the tertiary LC refiner 2, is controlled to that of the same desired value of the TMP process in Scheme A.

$$\min_{\mathbf{v}} \quad J^B_{spt}, \quad J^B_{spt} := \sum_{i=1}^{N^B} \|\xi_i^B - \xi^{B_s}_{k+i}\|^2_{Q_{\xi^B}} + \|v_{i-1} - u^{B_s}_{k+i-1}\|^2_{Q_{v^B}} \tag{6.11a}$$

$$\text{s. t.}: \quad z_0 = x_k, \tag{6.11b}$$

$$z_i = f^B_{tmp}(z_{i-1}, v_{i-1}), \tag{6.11c}$$

$$0 = g^B_{tmp}(z_{i-1}, y_{i-1}), \tag{6.11d}$$

$$z_{min} \le z_i \le z_{max}, \tag{6.11e}$$

$$y_{min} \le y_i \le y_{max}, \tag{6.11f}$$

$$u_{min} \le v_{i-1} \le u_{max}, \quad i = 1, \ldots, N^B \tag{6.11g}$$

In the econNMPC formulation, the following objective function (6.12) is minimized.

$$J^B_{econ} = \alpha^B_{tmp} \sum_{i=1}^{N^B} \text{Specific Energy} + \beta^A_{tmp} \sum_{i=1}^{N^B} \|\xi_i - \xi_{i+1}\|^2_{Q_{\xi^A}} + \|v_{i-1} - v_i\|^2_{Q_{v^A}}, \tag{6.12}$$

where Specific Energy is defined as

$$\text{Specific Energy} = \frac{\text{Total motor load}}{\text{Production rate}} \quad \text{MW/(tonnes/day)}$$
$$= \frac{\text{Primary refiner motor load + Tertiary refiner 1 motor load + Tertiary refiner 2 motor load}}{\text{Production rate}}. \tag{6.13}$$

α^B_{tmp} and β^B_{tmp} are positive weights.

6.5.2 Closed-loop Simulation

In this simulation study, the sptNMPC and econNMPC techniques are formulated for the TMP process in Scheme B discussed in Section 6.6. The simulation set-up is the same as that in Scheme A discussed in Section 6.4.2, and the disturbances presented in Table 6.1 are placed during the closed-loop simulation. The sampling time is 1s, and the prediction and control horizons are set as $N^B = 30$ for both the sptNMPC and econNMPC techniques. The controlled and manipulated weighting matrices are kept as $Q_{\xi^B} = diag([0.01\ 0.5\ 1\ 1\ 1\ 0.5\ 1\ 0.5\ 1]^T \times 10^{-1})$ and $Q_{v^B} = diag([0.8\ 8\ 0.8\ 0.8\ 0.8\ 8\ 8]^T \times 10^{-1})$. $\alpha^B_{tmp} = 1000$ and $\beta^B_{tmp} = 1$. The closed-loop simulation results are shown in Fig. 6.7 - 6.10. There is 88 kWh/tonne reduction in average specific energy, i.e. about 7.5%, in the system with econNMPC technique when disturbances are present, compared to the system with sptNMPC technique. Similar to Scheme A 6.4.2, both the sptNMPC and econNMPC techniques were able to maintain the pulp quality variables: long fiber content, and shive content, within the operating limits of $(50-75\%)$, and $(0-2.5\%)$, respectively, while keeping final freeness after the tertiary LC refining at the desired value of 106.5 (CSF).

6.6 Conclusion

In this chapter, optimal operations of two TMP process schemes have been studied. The Scheme A considers a conventional TMP process while Scheme B considers an improved TMP process with multi-stages of LC refining. The dynamic optimizations are performed within the NMPC framework for both the processes. Significant savings in specific energy are noticed when the disturbances are present, compared to setpoint tracking NMPC formulation, with the econNMPC technique for both the Schemes, while respecting the pulp quality requirements. Fig. 6.11 shows the specific energy comparison for both the Schemes with sptNMPC and econNMPC techniques. The average reduction in specific energy from the system with sptNMPC in Scheme A to the system with sptNMPC in Scheme B is around 252 kWh/tonne, about 18%. The average reduction is around 340 kWh/tonne, or 24%, from the system with sptNMPC in Scheme A to the system with econNMPC in Scheme B. Note that in [1], it showed that around 20% of specific energy reduction can be achieved with an improved TMP process at the steady state, compare to a convention TMP process in Scheme A. Finally, this simulation study concludes that multi-stage LC refining technology can save specific energy of approximately 18% with existing setpoint tracking control when disturbances are present. Further, approximately 6% reduction can be achieved with the proposed econNMPC technique.

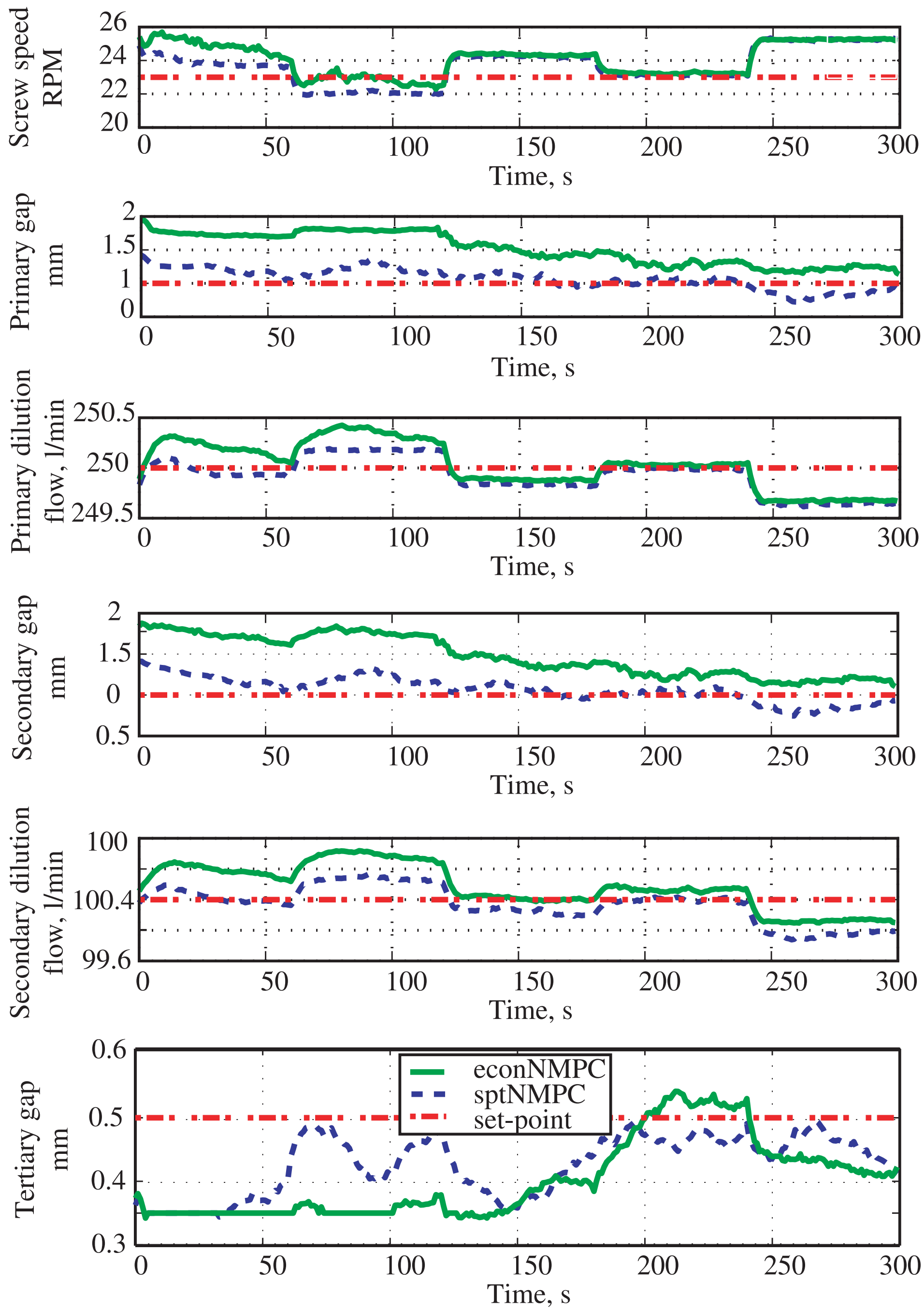

Figure 6.2: The manipulated input variables of the TMP process in Scheme A.

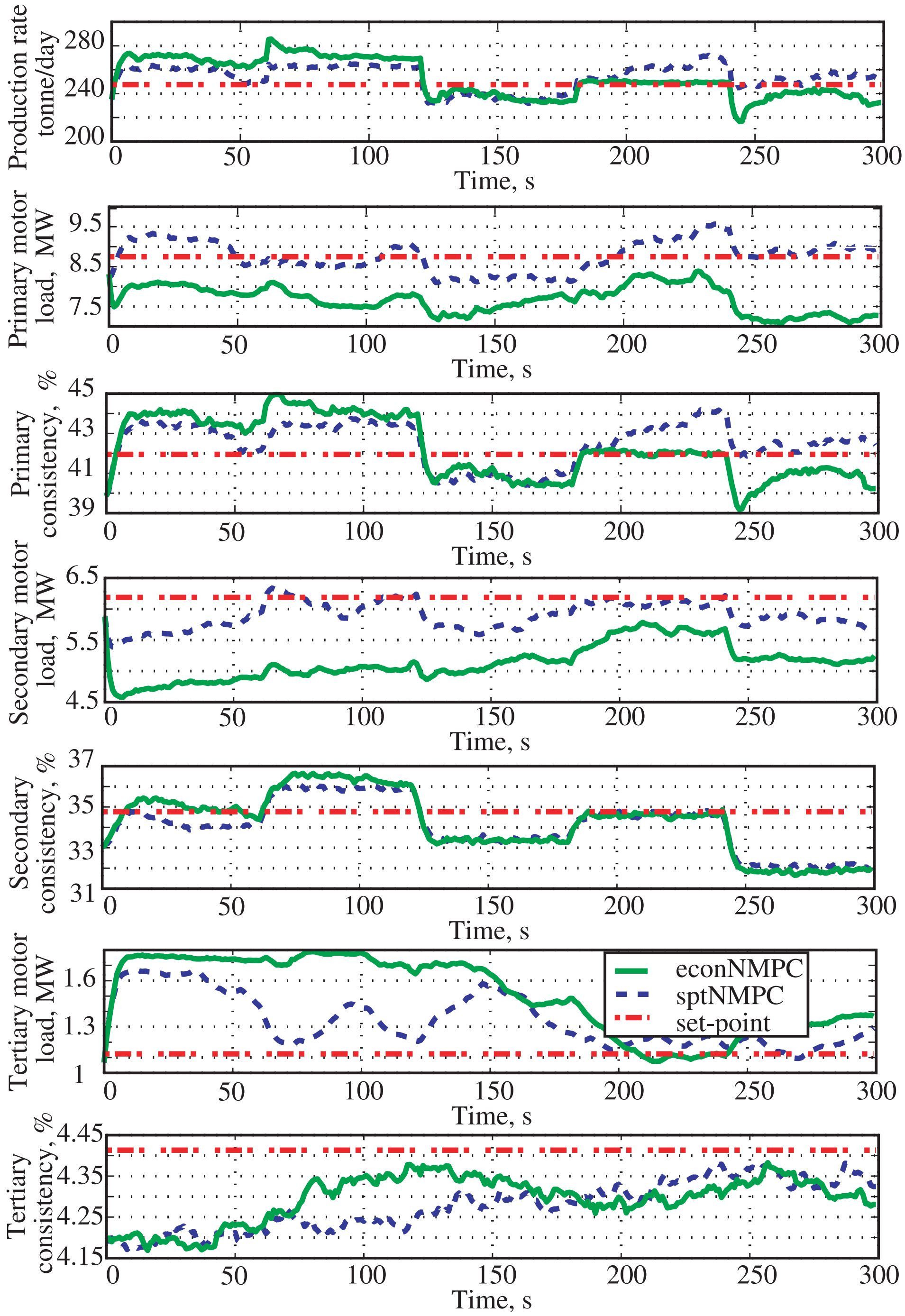

Figure 6.3: The controlled state variables of the TMP process in Scheme A.

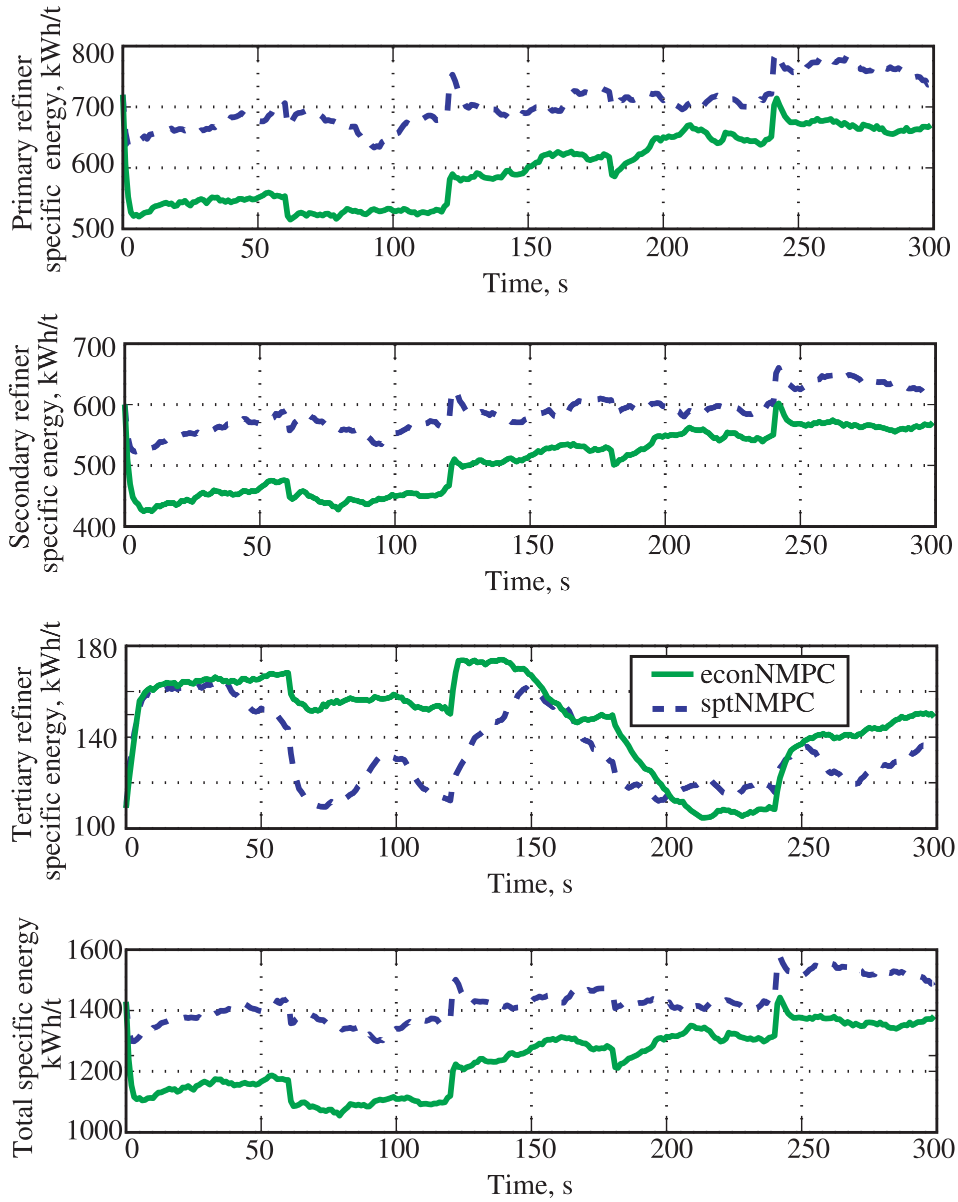

Figure 6.4: The specific energy consumptions of the primary, secondary, and tertiary refiners of TMP process in Scheme A.

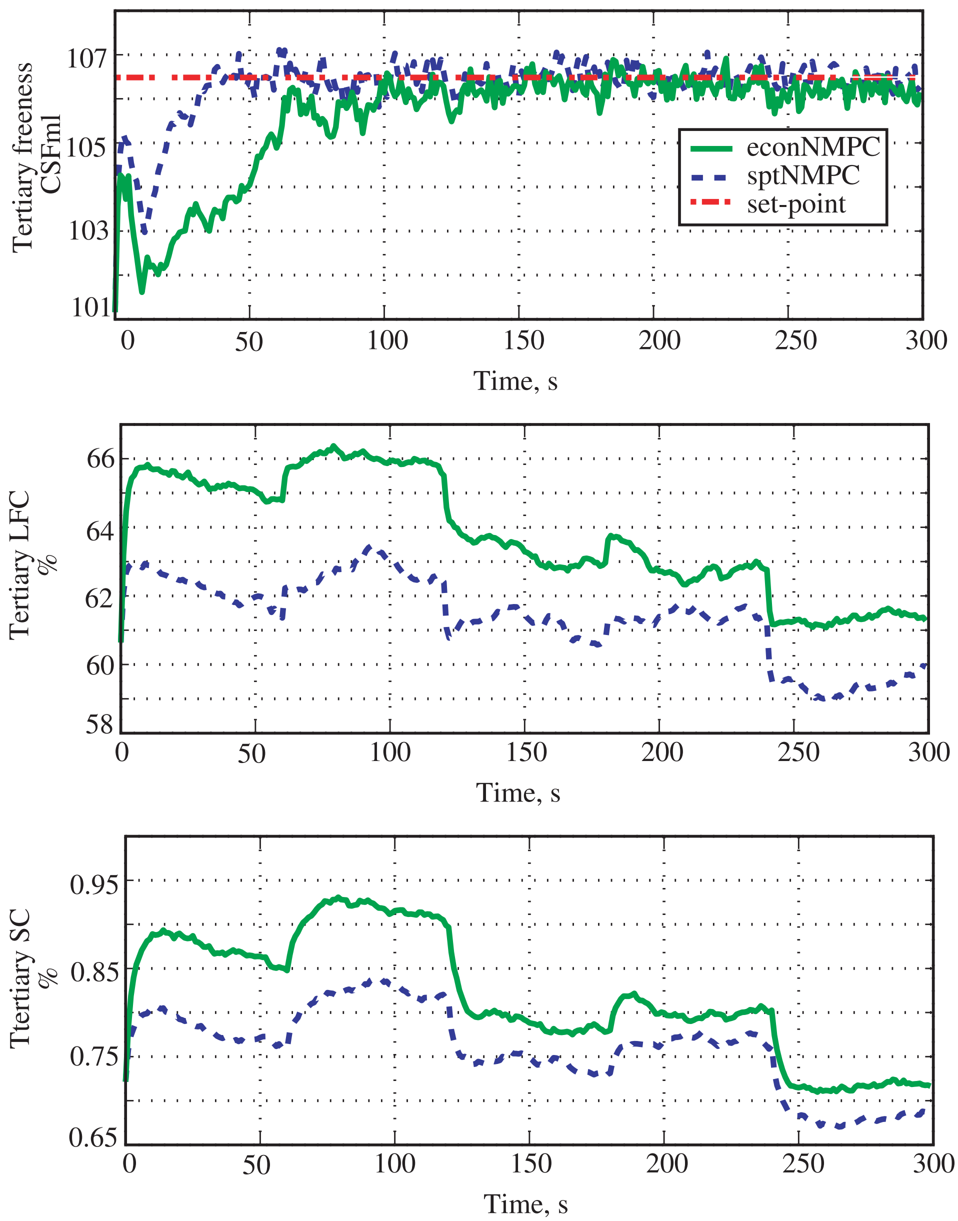

Figure 6.5: The pulp quality variables after the tertiary refining of the TMP process in Scheme A.

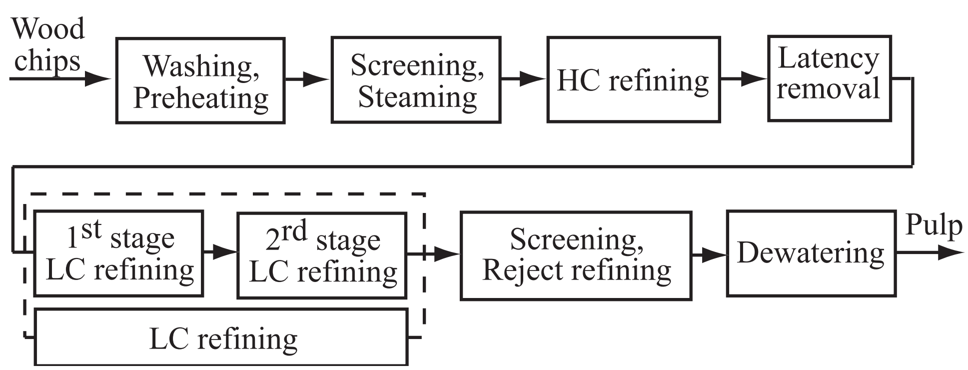

Figure 6.6: Scheme B: basic schematic of an improved TMP process with a two stages of LC refining

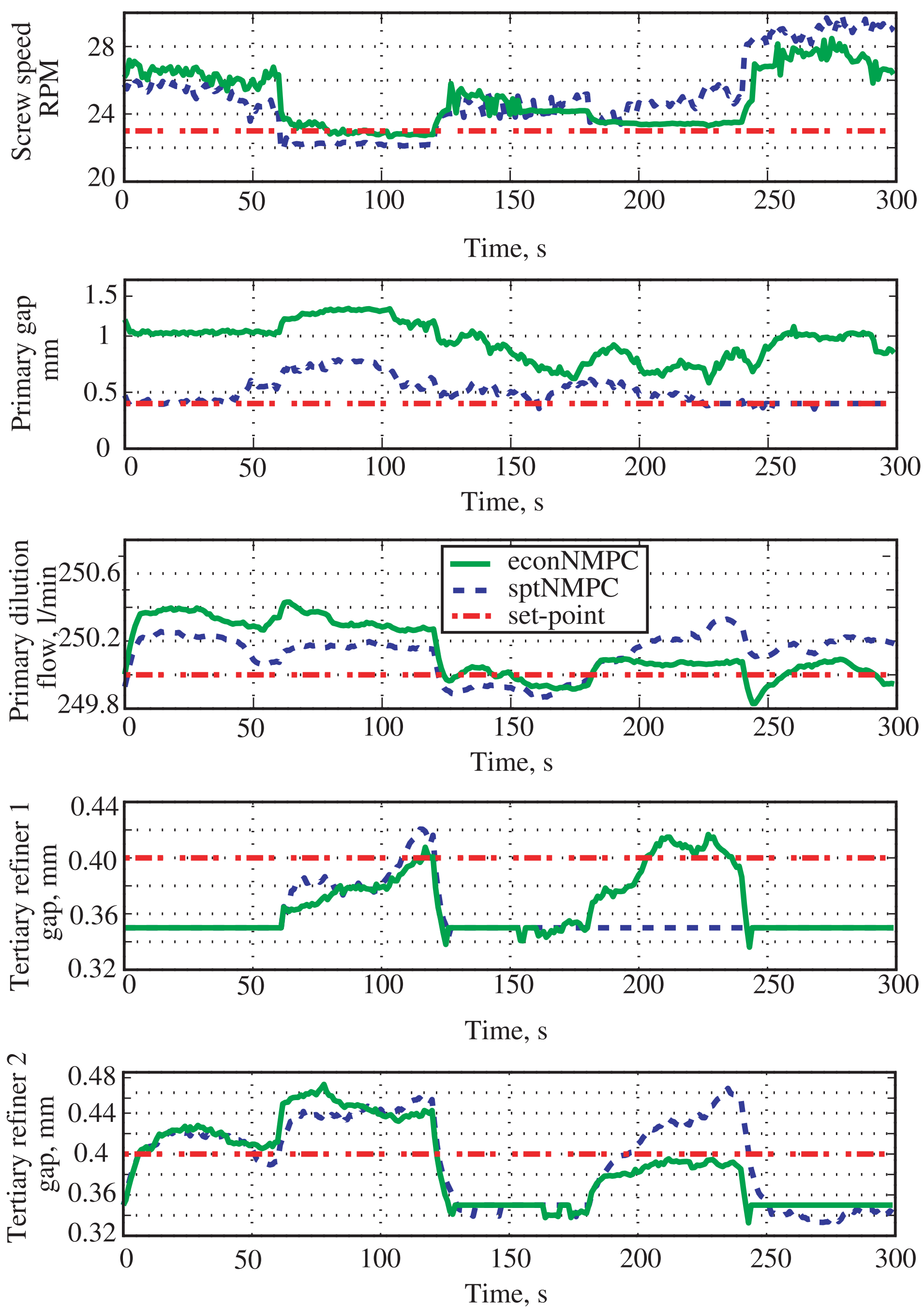

Figure 6.7: The manipulated input variables of the TMP process in Scheme B.

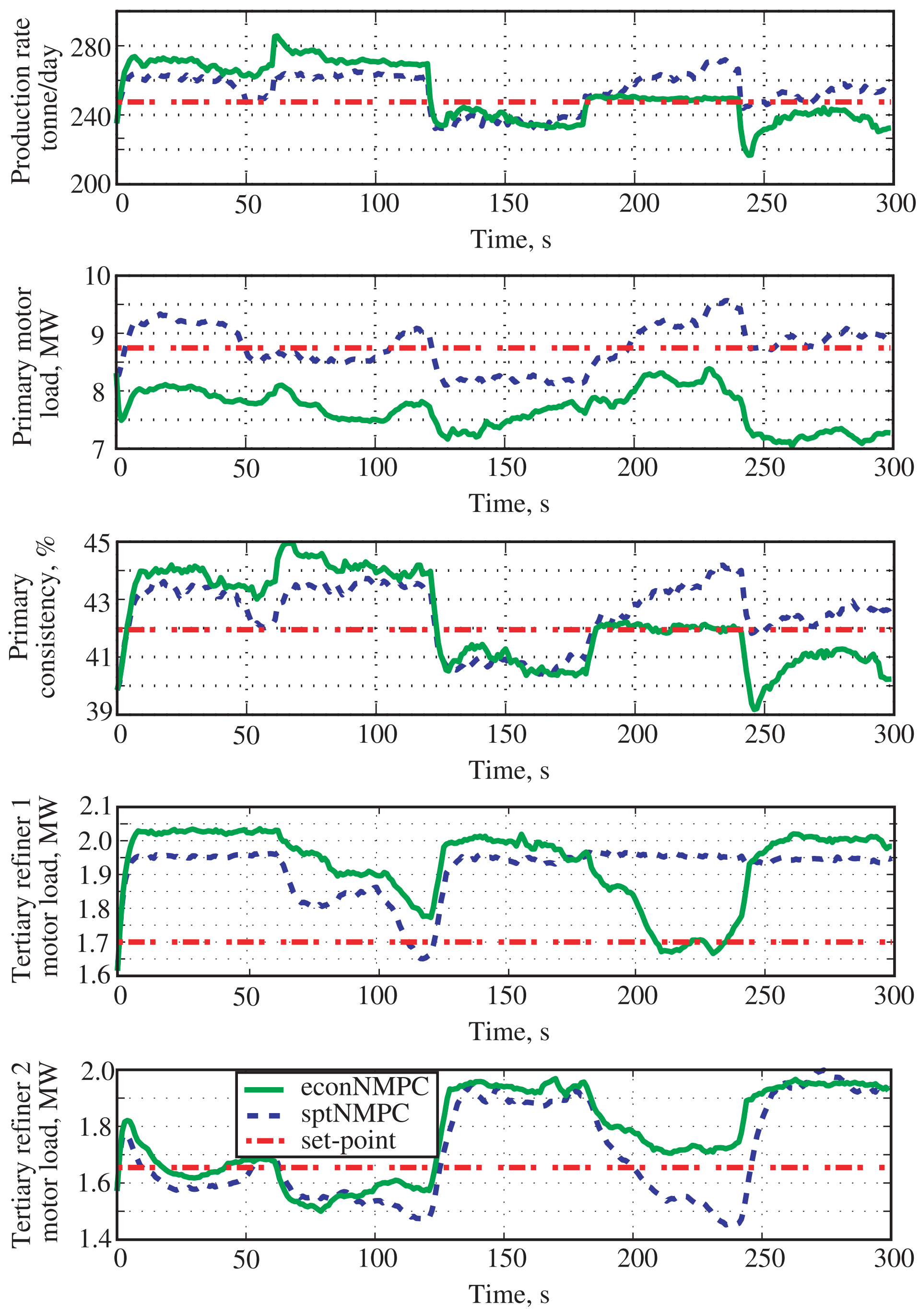

Figure 6.8: The controlled state variables of the TMP process in Scheme B.

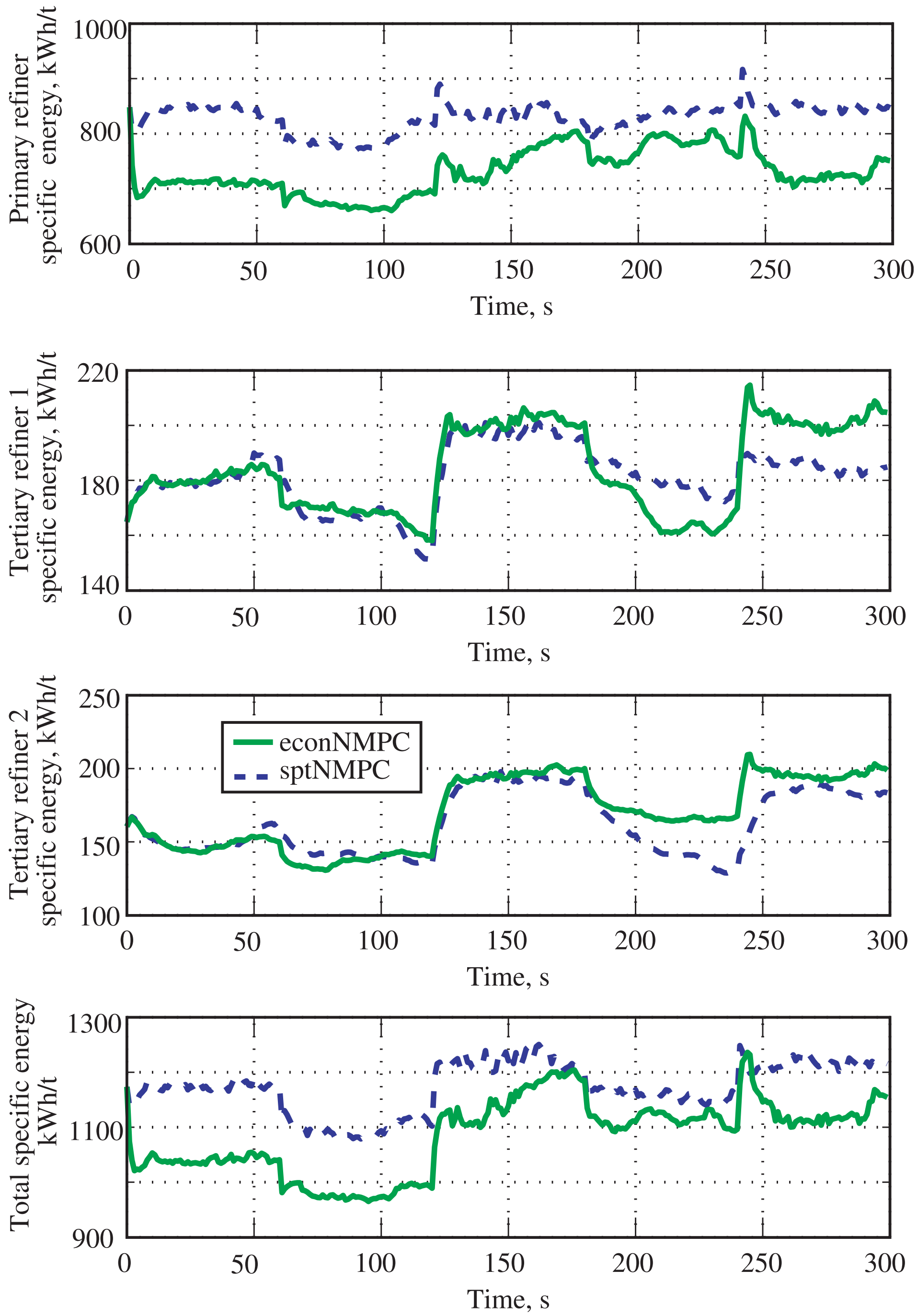

Figure 6.9: The specific energy consumptions of the primary refiner, tertiary refiner 1, and tertiary refiner 2 of TMP process in Scheme B.

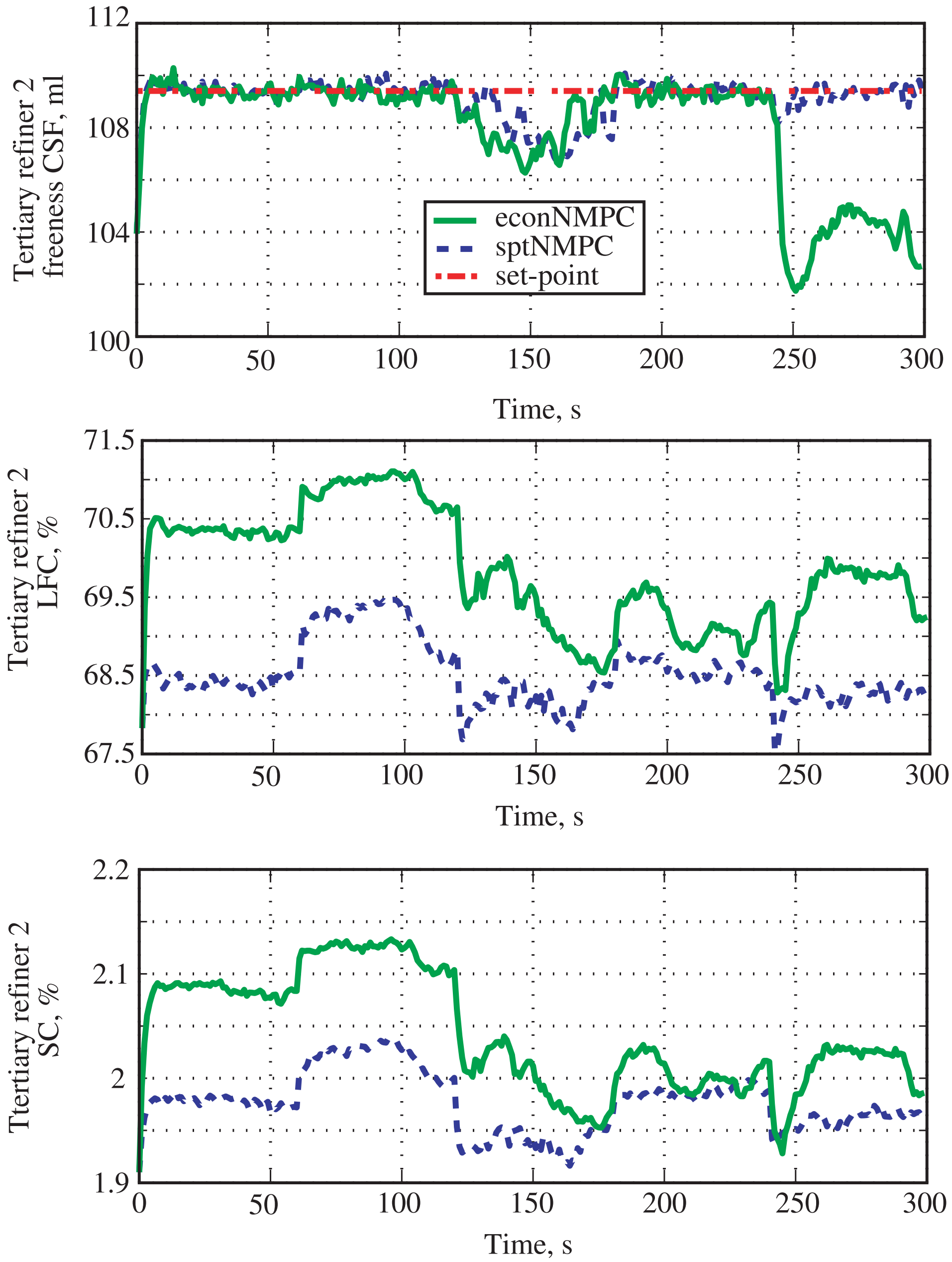

Figure 6.10: The pulp quality variables after the tertiary refining of the TMP process in Scheme B.

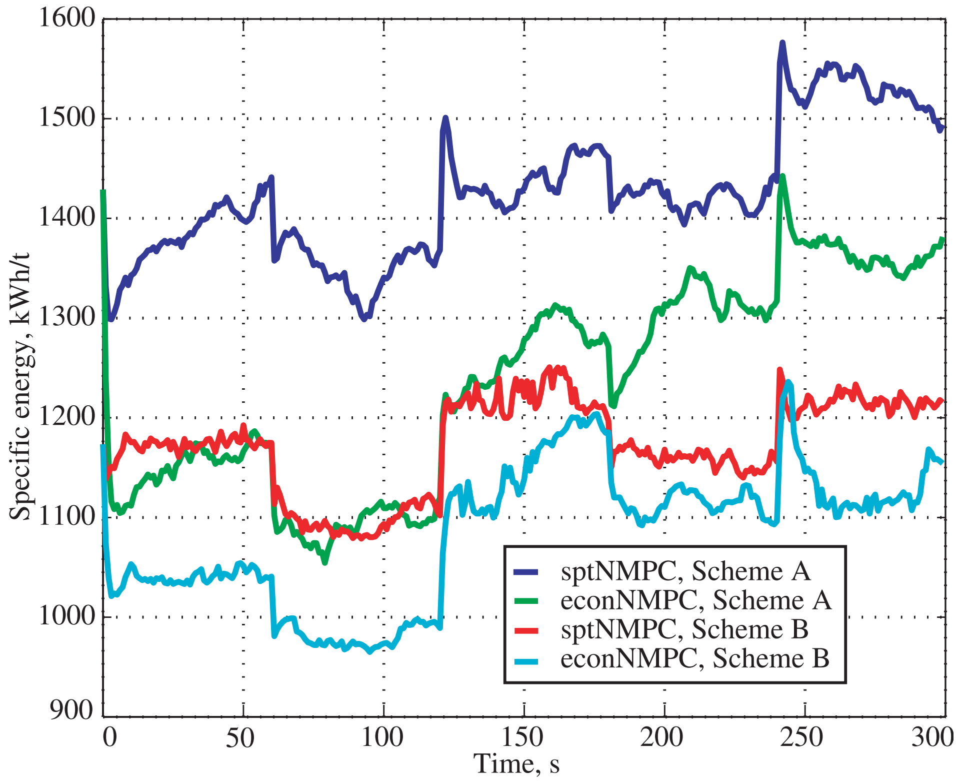

Figure 6.11: Specific energies of both Schemes A and B with sptNMPC and econ-NMPC techniques.

Chapter 7

Conclusions

In this work, we first studied closed-loop system identification techniques which can be applied to a Linear Time-Invariant (LTI) system controlled by a constrained Model Predictive Control (MPC) law. We investigated two techniques: 1) direct identification technique using Prediction Error Method (PEM), and 2) joint input-output technique using the PEM with the Long Range Predictive Identification (LRPI) criteria. In the direct identification technique, we studied how to use normal operational data for identification task without preforming any identification experiments. In the joint input-output identification technique, we studied LRPI criteria, a more meaningful identification criteria than the one-step ahead criteria in the context of identification for control using MPC. These techniques can be applied in the advanced control systems of the existing Thermo-Mechanical Pulping (TMP) processes to re-identify process models for improved performances, in particular, their low-level control systems where linear process model is being used in the MPC formulation.

In the second part of the thesis, we studied economical operation of the two-stage TMP process. A dynamic optimization problem is formulated to simultaneously regulate and optimize the TMP process when disturbances are present. The proposed economically oriented Nonlinear Model Predictive Control (econNMPC) minimizes the total specific energy consumption of both the primary and secondary refiners, respecting process constraints of such as motor loads, plate gaps, and pulp properties. In the simulation study, we first implemented setpoint tracking NMPC technique for the TMP process, where the controller task was to track the optimal steady state setpoint given by upper-level Real-Time Optimization (RTO) layer. Next, the econNMPC technique was implemented. Both the control schemes showed similar performances while the closed-loop system with econNMPC technique showed around 12% reduction in total specific energy compared to the closed-loop system with setpoint tracking NMPC technique.

In the third part of the thesis, an improved TMP process is studied for its optimal operation. The improved TMP process has a High Consistency (HC) refiner and two Low Consistency (LC) refiners. These refiners are dynamically coordinated using econNMPC technique. In a previous study [1], it is shown that around 20% specific energy reduction can be achieved with an improved TMP process at the steady state, compared to a convention TMP process consisting of two HC refiners and one LC refiner. In this study, we also showed that additional approximately 6% of specific energy reduction can be realized when the process is dynamically optimized.

Future Work

We have assumed that the state variables are measured for all NMPC formulations. However in practice, all the state measurements of TMP processes are not readily available to integrate with real-time controllers. For example, outlet consistencies of the refiners are not measured, but need to be estimated instantaneously. On the other hand, pulp qualities are usually measured just after the latency chest. Therefore, integration of those measurements with the NMPC scheme would require an estimation technique. However, this would increase complexity of the problem and require more computational power, and also would need to address theoretical issues such as stability of the overall scheme. Estimation methods such as Moving Horizon Estimation (MHE) technique or Extend Kalman Filter (EKF) would be more suitable for the TMP processes. Incorporation of such an estimation technique with NMPC algorithms for TMP processes is therefore our future research interest. At the same time, we are in the process of first preparing mill trials and then implementing the proposed techniques on a real HC and LC TMP plant. The implementation of the proposed optimal control strategy is based on the state space modeling of the TMP refiners.

Bibliography

[1] A. Luukkonen. *Development of a methodology to optimize low consistency refining of mechanical pulp*. PhD thesis, The University of British Columbia, June 2011.

[2] J. Sundholm. *Mechanical Pulping*. Papermaking Science and Technology. Fapet Oy, 1999.

[3] L. Euhus, B. C. Strand, D. Shearin, G. Fralic, and M. Edvall. Optimization of LWC TMP using advanced quality control. In *2003 International Mechanical Pulping Conference*, pages 375–378, Jun 2003.

[4] O. Johansson, M. Jackson, and N.W. Wild. Three steps to improved TMP operating efficiency. In *International Mechanical Pulping Conference 2007, TAPPI*, volume 1, pages 356–369. TAPPI, 2007.

[5] B. C. Strand and Greg Fralic. Economic benefits from advanced quality control of TMP mills. In *Control Systems 2000 Conference*, pages 11–15, May 2000.

[6] H. Du. *Multivariable Predictive Control of a TMP Plant*. PhD thesis, University of British Columbia, October 1998.

[7] D. D. Ruscio. *Topics in Model Based Control with Application to the Thermo Mechanical Pulping Process*. PhD thesis, The Norwegian Institute of Technology, 1993.

[8] M. S. Sidhu, R. V. Fleet, M. R. Dion, D. W. Anderson, and B. W. Weger. Modeling and advanced control of TMP refiner system. In *Control Systems 2004 Conference*, Jun 2004.

[9] F. Rosenqvist, D. Berg, A. Karlstrom, K. Eriksson, and C. Breitholtz. Internal interconnections in tmp processes. In *IEEE Conference on Control Applications*, pages 1010–1015, Sep 2002.

[10] G. A. Dumont and K. J. Åström. Wood chip refiner control. *IEEE Control Systems Magazine*, 8(2):38–43, 1988.

[11] H. M. Schwartz, G. Chang, and Y. Liu. Method of modeling, predicting and controlling tmp pulp properties. In *IEEE Conference on Control Applications*, pages 846–851, Sep 1996.

[12] I. Lama, M. Perrier, and P. Stuart. Controllability analysis of a tmp-newsprint refining process. *Pulp and Paper Canada*, 107(10):44–48, 2006.

[13] A. Karlstrom, K. Eriksson, D. Sikter, and M. Gustavsson. Refining models for control purposes. *Nordic Pulp and Paper Research Journal*, 23(1):129–138, 2008.

[14] M. Elsinga. TMP optimization using multivariable analysis. *IEEE Transactions on Industry Applications*, (3):893–898, May/June 2003.

[15] A. M. Brdys and P. Jatjewski. *Iterative Agorithms for Multilayer Optimizing Control*. Imperial College Press, 2005.

[16] J. B. Rawlings, D. Bonne, J. B. Jorgensen, A. N. Venkat, and S. B. Jorgensen. Unreachable setpoints in model predictive control. *Automatic Control, IEEE Transactions on*, 53(9):2209–2215, oct. 2008.

[17] R. Huang. *Nonlinear Model Predictive Control and Dynamic Real Time Optimization for Large-scale Processes*. PhD thesis, Carnegie Mellon University, December 2010.

[18] M. Sabourin, J. Aichinger, and R. Eksteen. Minimizing tmp energy consumption using a combination of chip pre-treatment, rts and multiple stage low consistency refining. In *International Mechanical Pulping Conference 2007, TAPPI*, pages 839–893, May 2007.

[19] S. J. Qin and T. A. Badgwell. A survey of industrial model predictive control technology. *Control Engineering Practice*, 11(7):733–764, July 2003.

[20] A. I. Propoi. Use of linear programming methods for synthesizing sampled-data automatic systems. *Automation and Remote Control*, 24(7):837–844, 1963.

[21] J. Richalet, A. Rault, J. L. Testud, and J. Papon. Model predictive heuristic control: Applications to industrial processes. *Automatica*, 14(5):413–428, 1978.

[22] C. R. Cutler and B. L. Ramaker. Dynamic matrix control-a computer control algorithm. In *AICHE national meeting*, April 1979.

[23] D. W. Clarke, C. Mohtadi, and P. S. Tuffs. Generalized predictive controlpart i. the basic algorithm. *Automatica*, 23(2):137–148, 1987.

[24] D. W. Clarke, C. Mohtadi, and P. S. Tuffs. Generalized predictive controlpart i. the basic algorithm. *Automatica*, 23(2):149–160, 1987.

[25] C. E. García, D. M. Prett, and M. Morari. Model predictive control: Theory and practice-a survey. *Automatica*, 25(3):335–348, 1989.

[26] R. Findeisen and F. Allgöwer. An introduction to nonlinear model predictive control. In C.W. Scherer and J.M. Schumacher, editors, *The Impact of Optimization in Control*, pages 3.1–3.45. Dutch Institute of Systems and Control, DISC, 2001.

[27] P. Tatjewski. *Advanced Control of Industrial Processes*. Advances in Industrial Control. Springer London, 2007.

[28] D. Q. Mayne. Nonlinear model predictive control: Challenges and opportunities. In Frank Allgöwer and Alex Zheng, editors, *Nonlinear Model Predictive Control*, pages 23–44. Birkhäuser, 2000.

[29] M. Diehl, R. Amrit, and J. B. Rawlings. A Lyapunov function for economic optimizing model predictive control. *IEEE Transactions on Automatic Control*, 56(3):703–707, 2011.

[30] H. K. Khalil. *Nonlinear Systems*. Prentice Hall, 2nd edition, 1996.

[31] E. G. Gilbert and K.T. Tan. Linear systems with state and control constraints: the theory and application of maximal output admissible sets. *Automatic Control, IEEE Transactions on*, 36(9):1008–1020, sep 1991.

[32] L. Magni and R. Scattolini. Robustness and robust design of mpc for nonlinear discrete-time systems. In Rolf Findeisen, Frank Allgöwer, and Lorenz Biegler, editors, *Assessment and Future Directions of Nonlinear Model Predictive Control*, volume 358 of *Lecture Notes in Control and Information Sciences*, pages 239–254. Springer Berlin / Heidelberg, 2007.

[33] M. Lazar, M. Heemels, A. Bemporad, and S. Weil. On the stability and robustness of non-smooth nonlinear model predictive control. In *in Workshop on Assessment and Future Directions of NMPC, Freudenstadt-Lauterbad*, pages 327–334, 2005.

[34] S. S. Keerthi and E. G. Gilbert. Optimal infinite-horizon feedback laws for a general class of constrained discrete-time systems: Stability and moving-horizon approximations. *Journal of Optimization Theory and Applications*, 57(2):265–293, 1988.

[35] D. Q. Mayne and H. Michalska. Receding horizon control of nonlinear systems. *IEEE Transactions on Automatic Control*, 35(7):814–824, 1990.

[36] H. Michalska and D. Q. Mayne. Robust receding horizon control of constrained nonlinear systems. *IEEE Transactions on Automatic Control*, 38(11):1623–1633, 1993.

[37] R. R. Bitmead, M. Gevers, and V. Wertz. *Adaptive Optimal Control*. Prentice Hall, 1990.

[38] T. Parisini and R. Zoppoli. A receding-horizon regulator for nonlinear systems and a neural approximation. *Automatica*, 31:1443–1451, October 1995.

[39] H. Chen and F. Allgöwer. Quasi-infinite horizon nonlinear model predictive control scheme with guaranteed stability. *Automatica*, 34(10):1205–1217, 1998.

[40] G. De Nicolao, L. Magni, and R. Scattolini. Stabilizing receding-horizon control of nonlinear time-varying systems. *IEEE Transactions on Automatic Control*, 43(7):1030–1036, 1998.

[41] M. Alamir and G. Bornard. On the stability of receding horizon control of nonlinear discrete-time systems. *Systems and Control Letters*, 23(4):291–296, 1994.

[42] E. S. Meadows, M. A. Henson, J. W. Eaton, and J. B. Rawlings. Receding horizon control and discontinuous state feedback stabilization. *International Journal of Control*, 62(5):1217–1229, 1995.

[43] Z. P. Jiang and Y Wang. Input-to-state stability for discrete-time nonlinear systems. *Automatica*, 37(6):857–869, June 2001.

[44] D. Limon, T. Alamo, D. M. Raimondo, D. de la Peña, J. Bravo, A. Ferramosca, and E. F. Camacho. Input-to-state stability: A unifying framework for robust model predictive control. In Lalo Magni, Davide Raimondo, and Frank Allgöwer, editors, *Nonlinear Model Predictive Control*, volume 384 of *Lecture Notes in Control and Information Sciences*, pages 1–26. Springer Berlin / Heidelberg, 2009.

[45] D. Q. Mayne, J. B. Rawlings, C. V. Rao, and P. O. M. Scokaert. Constrained model predictive control: Stability and optimality. *Automatica*, 36(6):789–814, June 2000.

[46] L. Magni, G. De Nicolao, R. Scattolini, and F. Allgöwer. Robust model predictive control for nonlinear discrete-time systems. *International Journal of Robust and Nonlinear Control*, 13(3-4):229–246, 2003.

[47] D. M. Raimondo, D. Limon, M. Lazar, L. Magni, and E. F. Camacho. Min-max model predictive control of nonlinear systems: A unifying overview on stability. *European Journal of Control*, 15(1):5–21, 2009.

[48] D. L. Marruedo, T. Alamo, and E. F. Camacho. Input-to-state stable mpc for constrained discrete-time nonlinear systems with bounded additive uncertainties. In *Decision and Control, 2002, Proceedings of the 41st IEEE Conference on*, volume 4, pages 4619–4624, dec. 2002.

[49] D. Q. Mayne, M. M. Seron, and S. V. Raković. Robust model predictive control of constrained linear systems with bounded disturbances. *Automatica*, 41(2):219–224, 2005.

[50] S. V. Raković, A. R. Teel, D. Q. Mayne, and A. Astolfi. Simple robust control invariant tubes for some classes of nonlinear discrete time systems. pages 6397–6402, San Diego, CA, United states, 2006.

[51] A. Bemporad and M. Morari. Robust model predictive control: A survey. In A. Garulli and A. Tesi, editors, *Robustness in identification and control*, volume 245 of *Lecture Notes in Control and Information Sciences*, pages 207–226. Springer Berlin / Heidelberg, 1999.

[52] J. B. Rawlings and D. Q. Mayne. *Model Predictive Control: Theory and Design*. Nob Hill Publishing, 2009.

[53] S. J. Wright. Applying new optimization algorithms to model predictive control. In *Proceedings of the CPC-V*, pages 147–155. CACHE Publications, 1997.

[54] J. M. Maciejowski. *Predictive Control with Constraints*. Prentice Hall, 2002.

[55] E. F. Camacho and C. Bordons. *Model Predictive Control*. Advanced Textbooks in Control and Signal Processing. Springer, 2 edition, 2004.

[56] A. Bemporad, M. Morari, V. Dua, and E. N. Pistikopoulos. The explicit linear quadratic regulator for constrained systems. *Automatica*, 38:3–20, January 2002.

[57] M. Diehl, H. G. Bock, and J. P. Schlöder. A real-time iteration scheme for nonlinear optimization in optimal feedback control. *SIAM Juournal on Cotrol and Optimization*, 43(5):1714–1736, 2005.

[58] V. M. Zavala and L. T. Biegler. The advanced step nmpc controller: Optimality, stability and robustness. *Automatica*, 45(1):86–93, January 2009.

[59] A. Wächter and L. T. Biegler. On the implementation of an interior-point filter line-search algorithm for large-scale nonlinear programming. *Mathematical Programming*, 106(1):25–57, May 2006.

[60] V. M. Zavala. *Computational Strategies for the Optimal Operation of Large-Scale Chemical Processes*. PhD thesis, Carnegie Mellon University, 2008.

[61] D. E. Kassmann, T. A. Badgwell, and R. B. Hawkins. Robust steady-state target calculation for model predictive control. *AIChE Journal*, 46(5):1007–1024, May 2000.

[62] A. C. Zanin, M. T. de Gouvea, and D. Odloak. Integrating real-time optimization into the model predictive controller of the fcc system. *Control Engineering Practice*, 10(8):819–31, 2002.

[63] L. T. Biegler. *Efficient Solution of Dynamic Optimization and NMPC Problems*. Progress in Systems and Control Theory. Birkhäuser, 2000.

[64] D. Q. Mayne. Nonlinear model predictive control: An assessment. Number 316, pages 217–217, 1997.

[65] V. M. Zavala and L. T. Biegler. Optimization-based strategies for the operation of low-density polyethylene tubular reactors: nonlinear model predictive control. *Computers & Chemical Engineering*, 33(10):1735–46, October 2009.

[66] V. Adetola and M. Guay. Integration of real-time optimization and model predictive control. *J. Process Control*, 20(2):125–133, February 2010.

[67] E. Harinath, L. T. Biegler, and G. A. Dumont. Control and optimization strategies for thermo-mechanical pulping processes: Nonlinear model predictive control. *Journal of Process Control*, 21(4):519–528, April 2011.

[68] R. Huang, V. M. Zavala, and L. T. Biegler. Advanced step nonlinear model predictive control for air separation units. *J. Process Control*, 19(4):678–685, April 2009.

[69] R. Huang, E. Harinath, and L. T. Biegler. Lyapunov stability of economically oriented NMPC for cyclic processes. *Journal of Process Control*, 21(4):501–509, April 2011.

[70] E. M. B. Aske, S. Strand, and S. Skogestad. Coordinator mpc for maximizing plant throughput. *Computers and Chemical Engineering*, 32(1-2):195–204, 2008.

[71] S. Engell. Feedback control for optimal process operation. *Journal of Process Control*, 17(3):203–219, 2007.

[72] J. Kadam and W. Marquardt. Integration of economical optimization and control for intentionally transient process operation. In Rolf Findeisen, Frank Allgöwer, and Lorenz Biegler, editors, *Assessment and Future Directions of Nonlinear Model Predictive Control*, volume 358 of *Lecture Notes in Control and Information Sciences*, pages 419–434. Springer Berlin / Heidelberg, 2007.

[73] J. B. Rawlings and R. Amrit. Optimizing process economic performance using model predictive control. In Lalo Magni, Davide Raimondo, and Frank Allgöwer, editors, *Nonlinear Model Predictive Control*, volume 384 of *Lecture Notes in Control and Information Sciences*, pages 119–138. Springer Berlin / Heidelberg, 2009.

[74] R. Huang, L. T. Biegler, and E. Harinath. Robust stability of economically oriented infinite horizon NMPC that include cyclic processes. *Journal of Process Control*, 22(1):51–59, January 2012.

[75] M. Heidarinejad, J. Liu, and P. D. Christofides. Economic model predictive control of nonlinear process systems using lyapunov techniques. *AIChE Journal*, 2011.

[76] L. Grüne. Optimal invariance via receding horizon control. Submitted in 50th IEEE Conference on Decision and Control and European Control Conference, 2011.

[77] L. Würth, J. B. Rawlings, and W. Marquardt. Economic dynamic real-time optimization and nonlinear model predictive control on infinite hoirzons, in international symposium on advanced control of chemical process. volume 7 of *7th IFAC International Symposium on Advanced Control of Chemical Processes*, 2009.

[78] J. Nocedal and S. J. Wright. *Numerical Optimization*. Operations Research. Springer, 2nd edition, 2007.

[79] H. Hjalmarsson. From experiment design to closed-loop control. *Automatica*, 41(3):393–438, March 2005.

[80] J. S. Conner and D. E. Seborg. Assessing the need for process re-identification. *Industrial & Engineering Chemistry Research*, 44(8):2767–2775, 2005.

[81] O. A. Z. Sotomayor, D. Odloak, and L. F. L. Moro. Closed-loop model re-identification of processes under mpc with zone control. *Control Engineering Practice*, 17(5):551–563, 2009.

[82] M. A. Hussain. Review of the applications of neural networks in chemical process control – simulation and online implementation. *Artificial Intelligence in Engineering*, 13(1):55–68, 1999.

[83] U. Forssell and L. Ljung. Closed-loop identification revisited. *Automatica*, 35(7):1215–1241, Jul 1999.

[84] L. Ljung. *System Indentification: Theory for the user*. Prentice-Hall, 2 edition, 1999.

[85] T. Söderström and P. Stoica. *System Identification*. Prentice Hall Internationl, 1989.

[86] P. M. J. Van den Hof and R. A. de Callafon. Multivariable closed-loop identification: from indirect identification to dual-youla parametrization. In *Decision and Control, 1996., Proceedings of the 35th IEEE*, volume 2, pages 1397–1402 vol.2, dec 1996.

[87] U. Forssell and L. Ljung. Projection method for closed-loop identification. *IEEE Transactions on Automatic Control*, 45(11):2101–2106, Nov 2000.

[88] J. Yan, E. Harinath, and G. A. Dumont. Closed-loop identification for model predictive control: Direct method. In *Proceedings of the IEEE Conference on Decision and Control*, pages 2592–2597, December 2009.

[89] M. Gevers, A. Bazanella, and L. Mikovic. Informative data: How to get just sufficiently rich? pages 1962–1967, 2008.

[90] X. Bombois, G. Scorletti, M. Gevers, P. M. J. Van den Hof, and R. Hildebrand. Least costly identification experiment for control. *Automatica*, 42(10):1651–1662, 2006.

[91] M. J. Van Den Hof and R. J. P. Schrama. Indirect method for transfer function estimation from closed loop data. *Automatica*, 29(6):1523–1527, Nov 1993.

[92] U. Forssell. *Closed-loop Identification: Methods, Theory, and Applications*. Linköping studies in science and technology. thesis no 566, 1999.

[93] D. S. Shook, C. Mohtadi, and S. L. Shah. Identification for long-range predictive control. *IEE Proceedings D: Control Theory and Applications*, 138(1):75–84, 1991.

[94] R. B. Gopaluni, R. S. Patwardhan, and S. L. Shah. The nature of data prefilters in MPC relevant identification - open- and closed-loop issues. *Automatica*, 39(9):1617–1626, 2003. Bias distribution;.

[95] R. B. Gopaluni, R. S. Patwardhan, and S. L. Shah. MPC relevant identification–tuning the noise model. *Journal of Process Control*, 14(6):699–714, 2004.

[96] M. Morari and J. H. Lee. Model predictive control: past, present and future. *Computers and Chemical Engineering*, 23(4-5):667–682, May 1999.

[97] D. D. Ruscio. Model predictive control and identification: a linear state space model approach. In *Proceedings of the 36th IEEE Conference on Decision and Control*. IEEE, December 1997.

[98] H. Du, G. A. Dumont, and Y. Fu. Nonlinear control of a wood chip refiner. In *Proceedings of the 4th IEEE Conference on Control Applications*, pages 1065–6. IEEE, 1995.

[99] S. Kidd. Implementation of a tmp advanced quality control system at a newsprint manufacturing plant. Technical report, Department of Energy, Washington, DC, 2005.

[100] M. Illikainen. *Mechanisms of thermomechanical pulp refining*. PhD thesis, University of Oulu, October 2008.

[101] X. Qian and P. Tessier. A mechanistic model for predicting pulp properties from refiner operating conditions. *Tappi journal*, 78(78):215–222, April 1995.

[102] L. O. Santos, P. A. F. N. A. Afonso, J. A. A. M Castro, N. M. C. Oliveira, and L. T. Biegler. Online implementation of nonlinear mpc: an experimental case study. *Control Engineering Practice*, 9(8):847–857, August 2001.

[103] W. H Chen, D. J. Ballance, and J. O'Reilly. Model predictive control of nonlinear systems: Computational burden and stability. *IEE Proc Control Theory Applications*, 147(4):387–394, July 2000.

[104] R. Findeisen and F. Allgöwer. Computational delay in nonlinear model predictive control. In *Int. Symp. Adv. Control of Chemical Processes, ADCHEM'03*, pages 427–432, 2004.

[105] S. Skogestad. Self-optimizing control: The missing link between steady-state optimization and control. *Computers and Chemical Engineering*, 24(2-7):569–575, July 2000.

[106] B. C. Strand, J. Straight, and D. Norris. Factors affecting energy reduction of newsprint from southern pine tmp.

[107] G. Mitchell, R. Musselman, and M. Sabourin. Third stage low consistency refining of tmp. In *52nd Appita general pulping conference*, pages 475–483, 1998.

[108] R. Musselman, D. Letarte, and R. Sinard. Third stage low consistency refining of tmp for energy saving and quality enhancement. In *PIRA 4th International Refining Conference*, 1997.

[109] J. Gao, C. P. J. Bennington, D. M. Martinez, and J. A. Olson. Latency removal in mechanical pulping processes. In *PAPTAC Annual Meeting*, pages 1293–1325. CD–ROM, 2012.